USGS
science for a changing world

Prepared in cooperation with the Alaska Division of Geological and Geophysical Surveys

GIS-Based Identification of Areas with Mineral Resource Potential for Six Selected Deposit Groups, Bureau of Land Management Central Yukon Planning Area, Alaska

U.S. Department of the Interior
U.S. Geological Survey

Prepared in cooperation with the Alaska Division of Geological and Geophysical Surveys

GIS-Based Identification of Areas with Mineral Resource Potential for Six Selected Deposit Groups, Bureau of Land Management Central Yukon Planning Area, Alaska

By James V. Jones, III, Susan M. Karl, Keith A. Labay, Nora B. Shew, Matthew Granitto, Timothy S. Hayes, Jeffrey L. Mauk, Jeanine M. Schmidt, Erin Todd, Bronwen Wang, Melanie B. Werdon, and Douglas B. Yager

Open-File Report 2015–1021

U.S. Department of the Interior
U.S. Geological Survey

U.S. Department of the Interior
SALLY JEWELL, Secretary

U.S. Geological Survey
Suzette M. Kimball, Acting Director

U.S. Geological Survey, Reston, Virginia: 2015

Suggested citation:
Jones, J.V., III, Karl, S.M., Labay, K.A., Shew, N.B., Granitto, M., Hayes, T.S., Mauk, J.L., Schmidt, J.M., Todd, E., Wang, B., Werdon, M.B., and Yager, D.B., 2015, GIS-based identification of areas with mineral resource potential for six selected deposit groups, Bureau of Land Management Central Yukon Planning Area, Alaska: U.S. Geological Survey Open-File Report 2015–1021, 78 p., 5 appendixes, 12 pls., *http://dx.doi.org/10.3133/ofr20151021*.

ISSN 2331-1258 (online)

COVER
Granitic rock exposures of the Melozitna pluton in the Kokrines Hills, central Alaska, contain multiple rare earth element (REE) occurrences. Gamma ray scintillometer on the outcrop in the foreground for scale. USGS photo by Sue Karl.

Contents

Appendixes

[Available online at http://pubs.usgs.gov/of/2015/1021/]

A. Stream-sediment geochemistry summary statistics and percentile cutoffs (Excel spreadsheet)
B. Igneous rock geochemistry peer-reviewed literature sources (text pdf)
C. Alaska Resource Data File (ARDF) mineral deposit keyword and scoring templates (Excel spreadsheet)
D. Lithology keyword search terms for an anticipated U.S. Geological Survey geologic map of Alaska (Excel spreadsheet)
E. Scoring results for HUC analysis of selected deposit groups (folder containing Excel spreadsheets and geospatial data files)

Figures

Tables

Plates

[Available online at http://pubs.usgs.gov/of/2015/1021/]

Conversion Factors

Inch/Pound to SI

Multiply	By	To obtain
	Length	
foot (ft)	0.3048	meter (m)
mile (mi)	1.609	kilometer (km)
yard (yd)	0.9144	meter (m)
	Area	
acre	0.4047	hectare (ha)
acre	0.004047	square kilometer (km^2)
square mile (mi^2)	259.0	hectare (ha)
square mile (mi^2)	2.590	square kilometer (km^2)
	Mass	
ounce, troy (troy oz)	31.103	gram (g)
ounce, troy (troy oz)	0.0000311	megagram (Mg)
ton, short (2,000 lb)	0.9072	megagram (Mg)

SI to Inch/Pound

Multiply	By	To obtain
	Length	
meter (m)	3.281	foot (ft)
kilometer (km)	0.6214	mile (mi)
meter (m)	1.094	yard (yd)
	Area	
hectare (ha)	2.471	acre
hectare (ha)	0.003861	square mile (mi^2)
square hectometer (hm^2)	2.471	acre
square kilometer (km^2)	0.3861	square mile (mi^2)
	Mass	
gram (g)	0.03215	ounce, troy (troy ounce)
megagram (Mg)	1.102	ton, short (2,000 lb)
megagram (Mg)	0.9842	ton, long (2,240 lb)

Other conversions used in this report		
metric ton (t)	1	megagram (Mg)
troy ounce per short ton	34.2857	gram per metric ton (g/t)
percent (%)	10,000	parts per million (ppm) or grams per metric ton (g/t)
percent	0.01 × ore tonnage, metric tons	metric tons of metal

List of Abbreviations Used

ADGGS	Alaska Division of Geological and Geophysical Surveys
AMRAP	Alaska Mineral Resource Appraisal Program
ANK	modal Al/[Na+K]
ASI	Aluminum Saturation Index
BLM	Bureau of Land Management
CYPA	Central Yukon Planning Area
GIS	Geographic Information System
g/t	grams per metric ton
ICP-MS	inductively coupled plasma mass spectrometry
HFSE	high field strength elements
HUC	hydrologic unit code
Mt	million metric tons
MALI	modified alkali-lime index
MUM	mafic and ultramafic rocks
NHD	National Hydrologic Dataset
NURE	National Uranium Resource Evaluation
NURE-HSSR	National Uranium Resource Evaluation Hydrogeochemical and Stream Sediment Reconnaissance
PGE	platinum-group elements
ppm	parts per million
REE	rare earth elements
ssU	Sandstone uranium deposit
t	metric ton
USGS	U.S. Geological Survey
WBD	Watershed Boundary Dataset

GIS-based Identification of Areas with Mineral Resource Potential for Six Selected Deposit Groups, Bureau of Land Management Central Yukon Planning Area, Alaska

By James V. Jones III[1], Susan M. Karl[1], Keith A. Labay[1], Nora B. Shew[1], Matthew Granitto[1], Timothy S. Hayes[1], Jeffrey L. Mauk[1], Jeanine M. Schmidt[1], Erin Todd[1], Bronwen Wang[1], Melanie B. Werdon[2], and Douglas B. Yager[1]

Abstract

This study, covering the Bureau of Land Management (BLM) Central Yukon Planning Area (CYPA), Alaska, was prepared to aid BLM mineral resource management planning. Estimated mineral resource potential and certainty are mapped for six selected mineral deposit groups: (1) rare earth element (REE) deposits associated with peralkaline to carbonatitic intrusive igneous rocks, (2) placer and paleoplacer gold, (3) platinum group element (PGE) deposits associated with mafic and ultramafic intrusive igneous rocks, (4) carbonate-hosted copper deposits, (5) sandstone uranium deposits, and (6) tin-tungsten-molybdenum-fluorspar deposits associated with specialized granites. These six deposit groups include most of the strategic and critical elements of greatest interest in current exploration.

This study has used a data-driven, geographic information system (GIS)-based method for evaluating the mineral resource potential across the large region of the CYPA. This method systematically and simultaneously analyzes geoscience data from multiple geospatially referenced datasets and uses individual subwatersheds (12-digit hydrologic unit codes or HUCs) as the spatial unit of classification. The final map output indicates an estimated potential (high, medium, low) for a given mineral deposit group and indicates the certainty (high, medium, low) of that estimate for any given subwatershed (HUC). Accompanying tables describe the data layers used in each analysis, the values assigned for specific analysis parameters, and the relative weighting of each data layer that contributes to the estimated potential and certainty determinations. Core datasets used include the U.S. Geological Survey (USGS) Alaska Geochemical Database (AGDB2), the Alaska Division of Geologic and Geophysical Surveys Web-based geochemical database, data from an anticipated USGS geologic map of Alaska, and the USGS Alaska Resource Data File. Map plates accompanying this report illustrate the mineral prospectivity for the six deposit groups across the CYPA and estimates of mineral resource potential.

[1]U.S. Geological Survey
[2]Alaska Division of Geological and Geophysical Surveys

There are numerous areas, some of them large, rated with high potential for one or more of the selected deposit groups within the CYPA. The CYPA has recognizable potential for REE deposits associated with the Hogatza plutonic belt and parts of the Ruby batholith. Another area of high potential surrounds a known carbonatite occurrence near Tofty, Alaska, in the Hot Springs placer district. Placer gold potential is relatively high along many drainages scattered across the CYPA. Prospecting for and production from relatively small placer gold deposits were widespread in the past and have continued to the present. Areas with high potential for PGE deposits associated with mafic and ultramafic rocks are in the northwestern Brooks Range to the west of the CYPA and in the Killik River quadrangle within the CYPA. Another area of high PGE potential flanks the Ruby batholith to the northwest, generally within and near the Kanuti River drainage. High potential for carbonate-hosted copper deposits exists outside the CYPA within the Gates of the Arctic National Park and Wildlife Preserve along the south flank of and into the core of the Brooks Range. A discontinuous belt of high potential extends far to the northeast and includes areas within the CYPA in the Wiseman, Chandalar, and Philip Smith Mountains quadrangles. Other areas with high potential for copper deposits in carbonate rocks are in the southeastern CYPA and in the Brooks Range foreland. Sandstone uranium potential within the CYPA appears most closely associated with areas proximal to felsic intrusive igneous rocks such as the Hogatza plutonic belt and the Ruby batholith; the potential appears highest for a basal-type sandstone uranium deposit analogous with the Death Valley (Boulder Creek) deposit adjacent to the Darby pluton on the eastern Seward Peninsula. The highest potential for tin-tungsten-molybdenum-fluorspar deposits is associated with the Hogatza belt and Ruby batholith plutons, but high potential also occurs along the Tofty-Livengood belt of intrusive igneous rocks and in scattered areas within the Yukon-Tanana uplands.

Introduction

The Bureau of Land Management (BLM) in Alaska is developing a resource management plan (RMP) for their Central Yukon Planning Area (CYPA; fig. 1), which includes consideration of mineral exploration and development activities and their management. The U.S. Geological Survey (USGS) was requested to provide an analysis of the geologic potential for selected types of as-yet-undiscovered mineral resources to contribute to the RMP. This analysis is not a comprehensive review of known mines, prospects, occurrences, or mineral deposit types that occur within the planning area. Instead, it is an evaluation of where mineral deposits of several specific groups might occur in the region on the basis of geoscientific data and (or) features such as geology (for example, lithology, mineralogy, known prospects), geochemistry (of rock, soil, water, and drainage sediment samples), and (or) geophysical properties.

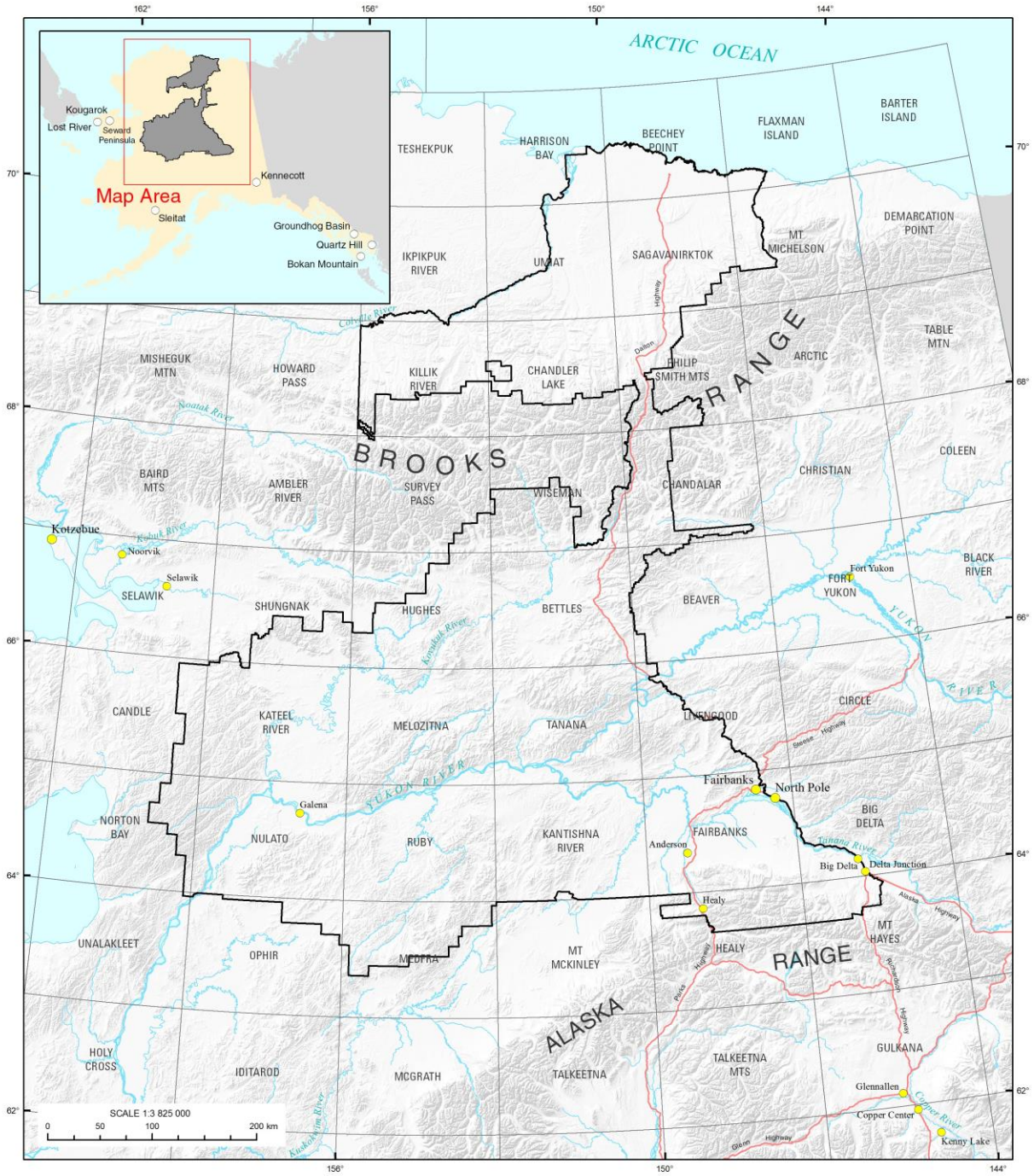

Figure 1. Reference map of northern Alaska showing the Bureau of Land Management Central Yukon Planning Area (outlined in black).

For this study, mineral "deposits" are localities with reported inventory or past production, whereas mineral "prospects" and "occurrences" describe localities where minerals of the mineral commodity are known but with no reported inventory. Mineral deposit "types" are recognized styles of mineralization with published deposit models, and mineral deposit "groups" contain two or more mineral deposit types with similar commodities that occur in broadly similar

geological settings. For example, the placer and paleoplacer Au group contains many different types of deposits on a global basis, but herein we focus on the alluvial placer, alluvial paleoplacer, and coastal placer types because they have the highest probability of occurrence within the CYPA.

This study considered six groups of mineral deposits that occur in Alaska and that contain critical elements (table 1; note that tables appear at the end of this report). Critical elements are those for which the United States imports more than half of its total supply and which come in large part from nations that cannot be considered reliable trading partners (National Research Council, 2008). Key characteristics of these deposit groups were identified and scored in terms of importance for indicating potential for the occurrence of each group. A geographic information system (GIS) was then used to systematically and simultaneously consider disparate types of geological, geochemical, mineral occurrence, and geophysical data as tools for prospectivity mapping for these six deposit groups within the CYPA. This study separates three levels of prospectivity on the basis of presence and abundance of favorable deposit-group attributes and three levels of certainty of the analysis. It is not a three-part probabilistic mineral resource potential assessment (Singer, 1993; Singer and Menzie, 2010) as conducted by the USGS for many areas in recent years (for example, Zientek and others, 2014).

The six specific mineral deposit groups considered in this study are (1) rare earth elements-thorium-yttrium-niobium(-uranium-zirconium) [REE-Th-Y-Nb (-U-Zr)] deposits associated with peralkaline to carbonatitic igneous rocks, (2) placer and paleoplacer gold (Au) deposits, (3) platinum group element(-cobalt-chromium-nickel-titanium-vanadium) [PGE (-Co-Cr-Ni-Ti-V)] deposits associated with mafic and ultramafic igneous rocks, (4) carbonate-hosted copper (-cobalt-silver-germanium-gallium) [Cu (-Co-Ag-Ge-Ga)] deposits, (5) sandstone uranium (-vanadium-copper) [U (-V-Cu)] deposits, and (6) tin-tungsten-molybdenum (-tantalum-indium-fluorspar) [Sn-W-Mo (-Ta-In-fluorspar)] deposits associated with specialized granites. For each deposit group, a map indicates the relative density of favorable data (high, medium, or low) for all of the 12-digit hydrologic units that constitute the CYPA (see below regarding 12-digit hydrologic units), as well as the relative certainty (high, medium, or low), derived by the method described below. Associated tables indicate which datasets were used in the analysis for each deposit group, which parameters were queried, and how much each parameter contributed to the estimate of mineral prospectivity. Data tables and associated geospatial data files (appendix E) provide the results for each deposit group and permit the user to analyze and query the findings in a spatial context.

Deposit Group Characteristics

The work here addresses the six deposit groups listed above and described below. These deposit groups do not include all of the mineral deposit types that are likely to occur in the CYPA. Instead, they were chosen for study because they are known to occur in Alaska and contain one or more critical elements as defined above (National Research Council, 2008). Table 1 summarizes the six deposit groups together with associated commodities, examples in Alaska and elsewhere in the world, and key references. In the lists of elements for each deposit group, elements preceding the parentheses are the major products of the deposit groups, or at least their most abundant elements of interest. Elements and minerals listed in parentheses are coproducts or byproducts that occur in some deposits of the group but are less common than those listed before. The following section provides an overview each deposit group that was the focus of this

study. Other deposit types known in the CYPA or elsewhere in central Alaska were not considered in this work.

REE-Th-Y-Nb (-U-Zr) Deposits Associated with Peralkaline to Carbonatitic Igneous Rocks

Worldwide, economic deposits of rare earth elements (REE) are most commonly associated with intrusive igneous rocks that are not fully saturated with silica, and, thus, have a paucity of quartz or none at all (Long and others, 2010). Associated intrusive-rock compositions vary from peralkaline granite to syenite and also include ultra-alkaline rocks and carbonatites. Mafic rocks within the same igneous complexes seldom contain ore. Although carbonatites are relatively rare worldwide, they are particularly rich in the REE (Rankin, 2005). Carbonatite and peralkaline intrusive complexes are derived from partial melting of mantle material, and deposits and associated rock types tend to occur within stable continental regions and are generally associated with intracontinental rift and fault systems (Verplanck and others, 2014). Protracted fractional crystallization of parental magmas leads to enrichment of REE and other incompatible elements. In carbonatites, REE mineralization can occur as either late stage mineral phases or as mineralization associated with late-stage orthomagmatic fluids. Deposits associated with carbonatite tend to be enriched in the light rare earth elements (atomic numbers from lanthanum, 57, through europium, 63). In alkaline intrusive complexes, REE mineralization may occur as primary phases in magmatic layered complexes or as late-stage dikes and veins (Verplanck and others, 2014). These deposits tend to be enriched in the heavy REE (atomic numbers from gadolinium, 64, through lutetium, 71). In some places, REE-bearing ore deposits of an intermediate enrichment pattern are found in association with intrusive rocks with compositions between the peralkaline granite and carbonatite end members.

Minerals that contain REE also commonly contain, or may contain, Nb, Th, and Y; these three elements form their own minerals, and they are most abundant in association with syenitic to ultra-alkaline to carbonatitic intrusive rocks (Notholt and others, 1990). Minerals containing REE might also contain U and Zr, and minerals with this latter set of elements together with Ta, Nb, and Sn are generally associated with peralkaline granite and syenite (Pollard, 1995). In syenitic to carbonatitic deposits, REE-bearing ore minerals are either fluorocarbonates such as bastnäsite [hexagonal $(Y,REE)CO_3(F,OH)$], synchysite [orthorhombic $Ca(REE,Y)(CO_3)_2F$], or parisite [rhombohedral $Ca(REE)_2(CO_3)_3F_2$] at places with carbonates like ancylite [orthorhombic $(Ca,Sr,REE)_2(CO_3)_2(OH,H_2O)$], or they are phosphate minerals like monazite [monoclinic $(Th,REE)PO_4$] and others closely related to it (Long and others, 2010). Carbonatites commonly contain large concentrations of apatite, another phosphate mineral that might be economically mineable for fertilizer (Richardson and Birkett, 1996). However, apatite typically does not contain REE in concentrations that are economically recoverable. The two largest producing REE mines in the world—Mountain Pass, California, and Bayan Obo, China—both produce more bastnäsite than any other mineral, and both are associated with carbonatites (Le Bas and others, 1992; Castor, 2008). Bastnäsite at Mountain Pass is probably igneous in origin, but bastnäsite at Bayan Obo is thought to be entirely hydrothermal (Chao and others, 1997; Castor, 2008). In less silica-undersaturated systems, such as peralkaline granite or syenite, the REE minerals that may be found in economic concentrations are mainly oxides like fergusonite [tetragonal(?) $(REE,Y)(Nb,Ti)O_4$] and silicates like allanite [monoclinic $(Ca,REE)_2(Al,Fe)_3(SiO_4)_3(OH)$] (Sheard and others, 2012). Uranium might occur in oxides with or without Nb, REE, Y, Th, or Ta in these deposits; for example, aeschynite, betafite, samarskite, and polycrase. Zirconium might occur in igneous and (or) hydrothermal zircon (tetragonal

$ZrSiO_4$) and eudialyte [rhombohedral $Na_{16}Ca_6Fe_3Zr_3(Si_3O_9)(Si_9O_{27})_2(OH,Cl)$]. The zircon of this kind of deposit might have greater economic value than any other REE, U, or Nb ore minerals.

Alaska currently has only one known REE deposit; it is associated with the Bokan Mountain peralkaline granite of Jurassic age in the far southeastern part of the State on Prince of Wales Island (fig. 1). The Bokan Mountain deposit has a 5.2 million metric ton (Mt) resource that contains 0.548 percent total REE (Bentzen and others, 2013), and the potential ore is concentrated in narrow, tabular dikes and veins that occur in a swarm and that display both quartz-vein and igneous-dike mineralogy and textures.

Placer and Paleoplacer Gold (Au) Deposits

Placer deposits are concentrations of high-density minerals formed by gravity separation during sedimentary processes. Heavy minerals are separated from their primary host rocks by weathering and erosion and then transported and concentrated in surficial deposits. Placer deposits exhibit a wide range of textures, form in many different environments, and host a variety of minerals, including valuable resources for gold, titanium, tin, platinum group elements, REE, and iron (Slingerland and Smith, 1986; Garnett and Bassett, 2005). Gold in placer deposits was initially derived from bedrock containing gold-quartz veins, disseminated gold, or other gold-bearing mineral deposits such as porphyry copper, Cu skarn, and polymetallic replacement deposits (Yeend, 1986). Primary gold-bearing deposits typically occur in igneous (Baker, 2002; Seedorff and others, 2005; Hart, 2007; Sinclair, 2007; Taylor, 2007) or metamorphic rocks (Berger and Henley, 1989; Groves and others, 1998; Goldfarb and others, 2005), although sedimentary deposits such as paleoplacers and modified paleoplacers (Pretorius, 1981; Minter, 2006) are also known to occur.

Alluvial placer deposits form in rivers and streams and represent the initial concentration of heavy minerals relative to source rocks within a drainage network. Heavy mineral deposition and concentration occurs where gradients flatten and (or) transport velocities decrease, such as at the inside of meanders, below rapids and falls, beneath boulders, and in vegetation mats (Yeend, 1986). Placer gold deposits are typically found in alluvial gravel and conglomerate. Gold grains and, more rarely, nuggets are most concentrated at the base of gravel deposits where natural traps such as riffles, fractures, bedding planes, or other features are oriented transverse to the water flow. Additional concentration can take place as sediment moves downstream and as older alluvial deposits are reworked by younger systems. The latter takes place in geomorphically stable areas where erosion has proceeded for a long time and multiple generations of sediment and (or) sedimentary rock are recycled into potentially multiple stages of terrace and streambed gravels (Yeend, 1986).

Coastal placer and paleoplacer deposits, or beach placers, form in a range of coastal sedimentary environments that are typically dominated by eolian, wave, and tidal processes (Hamilton, 1995). Heavy minerals in the coastal environment are derived from sources that could include deeply weathered local bedrock exposures, sediment deposited at river mouths, or offshore sand deposits scoured from the seafloor during storm events. Along wave-dominated coastlines, heavy mineral enrichment occurs in the foreshore and uppermost part of the shoreface environment where sediment is repeatedly reworked by wind, waves, and wave-induced currents. Strong onshore winds winnow shoreface deposits at low tide and ultimately transport sediment inland from the beach environment (Roy, 1999). Longshore-transport currents, or littoral drift, moves sand along the coast in the direction of prevailing winds, and headlands along drift-aligned coasts trap heavy minerals on the up-drift side of embayments. Most large coastal placer

deposits formed along passive tectonic margins with long histories of erosion and repeated cycles of sea level change (Force, 1991). Coastal placer deposits formed along convergent and transform tectonic margins are found worldwide but are generally much smaller in size and are dominated by sediment derived from relatively local sources.

PGE (-Co-Cr-Ni-Ti-V) Deposits Associated with Mafic and Ultramafic Igneous Rocks

The six platinum-group elements (PGE) are ruthenium (Ru), rhodium (Rh), palladium (Pd), osmium (Os), iridium (Ir), and platinum (Pt). These elements all share similar physical and chemical properties and, therefore, tend to occur together in mineral deposits (Harris and Cabri, 1991). The PGE are split into the iridium group (Os, Ir, Ru) and the palladium group (Rh, Pt, Pd) because these two subgroups tend to behave coherently during magmatic processes (Rollinson, 1993). PGE are found in many geologic settings and are hosted by igneous and sedimentary rocks; PGE ore deposits form from a variety of physical and chemical processes. In deposits associated with mafic-ultramafic (MUM) rocks, PGE are variably to strongly associated with Ni, Cu, Cr, Co, Ti, and V. Thus, for this study, only PGE ore-deposit models genetically associated with MUM rocks were considered because of the strong association with these critical elements.

Characteristics of MUM-rock-related deposit models are summarized by Naldrett (2004), and the specific deposit types that factored into this assessment are listed in table 1. Mafic and ultramafic magmas originate in the upper mantle and contain small amounts of copper, nickel, and PGE and variable but minor amounts of sulfur (Eckstrand and Hulbert, 2007). As the magma ascends through the crust and cools and the sulfur content of the magma is sufficient, sulfide liquid forms as droplets. These droplets can take in nickel, copper, and PGE, and they tend to sink toward the base of the magma body to form sulfide concentrations and, ultimately, ore deposits that contain the PGE and associated metals.

Carbonate-Hosted Cu (-Co-Ag-Ge-Ga) Deposits

Carbonate-hosted Cu deposits in Alaska consist of Kennecott and Kipushi types, and they contain four critical elements: Ag, Co, Ge, and Ga. Kennecott-type carbonate-hosted Cu deposits are named for the town of Kennecott, Alaska, where deposits were mined out by about 1938 (Price and others, 2014). The district is in southeastern mainland Alaska (fig. 1), now in the Wrangell-St. Elias National Park and Preserve. The deposits at Kennecott were northeast-striking, very high-grade (13 percent Cu) veins filling either normal or reverse faults that cut the Triassic Chitistone Limestone. They had considerable wall-rock replacement by copper sulfides and broad dolomitized alteration envelopes. The deposit bases were along probable bedding plane faults about 25 m above the contact between the Chitistone and the underlying Nikolai Greenstone. Silver (65 grams per metric ton, g/t) was recovered as well as Cu (MacKevett and others, 1997; Price and others, 2014).

The Ruby Creek deposit in the southwestern Brooks Range (fig. 1) is an Alaskan example of the Kipushi type, which is named for the Kipushi deposit, Democratic Republic of Congo (DRC). These are massive base-metal-sulfide replacement bodies or breccia fillings in carbonates, now dolomitized, that are either peneconcordant or cut the beds as high-angle breccia bodies, or both. All deposits classified as Kipushi type by Cox and Singer (1986) have Ge-bearing minerals. This appears to be a distinguishing characteristic for their classification, as there are other types of Cu-Pb-Zn-sulfide ores in carbonate rocks that also feature mineralized breccias and dolomitic alteration but that lack Ge minerals, such as the carbonate-hosted sulfide

deposits of Central Colorado (Beaty and others, 1990). The Ruby Creek deposit is hosted by the Middle Silurian to Early Devonian Cosmos Hills Sequence (Till and others, 2008). Copper-Co-Ge mineralization occurs as sulfide minerals that fill former open space in breccias or replace breccia matrix and wall-rock carbonates within a very large halo of hydrothermal dolomite containing minor sphalerite (Runnells, 1969; Bernstein and Cox, 1986; Hitzman, 1986). Copper sulfide minerals are mainly chalcopyrite, bornite, and chalcocite. Cobalt sulfides are mainly carrollite and cobaltiferous pyrite. Germanium sulfides are mainly renierite and germanite. Grades of the trace metals Co, Ge, and Ga in the Ruby Creek deposit have not been published. Elsewhere, Kipushi-type ores contain approximately 1,000 parts per million (ppm) Ge, but calculations from production figures from Kipushi, DRC, itself, suggest that recovery of Ge there ranged from 23 to 600 ppm and varied dramatically in time (Höll and others, 2007).

Sandstone U (-V-Cu) Deposits

Sandstone uranium deposits (ssU) are epigenetic deposits and have a worldwide distribution. They form in sandstone host rocks that range in age from Carboniferous to Tertiary. Sandstone uranium deposits are commonly divided into four types—basal, tabular, roll front, and tectonolithologic (table 1; Cuney and Kyser, 2009). Regardless of type, all ssU deposits are thought to form by redox-controlled processes that can be generalized as (1) oxidative mobilization of the uranium from the source rock, commonly granite or tuff, (2) transport of soluble uranyl (U^{6+}) complexes through an oxidized nonmarine-sandstone aquifer, and (3) reduction and precipitation as U^{4+} minerals by encounter with reduced host rocks that are laterally continuous with or lying below the aquifer in which uranium is transported (Guilbert and Park, 1986; Cuney and Kyser, 2009). Reducing conditions in the host rock typically result from entrained carbonized plant matter. In this analysis, all types of ssU deposits were initially targeted, but basal-type deposits are the most likely to occur in Alaska and the CYPA. Other U-enriched deposits that occur within similar host rocks are sediment-hosted V and sediment-hosted Cu deposits (Turner-Peterson and Hodges, 1986).

The best described ssU deposit in Alaska is the Death Valley deposit, located near the east end of the Seward Peninsula (fig. 1). It was discovered in 1977 by an airborne radiometric survey and has an average grade of 0.27 percent U_3O_8 in beds averaging 3 m thick and calculated reserves of about 1,000,000 pounds (~453.59 t) U_3O_8 (Dickinson and others, 1987). The host rocks are early-Eocene carbonaceous arkosic sandstones of fluvial or colluvial origin deposited in a graben formed on granitic bedrock (Dickinson and others, 1987). An underlying Late Cretaceous granitic pluton forms the western side of the graben. Basalt, coal and lacustrine laminated sideritic mudstone and turbidites are interbedded with the sandstone. An early-Eocene basalt flow dammed the ancestral river valley, forming the lake in which the lacustrine sediments were deposited (Dickinson and others, 1987).

Primary epigenetic mineralization took place in the early Eocene, and supergene enrichment occurred in the Holocene. The high-standing adjacent pluton is considered the likely source for the uranium. Primary mineralization is thought to have developed when uranium was dissolved by oxidizing surface water, carried east from the pluton, recharged into the alluvial aquifer, and then deposited in the reducing environment of the carbonaceous Tertiary sedimentary rocks (Dickinson and others, 1987). The mineralized rocks are fairly widespread in the subsurface, occurring both above and below the Eocene basalt and lacustrine rocks, and extending to a depth of about 91 m. Uranium minerals in the primary ore are coffinite ($U(SiO_4)\cdot nH_2O$) in the reduced zones and autunite ($Ca(UO_2)_2(PO_4)_2\cdot 10\text{-}12H_2O$) where the

primary ore has been oxidized. The secondary supergene enrichment is related to the present surface exposure and is possibly ongoing since the involvement of recent surficial mudflows and soil formation processes indicate a recent age (Dickinson and others, 1987). Uranium minerals in the secondary enrichment include meta-autunite ($Ca(UO_2)_2(PO_4)_2 \cdot 6H_2O$). The uranium-rich rocks of the Death Valley deposit are strongly carbonaceous and have anomalously low manganese (Mn) concentrations. The features of Death Valley are most consistent with those of a basal-type ssU deposit (Dickinson and others, 1987), and the low Mn concentration of the U-bearing rock is inconsistent with roll-front type deposits (Harshman, 1972).

Sn-W-Mo (-Ta-In-Fluorspar) Deposits Associated with Specialized Granites

Fluorspar (industry term for fluorite, cubic CaF_2) and ore minerals containing Sn, W, Mo, Ta, In, and do not always occur as a group, but they are commonly found in various combinations closely associated with highly evolved felsic intrusive rocks that are grouped herein as specialized granites (for example, Reed, 1986). Specialized granites include granite porphyries, peraluminous granites, and high-silica (>73 percent SiO_2; Rogers and Greenberg, 1990; Blatt and others, 2006) granites. Such granites tend to be found in tectonic environments that involve thickening, contraction, or extension of continental crust. With some exceptions, the common petrogenetic characteristics of specialized granites and their associated dikes and sills are that they (1) are late-stage magmatic phases containing enriched concentrations of incompatible elements as a result of fractional crystallization and (2) have sources that include continental crust. Mineral deposits associated with specialized granites mainly occur in dikes, veins, stockworks, and greisens or hydrothermally altered zones near the top of granite intrusions and in carbonate wall rocks as skarns. In systems associated with specialized granites, Sn ore minerals are mainly cassiterite and less commonly stannite; W is mainly found in scheelite and wolframite, and Mo is mainly found in molybdenite. Tantalum occurs mainly in tantalite ($MgTa_2O_6$) and less commonly in wodginite ($Mn^{2+}Sn^{4+}Ta_2O_8$) or microlite ($(Na,Ca)_2Ta_2O_6(O,OH,F)$). Indium typically occurs as a substitution in sphalerite, cassiterite, and (or) stannite and is found rarely as roquesite ($CuInS_2$).

Specialized granites include a wide variety of compositions because many factors can influence production and crystallization of silicic magma. The formation of specialized granites may include late phases associated with large magma systems or localized anatectic melts, and a common characteristic of these diverse granites is their relatively small volume. Most economic concentrations of Sn, W, Mo, Ta, and In, with or without fluorspar, are associated with peraluminous granites. Veins, dikes, and pegmatites that contain enriched concentrations of Sn, Ta, W, Mo, Cs, and Li are classified as lithium-cesium-tantalum (LCT) pegmatites (Černý and others, 2005), which commonly occur within and peripheral to the cupolas of peraluminous and highly evolved granites (Černý, 1991; Černý and others, 2005; Johan and others, 2012). Indium is a common impurity in Zn-, Sn-, and Cu-sulfides and in Sn oxides (cassiterite) in Sn-W veins, pegmatites, and skarns associated with evolved granitic rocks (Černý and others, 2005; Ishihara and others, 2006; Sinclair and others, 2006). Fluorine and H_2O are important agents for transport of Sn, In, Ta, and W in fluids exsolved from peraluminous granite melts (Dobson, 1982; Swanson and others, 1990; Černý and others, 2005; Johan and others, 2012). Highly fractionated LCT granites and pegmatites are also thought to be enriched in F by anatectic crustal melts (Černý, 1991), which is consistent with strontium isotopic ratios for tin-bearing granites in Alaska (Hudson and Arth, 1983; Arth and others, 1989).

Mineable deposits of tin are mainly found in skarns, greisens, simple Sn-veins and Sn-polymetallic veins (table 1). Greisens associated with evolved granites consist of quartz, white mica, and cassiterite, with or without scheelite, molybdenite, pyrite, and (or) fluorite, that form in the upper roof zones of hydrothermally altered granite (endogreisen), or as alteration of wall rocks of the intrusions (exogreisen). Additional minerals found less commonly in greisen include tourmaline, topaz, garnet, axinite, arsenopyrite, sphalerite, and chalcopyrite. A characteristic mineral that occurs in greisens in cupolas of Sn-granites is Li-rich annite ($KFe^{2+}{}_3(AlSi_3O_{10})(OH)_2$) (formerly "zinnwaldite"), where annite is the iron-rich end member of the biotite-phlogopite micas. Alaska has a well-known province of Sn-granites and associated Sn occurrences on the northwestern Seward Peninsula (fig. 1; Hudson and Arth, 1983), as well as widely scattered Sn occurrences in interior Alaska between the central Alaska Range and the central Brooks Range and to the west of the Alaska Range (fig. 1).

Concentrations of tungsten are recognized in both oxidized (magnetite-series) and reduced (ilmenite-series) granites. Porphyry-W deposits are rare (Seedorff and others, 2005), although granite porphyries with associated W are described in the Fairbanks area in Alaska (fig. 1; Newberry and others, 1990). Tungsten is typically concentrated in veins and greisens around the margins of highly evolved granites (Werner and others, 1998) and is mined mainly from skarns and veins (table 1). Although high W contents result from extended melt fractionation, W contents of granites associated with scheelite skarns are not commonly elevated relative to other igneous rocks (Newberry and Swanson, 1986; Černý and others, 2005). It is common for W skarns to contain Sn and some Mo and common for Sn skarns to contain W. Fluorspar is typically found as either a principal product with Sn and W in vein, greisen, and skarn deposits associated with highly evolved granites. Late-stage Sn-, Zn-, and Cu-sulfide veins and breccias that postdate W-Mo mineralization can contain significant concentrations of indium (Sinclair and others, 2006).

Magmatic-associated Mo deposits include a broad range of compositions for shallowly emplaced to hypabyssal intrusive rocks, but molybdenum is mined principally from two types of deposits—(1) Climax-type porphyry Mo systems, where it is the principal product (White and others, 1981; Seedorff and Einaudi, 2004), and (2) porphyry Cu (-Mo) systems, where it is a byproduct of mining large-tonnage, low-grade copper deposits (Seedorff and others, 2005). In the range of compositions between those two granite porphyry types are other deposits classified as low-fluorine porphyry Mo deposits (Theodore, 1986; Ludington and Plumlee, 2009). In Climax-type deposits, molybdenum is associated with high-K, aluminous granite and rhyolite porphyry with more than 73 weight percent SiO_2 (White and others, 1981).

Late intrusive or hydrothermal activity associated with specialized granites can remobilize Sn, W, Mo, Ta, and In. However, high volatile (especially F) contents in near-solidus melts make it difficult to distinguish magmatic versus aqueous fluid effects (Černý and others, 2005, and references therein).

Datasets

To evaluate mineral potential in the CYPA for the deposit groups described above, the following datasets were assembled and analyzed using ArcGIS. Most of the data are publicly available, and direct links to the Internet resources are included in the dataset descriptions or at the end of this report.

Geochemical Data Sources

The geochemical dataset used in this study is a compilation of three geochemical databases with a statewide distribution of geologic material samples for Alaska. The file structure and data format of each database is markedly different. They were reformatted for consistency and optimized for geochemical mapping and statistical evaluation.

The Alaska Geochemical Database, version 2.0 (AGDB2), of the USGS is the most recent compilation for new and historical geochemical analyses of rock, stream sediment (henceforth, simply, "sediment samples"), soil, and heavy-mineral concentrate samples in Alaska (Granitto and others, 2013). The AGDB2 includes analyses of 108,966 rock samples, 92,694 sediment samples, 6,869 soil samples, 7,470 mineral samples, and 48,096 heavy-mineral concentrate samples. These samples were collected between 1962 and 2009 and prepared according to various USGS standard methods (Miesch, 1976; Arbogast, 1990, 1996; Taggart, 2002). For this work, data for all sediment and heavy-mineral concentrate samples, as well as data for 48,731 igneous rock samples and 18,281 sedimentary rock samples, were used.

The National Uranium Resource Evaluation (NURE) database contains data derived from the NURE Hydrogeochemical and Stream Sediment Reconnaissance (NURE-HSSR) program that was overseen by the U.S. Atomic Energy Commission. NURE sediment samples were collected in Alaska between 1976 and 1979 and prepared according to various standard methods. For this work, data from 65,993 of these Alaska sediment samples were used.

The Alaska Division of Geological and Geophysical Surveys (ADGGS) geochemical database includes analyses of 12,437 rock samples, 10,919 sediment samples, 100 soil samples, and 1,061 heavy-mineral concentrate samples that were collected between 1960 and 2014. These data were provided by the ADGGS and are also available for download from their Web site (http://www.dggs.alaska.gov/webgeochem). For this work, the data for all the ADGGS sediment and heavy-mineral concentrate samples, as well as the data from 5,653 igneous rock samples, were used.

Many samples in the AGDB2 and ADGGS databases were analyzed by more than one analytical method, and therefore, some samples have more than one determination for a given element. Some elements have as many as four determinations for a given sample analyzed by different techniques; Ag, As, Au, Bi, Cd, Cu, Mo, Pb, Sb, and Zn have the greatest number of multiple determinations. To minimize the complexity of multiple determinations for individual elements, a single best value was used for each element for each sample. Granitto and others (2013) provide a detailed description of the ranking criteria accompanying analytical methods and how they were used to determine best values.

Many of the samples in the geochemical datasets have also been reanalyzed. For these samples, the original and the reanalyzed data might coexist because the samples were issued a second laboratory identification number on submission for reanalysis, effectively creating a second data record in the datasets. In this work, for each element for which there was more than one analysis at a specific location, the larger value of the two analyses was selected for use in calculation of statistics, to display on point plots, and to use for gridded map layers.

Stream-Sediment Geochemistry

Geochemical data of sediment samples represents one of the most comprehensive, evenly spaced, and highest-density datasets for examining mineral resource potential across Alaska. Bedrock is obscured in many areas by unconsolidated sediment and vegetation. Sediment data

show patterns of element concentration that reflect rock types in their respective drainage basins and, thus, provide clues about the composition of rocks in areas of poor exposure or that lack geologic mapping. This dataset is herein referred to as sediment geochemistry because, although some samples were collected from a variety of surface water bodies, more than 80 percent of the sediment samples in the AGDB2 were collected from streams.

For this analysis, sediment geochemical data from the AGDB2, NURE, and ADGGS datasets were combined into a single dataset for which the median, 75th, 91st, and 98th percentiles were calculated. These percentile cutoff values were used in the mineral potential scoring methods described below. Appendix A shows summary statistics for each element, which database(s) contained data for each element, and the statistical method by which percentile values were determined (see below). The combined dataset produces the greatest statewide coverage of geochemical data, but analytical methods differed among samples. Furthermore, the combined datasets contain multiple detection limits for a single element, thus resulting in multiple data censoring limits. Censored data are those that fall outside the detection limit for a specific element analyzed by a particular method. Some elements have highly censored data. For these elements, summary statistics were strongly skewed if censored data were omitted or if substitute values were introduced for the censored values. For example, if the geochemical data for an element are 90 percent censored, then substitution of a value such as one-half of the lowest determination limit for the censored data will yield artificially low mean, median, and percentile values. Similarly, if the data are 90-percent censored, then omission of the censored data will leave only anomalously enriched data, and statistics calculated on that portion of the data will yield artificially high mean, median, and percentile values. Therefore, two methods were used to calculate statistical values for each element depending on the amount of censored data—substitution method and Kaplan-Meier method.

Both methods were initially applied to data for several elements that have different degree of censoring. For low degree of censoring, results were nearly identical when summary statistics were calculated by both methods. Critical assessment of these comparisons indicated that for data with less than about 40-percent censoring, the differences for the median and upper percentiles were negligible to insignificant. As a result, for elements with 40 percent or less censored data, substitution was used, and all censored values were replaced with a value of half the minimum noncensored value, or half of the minimum lower limit of detection, whichever was the lesser of the two. The digits “1, 1” were added at the end of the substitutes to make those replaced values identifiable in the database. Summary statistics were then calculated by standard procedures on the combination of the analyzed and substituted values. For elements with more than 40 percent censored data, the Kaplan-Meier method was used for estimating summary statistics. This method is a nonparametric statistical approach to calculating cumulative probability distributions from which summary statistics for censored data are calculated (Helsel, 2012). The procedure used here is detailed in Helsel (2012) and was run using Minitab. Appendix A shows the level of censoring for each element and for which elements the Kaplan-Meier method was used.

Igneous-Rock Geochemistry

Igneous rock geochemical indices were calculated for nearly 49,000 igneous rock samples statewide for use in identifying permissive rock types for REE deposits and Sn-W-Mo deposits. The REE deposits considered herein are associated with igneous rocks with peralkaline, alkaline, or carbonatitic composition; Sn-W-Mo deposits of greatest interest in this study are

associated with high-silica, peraluminous intrusive igneous rocks. These distinctive igneous rock compositions are relatively easy to identify using geochemical data from individual rock samples or suites of rock samples. The distribution of igneous rock samples across the State provides more detail than geological maps can portray, especially considering the compositional complexity of many igneous systems and general lack of detailed geologic mapping statewide. Thus, the geochemical characteristics of individual rock samples provides a means of identifying favorable rock types within broader belts of igneous rock outcrop, in areas where igneous rocks were exposed at a scale not represented on available geologic maps, or in cases where geochemical trends of interest were not obvious or apparent in outcrop.

Major and trace element geochemical data for igneous rock samples were compiled from four primary sources—the AGDB2, the ADGGS database, peer-reviewed literature (see appendix B for a list of literature sources), and unpublished USGS data. For all geochemical ratios discussed below, available data were screened to include only high-resolution analyses, as follows. For an igneous rock analysis to be used, where two or more elements for an igneous rock sample contribute to a ratio or geochemical index (see below) both data components of the ratio had to be of similarly high precision. In general, only major-element data were used for samples where all major rock forming element oxides were measured such as by x-ray fluorescence (XRF) methods. For trace elements such as Y and Nb, only XRF and inductively coupled plasma mass spectrometry (ICP-MS) analyses were used, avoiding methods for which there is an increased risk of insoluble residues of accessory phases that may contain these elements. In addition, all major-element-oxide concentrations used in calculating geochemical indices were normalized to an anhydrous basis.

Use of single-element geochemical data can, in a broad sense, help identify geochemical anomalies. However, all commonly used igneous classification schemes using geochemical data require two or more elements or element oxides. Well-developed geochemical criteria exist for the classification of the igneous rocks, including the discrimination of alkaline and silica-undersaturated rock types using major and trace elements (for example, Irvine and Baragar, 1971; Frost and others, 2001; Frost and Frost, 2008; Frost and Frost, 2011). Similar conventions were followed in classifying the igneous rocks by using major element ratios to calculate the aluminum saturation index, or ASI (modal Al/[(Ca-1.67×P)+Na+K]) (Shand, 1947), and modal Al/[Na+K] (ANK). These parameters allow the differentiation between peraluminous (ASI>1), metaluminous (ANK>1), and peralkaline (ANK>1) rock types.

In some cases, trace element concentration ratios (for example, Nb/Y>1; 10,000×Ga/Al>2.6) can distinguish alkaline and subalkaline igneous rock types (Winchester and Floyd, 1977; Pearce and others, 1984; Whalen and others, 1987; Pearce, 1996). However, many useful geochemical discrimination diagrams are X-Y plots that have subfields defined by one or more established boundaries. For example, distinctions between the various rock types using major elements (that is, alkaline versus calcic; ferroan versus magnesian) can be made using plots of SiO_2 versus the modified alkali-lime index (MALI, which is Na_2O+K_2O-CaO), and the Fe# (FeO/[FeO + MgO]) which were proposed by Frost and others (2001).

Igneous classifications based on elemental comparisons relative to a boundary or array in geochemical X-Y space is traditionally done by eye and, thus, is inefficient for large data sets containing thousands of samples, such as those for the State of Alaska (for example, ADGGS and AGDB2; Granitto and others, 2013). Instead, a method was devised to quantify a sample's displacement from established boundaries in geochemical x-y space. Specifically, for each igneous rock sample, the displacement was calculated in the y-axis direction above or below the

accepted boundaries. For example, relative to the MALI array (the alkali-calcic/calcic-alkalic boundary in Frost and others, 2001), the displacement equation for a sample is:

$$MALI_{displacement} = MALI_{calculated} - MALI_{expected},$$

where $MALI_{expected}$ is the MALI predicted by the boundary equation for the SiO_2 content in a given sample. In this way, the $MALI_{displacement}$ and $Fe\#_{displacement}$ index values were calculated for each sample for which the appropriate data are available. For the Fe# versus SiO_2 plot, the boundary proposed by Frost and Frost (2008) was used because all data could be converted to total iron (FeO_{total}), but not all samples were analyzed for FeO and Fe_2O_3 (compare to Fe-Index in Frost and others, 2001). In general, both Fe# and MALI displacements are more positive for samples representing more ferroan and alkalic compositions and more negative for magnesian and subalkaline compositions, respectively.

These displacement-type ($MALI_{displacement}$, and $Fe\#_{displacement}$) and simpler cutoff-type (that is, Nb/Y, Ga/Al) geochemical discriminant indices allow rapid recognition of geochemical spatial trends and anomalies potentially associated with mineral deposits considered herein. Different combinations of multiple indices provide robust petrologic constraints on the composition, sources, and probability of mineral potential of igneous rocks in the CYPA. Greater detail on the use of these indices is given within each relevant section below.

Heavy Mineral Concentrate Mineralogy and Geochemistry

Mineralogical data based on visual identifications are available for more than 18,000 nonmagnetic bulk-panned concentrate or heavy-mineral concentrate (HMC) samples in the AGDB2 (Granitto and others, 2013). The HMC samples were derived from sediments, soils, or rocks, and the data were derived from data entry sheets, USGS Open-File Reports, and archival digital spreadsheets. The entries include several different ways to quantify heavy minerals such as gold, cassiterite, monazite, and scheelite (Granitto and others, 2011; Granitto and others, 2013). Some samples have grain count data, and other samples are described by a variety of qualitative values (for example, “present” or “abundant” or “trace”), estimated percentages, or percentage ranges. Null values indicate that the mineral was not observed in the sample. The mineralogy data in the AGDB2 are presented as they were originally recorded and interpreted, and the data sources are listed in Granitto and others (2011). The AGDB2 also contains best-value geochemical data for more than 48,000 HMC samples across the State of Alaska. The specific methods for incorporating HMC mineralogy and (or) geochemistry into our assessment of mineral resource potential are described in more detail in the relevant sections below.

Alaska Resource Data File

The Alaska Resource Data File (ARDF; http://ardf.wr.usgs.gov/) contains more than 7,000 reports of mines, prospects, and mineral occurrences in Alaska. The ARDF records are published for individual USGS 1:250,000-scale quadrangles. USGS Open-File Reports containing records for each quadrangle are available for download separately or as part of a single composite ARDF database from the Web address shown above. The ARDF records represent a broad spectrum of mineral deposit types. For this study, methods were developed to search for records that were most likely to represent each of the six deposit models described below. For each deposit group, a list of searchable keywords was developed for key ARDF record fields. The keywords were weighted for their relevance to the mineral deposit of interest and were also assigned to a “definite” or “maybe” column depending on the strength of their

association with, or relevance to, the model of interest (appendix C). In some cases, keywords were assigned negative scores if they were indicative of a geological system known to be not associated with the mineral deposit of interest. Complete lists of keywords and associated weights are shown in appendix C for each deposit group.

Using a custom Python script in ArcGIS, all ARDF records were searched and assigned a total score for each deposit group on the basis of the total keyword hits and sum of the associated scores. High-scoring ARDF records for each deposit group were initially reviewed against areas of known mineral potential and (or) mining activity to ensure that known occurrences were identified by the keyword search method. If ARDF scoring results did not adequately reflect deposits of known type, then scoring parameters were modified to better calibrate the method. In some cases, scrutiny of individual ARDF records revealed problems such as misspellings and imprecise location information. All records that were discovered to contain errors were corrected in the original database before the final analyses described below. However, individual users are cautioned that ARDF records might contain other errors that were not recognized but that ideally would be outweighed or counteracted by other datasets used herein. The specific deposit-group sections below provide more information on how the ARDF scores were used to help assess mineral potential.

Geologic Map Data for the State of Alaska

An anticipated geologic map of Alaska (Wilson, Frederic H., and others, USGS, written commun.) portrays the distribution of different rock types across the State. For most mineral deposit groups, the catalog of lithology descriptions for the geologic-map database was used to search for and identify rock types that were most prospective and (or) best suited for hosting the deposit group. The lithology query results were used to develop derivative, generalized lithology map layers to show the distribution of favorable rock types for each deposit group across the State. The specific lithologies queried for each deposit group are described in detail below and are summarized in appendix D.

Aerial Gamma-Ray Surveys

Aerial gamma-ray surveys for the State of Alaska were calibrated and compiled by Duval (2001) and Saltus and others (1999), and they reflect the radioactive signatures of bedrock and surficial materials. These surveys, flown as part of the National Uranium Resource Evaluation (NURE) Program (conducted by the U.S. Department of Energy from 1976 to 1984), cover most of Alaska except for parts of the Brooks Range. These surveys measured the flux of gamma rays emitted as a result of the radioactive decay of the naturally occurring radioactive elements ^{40}K, ^{238}U, and ^{232}Th and were used to identify areas with potential for REE, Sn-W-Mo, and uranium deposits, as described below.

National Hydrography Dataset and Watershed Boundary Dataset

The USGS National Hydrography Dataset and Watershed Boundary Dataset (NHD and WBD; http://nhd.usgs.gov/) delineate surface water networks and drainage basins throughout the United States using standardized criteria based on topography and hydrology. Relative drainage basin size, geographic location, and nested hierarchy are encoded within a string of digits known as a hydrologic unit code (HUC). A classical hydrologic unit is a division of a watershed with but a single discharging stream, so it corresponds with a physical watershed on the ground

defined by topography. The great majority of the 12-digit HUCs comprising the CYPA are classical HUCs. The WBD currently reviews and certifies HUCs that range in length from two digits, for the largest drainage systems known as regions, to as many as 12 digits, for systems known as subwatersheds. For this study, 12-digit HUC boundaries were used as a geographic reference frame for evaluating mineral resource potential across the CYPA. Scores assigned for favorability for each deposit group were summed on a HUC by HUC basis. Numeric codes, names, and boundaries that are associated with each HUC provide unique identifiers that can be used in a GIS to geographically associate other digital data from multiple sources. In this report, we commonly use the term "HUC" to refer to a physical drainage subbasin and not solely the string of digits used to identify the subbasin. Rivers and streams from the NHD were used primarily for the placer model to map drainage networks downstream from areas with high placer potential (see below).

GIS-Based Methodology and Results by Deposit Group

General Methodology

The goal of this project was to identify and rate areas of mineral resource potential across the CYPA for the selected deposit groups described above. The six deposit groups were prioritized for reasons described above, and it is acknowledged that there are likely many other important deposit groups that exist or for which there is potential across the CYPA. Subwatersheds defined by 12-digit HUCs were chosen as the primary spatial feature for evaluating and mapping mineral potential (fig. 2). The use of HUCs as analysis cells provided a few key advantages over other types of surveyed units (for example, Public Land Survey System, or latitude-longitude quadrangle). First, each HUC in the CYPA has unique, numeric identifiers and names that can be used in a GIS to geographically associate other digital data from multiple sources. This feature could be useful to the BLM in addressing multiple issues involving land-use decisions. Second, the HUC dataset is standardized, available for, and continuous across most of the State and surrounding region. The 2,460 12-digit HUCs in the CYPA (fig. 2) have an average area of approximately 100 square kilometers (km^2), or 27,500 acres. This average unit size is generally larger than any single mineral deposit or some mining districts; however, with 2,460 HUCs within the CYPA, this unit size provides sufficient detail for comparison and contrast. The HUCs represent a balance between an appropriate level of detail for displaying data patterns at large scales and optimizing computing efficiency when employing data from large relational databases. However, perhaps most importantly, subwatershed boundaries (most commonly, drainage divides) are typically well marked on the ground; they are actual physiographic features with a direct link to processes (for example, erosion and weathering) and features (for example, streams and rivers) that expose, transport, and potentially enrich the sought-after ore minerals. Using subwatersheds as an analysis unit also provides a direct link to sampling that was focused along streams and other surface water bodies.

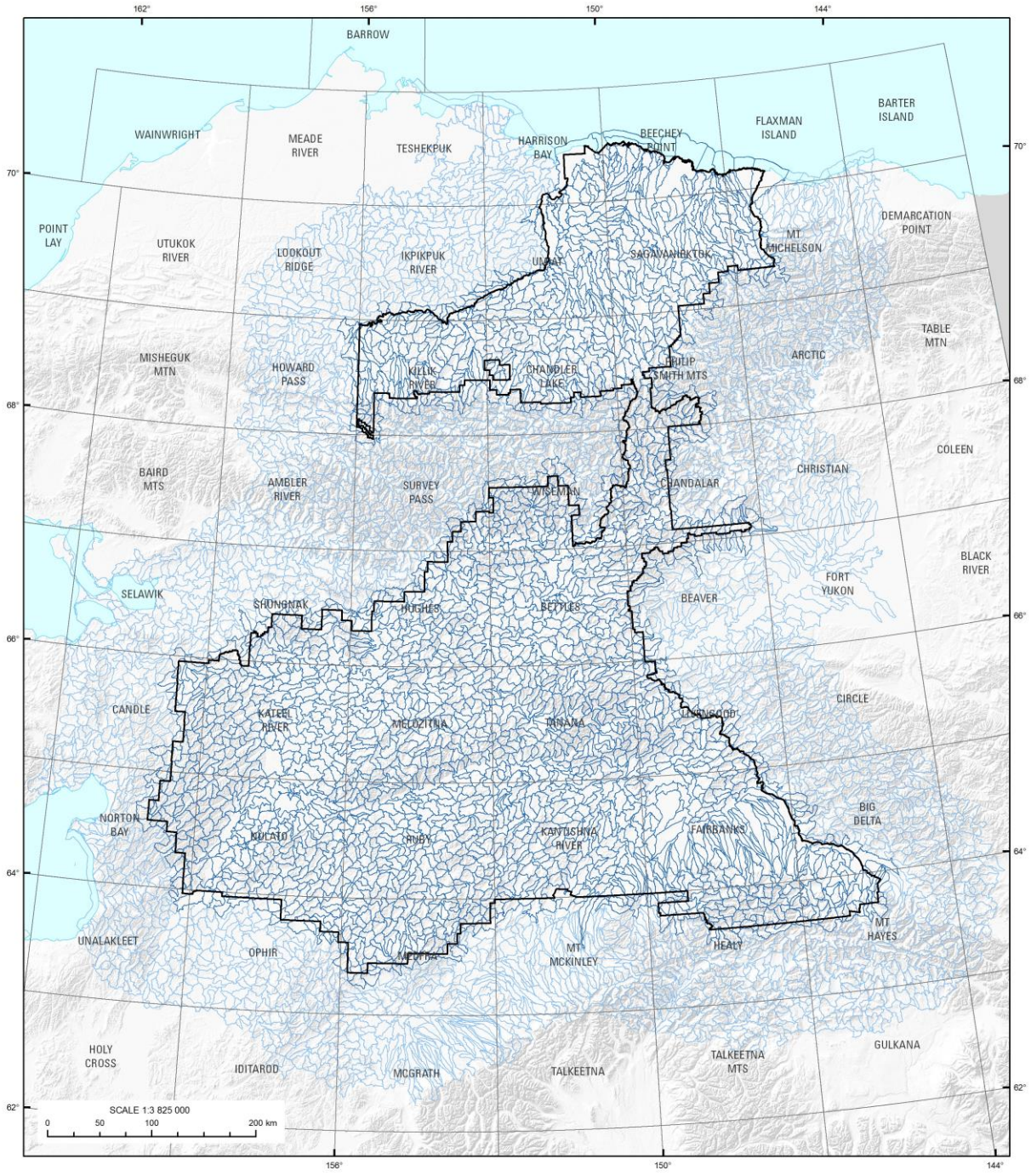

Figure 2. Map showing the boundaries (blue) for 12-digit hydrologic unit codes (HUCs) within and surrounding the Bureau of Land Management Central Yukon Planning Area (outlined in black).

The analysis area included HUCs within a 100-kilometer (km) buffer outward from the CYPA boundary (fig. 2), providing a more continuous view of geologic-scale trends in mineral prospectivity over the CYPA and its surroundings (fig. 2). Using a customized Python script in ArcGIS, each HUC was assigned a mineral prospectivity score using the criteria and treatments described for each deposit group below. Total scores were used to guide the classification for

each HUC as having high, medium, low, or unknown potential for each deposit group. The relative certainty of the estimated potential for each HUC was also assigned high, medium, low, or unknown values by procedures described for each deposit group below. Scoring templates and potential versus certainty classification templates (tables 2–15) accompany the following sections and are unique to each mineral deposit group. Plates 1 through 12 show maps with results for each deposit group and annotated maps highlighting specific deposits and (or) selected areas with high to medium potential for each deposit group. The accompanying tables in appendix E present results by deposit group and include the scores for each HUC by individual component, the percent contribution of each scoring element to the total score, and resulting classification. Results for all HUCs within the analysis area (5,365 HUCs total) are shown in plates 1 through 12 and in appendix E. However, because this effort was ultimately focused on mineral potential in the CYPA proper, only the results for the 2,460 HUCs intersecting or within the CYPA are described and discussed in the following sections.

REE-Th-Y-Nb (-U-Zr) Deposits Associated with Peralkaline to Carbonatitic Intrusive Rocks

REE-Th-Y-Nb (-U-Zr) deposits are most commonly associated with alkaline igneous rocks, in particular peralkaline, syenitic, and carbonatitic intrusive rocks, and their weathering products (Wall, 2013; Verplanck and others, 2014). Mineralization in alkaline intrusive rocks can occur as primary minerals within the main intrusive phase, in late-stage orthomagmatic fluids, or as secondary minerals in late-stage hydrothermal deposits (Verplanck and others, 2014). Late-stage orthomagmatic fluids form deposits in cupolas, pegmatites, veins, and dikes, which are included in the alkaline intrusive deposit model because of the association of these features with the alkaline igneous complexes. REE-Th-Y-Nb (-U-Zr) mineralization in hydrothermal deposits and alteration zones associated with alkaline igneous complexes (Wall, 2013) are also included in this deposit model because of their direct association with the alkaline igneous complexes. There are other deposit types that contain REE- and HFSE-bearing minerals but in relatively minor amounts. REE-bearing minerals can also occur in placer deposits and, thus, might indicate a bedrock source in the drainage basin. However, for this study, these types of deposits were not evaluated as independent prospective REE resources. For the purposes of this study, the most permissive and prospective rock types for REE-Th-Y-Nb (-U-Zr) deposits were restricted to carbonatites, alkaline and peralkaline igneous rocks, and felsic igneous rocks enriched in U and Th.

Alkaline igneous rocks are enriched in Na_2O, K_2O, and CaO relative to SiO_2 and Al_2O_3, in excess of amounts needed to form feldspars. Peralkaline igneous rocks have (Na + K)/Al greater than 1, and aluminum saturation index (ASI) [Al/(Ca-1.67P+Na+K)] values less than 1 (Frost and others, 2001). For the purposes of this study, alkaline rocks include peralkaline and alkali granites and their volcanic equivalents (for example, rocks with alkali contents within or above the saturation field on the total alkali versus silica diagram of Le Bas and others [1986]). Alkaline igneous rocks are common in Alaska and the CYPA. Carbonatites, which are classified with alkaline rocks, contain more than 50 modal percent primary carbonate minerals and less than 20 percent silica (Le Maitre, 2002). They may also contain albite and (or) potassium feldspar. Carbonatites are rare, with few known occurrences in Alaska, but there are small occurrences in the CYPA.

Carbonatites and alkaline granites include a range of compositions, and the petrogenesis of these rocks is debated. They can evolve through a variety of processes, but all igneous rocks of this type require a mantle source that has been enriched in lithophile elements, H_2O, and CO_2

(Bailey, 1987, 1989). A similar mantle source for alkaline rocks in general is also supported by the common spatial association of carbonatitic and peralkaline complexes in addition to their association with REE concentrations (Verplanck and others, 2014). Magma sources that are enriched in REE and HFSE include primary magma derived from enriched mantle and magma derived from partial melting of continental mantle and continental crust (Arth and others, 1989). Magmas derived from enriched mantle tend to be found in tectonic environments that involve thickening, contraction, or extension of continental crust. Processes such as protracted fractional crystallization of enriched mantle magmas can result in concentrations of rare earth metals and other incompatible elements, including Y, Nb, Zr, U, and Th, have been inferred by multiple workers for mineralization at Bokan Mountain in southeast Alaska (fig. 1; Thompson, 1988; Philpotts and others, 1998; Dostal and others, 2013). Neodymium isotopic data from peralkaline granite at Bokan Mountain are consistent with these incompatible elements being derived from a parental mantle magma (Philpotts and others, 1998).

Fractional crystallization of alkaline magmas results in the formation of late-stage phases rich in Na, K, SiO_2, HFSE, U, Th, and REE. These elements are commonly incorporated in monazite, allanite, brannerite, and zircon; trace amounts are present in apatite, fluorite, hematite, feldspars, and micas. It is thought that fluorine, which is also concentrated in highly fractionated magmas, is crucial for the transport of REE and Th in late-stage melts and aqueous fluids because it reduces minimum melt temperatures and viscosity and increases solubility of trace mineral phases, extending fractionation of REE and HFSE to lower temperatures (Whalen and others, 1987; Černý and others, 2005). As a result, REE and Th concentrations are further enhanced. In alkaline magmatic systems, because incompatible elements become concentrated in late-stage melts and aqueous fluids, REE- and HFSE-bearing minerals are often deposited in cupolas, greisens, alteration zones, pegmatites, veins, and dikes near the top of the intrusive complex. These minerals can also crystallize in hydrothermal alteration zones associated with pluton emplacement.

Rare earth and HFSE are concentrated in late-stage magmatic phases because they are incompatible elements. The REE consist of 15 elements in the lanthanide series (La to Lu). They typically have small ionic radii and a 3+ valence (with notable exceptions of Ce and Eu, which can also be 4+ and 2+ depending on f_{O2}). The atomic radii of REE increase systematically from light (LREE) to heavy (HREE), so LREE tend to be more incompatible than HREE (for example, Blundy and Wood, 2003). REE do not easily substitute into crystal lattices of the common rock-forming minerals, and, thus, they behave as incompatible elements in most igneous systems. As a result of their incompatibility, they are often concentrated in the last minerals to crystallize from magma or aqueous fluid.

The high field strength elements (HFSE), including Nb, Zr, Hf, Ti, and Ta, have similarly low atomic radii and high valences (4+ to 6+), so they behave similarly to REE. Lanthanide series REE have similar electron configurations to other group 3 elements that include transition metals Sc and Y, which are sometimes called rare earth metals. They have chemical and physical properties similar to the REE and for the purposes of this model are included with REE. Similarly, the actinide series elements, of which only Th and U are naturally occurring, typically have similar ionic radii and valences to Zr, Hf, and Ce and, thus, easily substitute for LREE and HFSE in accessory mineral phases. As a result, REE (that is, lanthanides plus rare earth metals), HFSE, and actinides (Th + U) tend to be concentrated together in igneous systems. For this reason, the interpretation of deposits that contain REE, Th, Y, Nb, U, and (or) Zr was focused into a single model. Because they contain the largest concentrations of REE and HFSE, alkaline intrusive-rock associations are a first-order exploration tool for REE and HFSE deposits.

Alkaline magmas are also associated with magmatic gold deposits, but pluton-related gold in Alaska is found in unfractionated plutons that do not contain REE mineralization (Newberry and Solie, 1995). REE and HFSE have also been variably associated with a range of peralkaline to peraluminous granites (Černý and others, 2005). Peraluminous granites are characterized by high alumina with respect to sodium and potassium, and may contain subordinate REE. However, increasing aluminum saturation correlates with depletion of REE, Y, Th, and U (Bea, 1996), and these rocks are more appropriately included in the specialized granite model below.

Carbonatitic and alkaline intrusions tend to be associated with cratons or areas of thickened crust affected by active deformation, including extension, transtension, and contraction, accompanied by some combination of processes such as metasomatism of mantle magma, crustal assimilation, and fractional crystallization. Carbonatitic and alkaline intrusions are commonly associated with continental rift settings (Verplanck and others, 2014, and references therein) but are not uniquely constrained to such rift settings. An example of an exception to this tectonic setting is the Bokan Mountain peralkaline granite, which was emplaced in an oceanic arc complex (Dostal and others, 2013). Alternative tectonic settings and magmatic and metasomatic processes that can produce carbonatitic and alkaline igneous suites have not been fully investigated.

There are few known REE-Th-Y-Nb (-U-Zr) deposits in Alaska at present (table 1), and there are no known deposits in the CYPA at this time. Most known REE-Th-Y-Nb (-U-Zr) prospects and occurrences in the CYPA are either placer deposits containing REE-bearing ore minerals (for example, Barker and others, 2009) or relatively localized features such as veins or greisens associated with larger igneous bodies (for example, Barker and Foley, 1986).

Mineral Resource Potential Estimation Methodology

For the REE-Th-Y-Nb (-U-Zr) analysis, HUCs were scored on the basis of the following criteria: (1) igneous rock geochemistry, (2) ARDF records, (3) stream-sediment chemistry for elements of interest (HFSE + REE + Th), and (4) aerial gamma-ray surveys. These criteria are briefly described below and summarized in table 2.

Igneous-Rock Geochemistry

Igneous rock geochemical data were used to identify permissive rock types for REE-Th-Y-Nb (-U-Zr) deposits, particularly igneous rocks with peralkaline, alkaline, or carbonatitic composition. These distinctive igneous rock compositions are relatively easy to identify using geochemical data from individual rock samples or suites of rock samples. The distribution of igneous rock samples across the CYPA provides more detail than geological maps can portray, especially considering the compositional complexity of many igneous systems and a general lack of detailed geologic mapping. The method of discriminating the presence of alkaline rocks described herein offers three advantages—(1) geochemistry provides an objective test of key compositional criteria for identification of alkaline rocks, (2) geochemical data are also spatially referenced to dikes and small satellite bodies that can be associated with REE mineralization but are not typically captured in mapped units, and (3) rock-sample data correspond to discrete locations within a HUC, which provides greater geospatial precision for rock compositions than is provided by granite map units that typically span several HUCs. For these reasons, igneous rock geochemistry was favored over using geological map units alone to better identify the specific compositions of interest across the area.

The geochemical criteria selected to identify igneous rocks that are favorable for REE-Th-Y-Nb (-U-Zr) deposits are (1) $MALI_{displacement}$ and $Fe\#_{displacement}$ (described above), (2) Ga/Al, and (3) Nb/Y. As discussed in detail above, positive values for $Fe\#_{displacement}$ and (or) $MALI_{displacement}$ are typical of rocks more likely to be associated with REE-Th-Y-Nb (-U-Zr) deposits (that is, A-type, intraplate peralkaline to alkaline rocks). However, caution must be used when deciding which rocks to include in scoring. Few, if any, exploitable REE deposits are known to be associated with mafic rocks (for example, Linnen and others, 2014). In addition, in scoring $MALI_{displacement}$ it is crucial to avoid mafic rocks, especially those that might be cumulates because, for example, olivine or biotite will increase MALI, while decreasing SiO_2; in this case, a high value of $MALI_{displacement}$ is not characteristic of the equilibrium liquid composition. Therefore, the $MALI_{displacement}$ calculation was only applied to rocks with SiO_2>56 weight percent (or >200 ppm Ni); more mafic rocks were excluded in scoring this parameter.

Similarly, use of the Ga/Al ratio to classify A-type granites (Whalen and others, 1987) has only been calibrated for granitic (intermediate to felsic) compositions. The Ga/Al ratio is a proxy monitor of fluorine contents because of the higher solubility of GaF_6 relative to AlF_6. However, for fluorine content to be an effective index of a potential REE deposits, highly incompatible element concentrations must be high enough to combine with fluorine to form accessory mineral phases in which REE and HFSE are compatible. Thus, late-stage, differentiated magmas are preferred when using the Ga/Al ratio. For this reason, scoring of Ga/Al was restricted to rocks with SiO_2>60 weight percent.

On the other hand, $Fe\#_{displacement}$ and Nb/Y are important proxies for broader patterns of differentiation and tectonic setting for a range of igneous rocks. For example, Frost and others (2001) and Frost and Frost (2008) demonstrated that plutonic and volcanic alkaline rocks with SiO_2>48 weight percent are generally ferroan (that is, $Fe\#_{displacement}$>0). A similarly broad range of compositions are appropriate for interpretation using Nb/Y ratios. The distinction of alkaline and subalkaline rock types associated with different tectonic settings using this ratio is well established (Winchester and Floyd, 1977; Pearce and others, 1984; Eby, 1990; Pearce, 1996). In both cases, even primitive mafic rock compositions were included for scoring. Although $Fe\#_{displacement}$ and Nb/Y do not directly indicate the possible occurrence of REE-enriched rocks, they can be used to identify the tectonic environments such as within-plate settings where REE-rich rocks are expected to occur. Therefore, all igneous rocks were scored for Fe# and Nb/Y indices.

Databases of element ratios from igneous geochemistry in Alaska generally have poor coverage in some areas because of limited sample collection and inconsistent igneous rock exposure. However, some HUCs contain multiple igneous rock sample analyses for reasons such as high interest, good outcrop, and (or) relative ease of access. To minimize possible effects of inconsistent sample density on HUC scoring results, only a single point was assigned for each geochemical index if one sample within the HUC had a value exceeding the cutoffs listed in table 2. Thus, the maximum possible igneous rock score contributing to the composite HUC score is 4.

Alaska Resource Data File

Records in the ARDF were scored for their relevance to REE-Th-Y-Nb (-U-Zr) potential on the basis of keywords used in various categories of the ARDF record (see appendix C). Examples of keywords for the REE-Th-Y-Nb (-U-Zr) deposit group include “carbonatites,” “alkaline rock associated,” “hydrothermal,” “radioactive,” “replacement,” and “uraniferous.”

Keywords scored for alteration include terms such as “carbonatization,” “dolomitization,” “albitization,” “metasomatism,” “potassic,” “Fe-carbonate,” and “pyroxene-fluorite.” Keywords for commodities include individual elements (La, Ce, Pr, Nd, Pm, Sm, Eu, Gd, Tb, Dy, Ho, Er, Tm, Yb, Lu, Sc, U, Th, Y, Zr, and Nb), as well as “REE” and “HFSE.” Keywords were also ranked such that REE ore or gangue minerals such as xenotime, bastnaesite, and synchysite received 3 points, whereas less economic minerals such as monazite received 2 points. Other relevant minerals such as zircon and fluorite received 1 point. The cumulative keyword hits contributed to a net ARDF keyword score, and ARDF keyword scores higher than 2 appeared to capture any occurrences in a HUC with potential for a REE-Th-Y-Nb (-U-Zr) deposit. Many ARDF localities with scores greater than 2 are placer occurrences of REE-, HFSE-, or U-Th-bearing minerals, which were considered to be important in the CYPA because bedrock is generally poorly exposed and placer occurrences suggest a bedrock source nearby. An ARDF keyword score higher than 5 corresponded to prospects and occurrences with keyword hits for multiple categories in an ARDF record and was considered to be most favorable for REE-Th-Y-Nb (-U-Zr) deposit potential. By this reasoning, HUCs containing ARDF localities with scores of 2 to 4 were assigned 1 point, and HUCs containing localities with scores of 5 or higher were assigned 2 points (table 2). Multiple ARDF localities in a HUC were not considered to significantly add to the REE deposit potential, so the maximum possible ARDF score for any given HUC was 2. This score cap was also chosen to limit the potential impact of ARDF records with long, detailed descriptions that are simply artifacts of the ARDF recording process. In some cases, more verbose records received higher keyword scores that did not necessarily indicate higher potential for a REE-Th-Y-Nb (-U-Zr) deposit.

Stream-Sediment Geochemistry

Stream-sediment sampling and geochemical analysis for the CYPA is more comprehensive, more evenly spaced, and higher in density than any other database available. Bedrock is obscured in many areas by unconsolidated sediment and vegetation, and thus, stream-sediment data can provide important clues about the composition of obscured bedrock. Stream-sediment geochemical data show patterns of element concentration that reflect rock types in their respective drainage basins and provide clues to the composition of rocks in areas of poor exposure and limited geologic mapping. In general, high values for REE and other HFSE in stream sediments in the CYPA closely follow mapped belts of igneous rocks that contain alkaline phases and also coincide with known occurrences and prospects that contain these elements. This agreement provides some measure of confidence that high geochemical values for target elements in stream sediments in areas of poor exposure have high potential for indicating the presence of permissive rock types. In addition, enriched values for multiple elements of interest reinforce the potential for as-yet-undiscovered concentrations of these elements in a given HUC.

The most comprehensive coverage for LREE in the CYPA area is best represented by the elements lanthanum (La) and cerium (Ce). The element ytterbium (Yb) has the most extensive regional coverage of the HREE in the database in the CYPA, and the distribution of Th in stream sediments is quite similar to that of the HREE in general. Thorium is an important trace element and that is commonly associated with REE (Bea, 1996). Because it is radioactive, it is also a very useful exploration tool. Niobium (Nb) also has strong affinities with REE. Geochemical data for Ce (representing LREE), Yb (representing HREE), Nb (representing HFSE), and Th in stream-sediment samples were used as proxies in scoring HUCs for REE-Th-Y-Nb (-U-Zr) potential.

The 91st and 98th percentile concentration values for each element (listed in appendix A) were used as scoring value cutoffs. If a HUC contained samples with concentrations of Ce, Yb, Nb, and (or) Th above the 98th percentile value, a score of 2 was added for each element. If a HUC contained samples with concentrations of Ce, Yb, Nb, and (or) Th between the 91st and 98th percentile values, a score of 1 was added for each element. Each of the four elements considered here could only contribute once to a HUC's score. Thus, the maximum for any HUC on the basis of stream-sediment chemistry was 8.

Aerial Gamma-Ray Survey Data

Aerial gamma-ray survey data do not cover all of Alaska, but the coverage is relatively complete in the CYPA. The aerial survey data are gridded in 5 km cells. Areas with high Th/K ratios characterize Sn, W, REE, and rare-metal deposits (Portnov, 1987), and a Th/K ratio >5 indicates Th and HFSE concentrations in igneous rock or sediment that substantially exceed background levels in Alaska (Saltus and others, 1999). Scintillometer readings are commonly used to identify outcrop sources of Th (and REE by proxy, because of the affinity between Th and REE) concentrations in minerals, veins, seams, and alteration zones, and provide ground-based data to determine sources of radioactivity in areas that stand out in airborne radiometric surveys. Thus, radiometric surveys provide a remote-sensing proxy for identifying areas possibly underlain by Th-bearing (and REE-bearing) rocks. Th/K ratios above 12 represent the highest 1 percent of rocks in the CYPA. Accordingly, HUCS with Th/K ratios above 5 were given a score of 1, and those with Th/K ratios above 12 were given a score of 2 (table 2).

Results and Discussion

The total scores for HUCs in the CYPA were classified using natural statistical breaks (Jenks method) into three categories corresponding to high, medium, and low potential for REE mineral deposits (table 3), The respective score range for each category was 16–6, 5–3, and 2–0. There are 18 HUCs with a null value (indicating lack of data) for all 4 datasets in the CYPA and the buffer zone, and these were assigned a potential of unknown. Some measure of certainty was also assigned to our estimation on the basis of how many datasets contributed to the mineral potential score (table 2). A HUC assigned high certainty received scores from all four contributing datasets. There are 211 HUCs, approximately 9 percent of the 2,460 HUCs in the CYPA, that were ranked as having high potential to contain REE-Th-Y-Nb-(U-Zr) mineralization associated with alkaline igneous rocks in the area. High certainty was assigned to 48 of the 211 high-potential HUCs on based on contributions from 4 datasets, 157 have medium certainty based on contributions from 2–3 datasets, and 6 have low certainty based on contributions from only 1 dataset (table 3; plate 1). There are 453 HUCs that have medium potential for REE-Th-Y-Nb-(U-Zr) mineralization, representing 18 percent of the HUCs. Of these, 51 have high certainty, 372 have medium certainty, and 30 have low certainty (table 3, plate 1). The remaining 1,780 HUCs have low potential for REE-Th-Y-Nb-(U-Zr) mineralization on the basis of our scoring method. Of these, 381 have high certainty, 1,325 have medium certainty, and 741 have low certainty (table 3; plate 1).

The areas that stand out as having high to medium potential for REE-Th-Y-Nb-(U-Zr) mineralization in the CYPA include the Hogatza igneous belt—especially the Zane Hills and Indian Mountain—the Ruby batholith, the Sischu-Prindle igneous belt, parts of the central Brooks Range, parts of the northern Alaska Range, and parts of the Yukon Tanana Upland.

These areas are all highlighted in plate 2. Many of these areas contain known or suspected REE-Th-Y-Nb-(U-Zr) mineral prospects and (or) occurrences. The Hogatza igneous belt contains numerous middle to Late Cretaceous alkaline intrusive and extrusive rocks that cross into the western part of the CYPA. The Hogatza belt includes syenite, nepheline syenite, lamprophyre, monzonite, and granite that variably contain disseminated fluorite, goethite, xenotime, zircon with radioactive haloes, and radioactive minerals. Many of the igneous rocks are cut by contemporaneous shear zones that contain quartz, xenotime, and radioactive minerals (Barker, 1985). In the Zane Hills, monzonite, syenite, bostonite stocks, dikes, and associated polymetallic quartz veins contain allanite, betafite, fluorite, and tourmaline (plate 2; Miller and Ferrians, 1968; Miller and others, 2002). These rocks also contain known U-Th-Nb-Y mineralization and are overlain by sedimentary rocks that also contain U-bearing minerals presumably sourced from these alkaline intrusive rocks (Miller and Ferrians, 1968). Stream-sediment geochemical samples throughout this belt have high values for LREE, HREE, Th, and U, and placer deposits in the Hogatza River area (plate 2) contain gold, uranothorite, and titanite; pan concentrates have high values for Au, REE, U, Th, and PGE (Miller and Ferrians, 1968).

The Ruby batholith, extending from the southeastern Brooks Range to the Kaiyuh Mountains (plate 2), contains a mix of HUCs with high and medium potential. The Ruby batholith contains late Early Cretaceous calc-alkaline, alkaline, and peraluminous intrusive rocks with localized HFSE and Sn mineralization. Multiple placer occurrences throughout and around the Ruby batholith exposure area contain REE- and (or) HFSE-bearing minerals such as monazite and uranothorite. Although these placer deposits could have a variety of sources including granitic rocks in the Brooks Range to the north, their proximity to exposures of the Ruby batholith raise the possibility of local sources. Individual plutons within the Ruby batholith have associated Sn-bearing veins that also have high values for HSFE including Rb, Ta, and W. The Sithylemenkat pluton has associated tin greisen deposits as thick as 3 m and as long as 400 m that contain a large assortment of minerals, including cassiterite, tourmaline, magnetite, hematite, ilmenite, garnet, wolframite, monazite, and molybdenite. The greisens also yield high values for Sn, Nb, Ta, W, Cs and variable amounts of REE, Th, and U (Barker and Foley, 1986). The Ray Mountains pluton is cut by polymetallic veins that contain hematite, Ag, Pb, Zn, Bi, La, Mo, Sn, U, and W, and adjacent gravel deposits contain monazite and xenotime inferred to be derived from the pluton. In the southwestern part of the Ruby batholith, porphyritic granite of the Melozitna pluton contains fluorite, monazite, tourmaline, pyrite, and molybdenite, and Th-, and U-bearing veins cut coarse-grained biotite quartz monzonite (Solie and others, 1993).

In a belt southeast of the Ruby batholith, alkaline intrusive rocks of Late Cretaceous to Paleocene age include the granite at Mount Prindle (plate 2) and associated tin greisens, Sn-polymetallic veins, Pb-, Zn-, Mn-, and U-bearing epithermal veins. The Late Cretaceous Roy Creek syenite contains U-Th-REE mineralization (plate 2; Burton, 1981; Armbrustmacher, 1989). In the Sischu Mountain area (plate 2), early Tertiary volcanic rocks consistently yield high values for U, Th, and REE (Miller and others, 1980). The location, age, composition, and mineralization of these rocks suggests they may be on trend and geologically related to igneous rocks in the Mount Prindle area, and this area is herein referred to as the Sischu-Prindle igneous belt (plate 2). Carbonatite sills containing aeschynite, apatite, monazite, hematite and magnetite (Warner and others, 1986; Reifenstuhl and others, 1998) also outcrop to the northwest of this area, and associated placer deposits in the Hot Springs district (plate 4; Nokleberg and others, 1987) contain gold, cassiterite, monazite, aeschynite, apatite, ilmenite, magnetite, euxenite, and xenotime. The mineralogical diversity of the placer deposits reflects the variety of sources in this zone, shown as the Tofty belt in plate 2.

One intriguing result of this study is the distribution of HUCs with medium potential and low certainty in parts of the CYPA. A number of these HUCs occur in the western Yukon-Koyukuk Basin (plate 2) and the southeastern corner of the CYPA. These areas are not associated with known or suspected REE-Th-Y-Nb-(U-Zr) mineralization, and the low certainty indicates that the assignment of medium potential is based on relatively limited data. These areas warrant further study and more detailed sampling to better quantify the mineral potential and assess the relative certainty of the mineral potential in these areas.

Placer and Paleoplacer Au

Placer deposits are concentrations of high-density minerals formed by gravity separation during sedimentary processes. Heavy minerals are separated from their primary host rocks by weathering and erosion and then transported and concentrated in surficial deposits. Placer deposits exhibit a wide range of textures, form in many different environments, and host a variety of minerals, including valuable resources for gold, titanium, tin, platinum group elements, REE, and iron (Slingerland and Smith, 1986; Garnett and Bassett, 2005; Van Gosen and others, 2014). Gold in placer deposits was initially derived from bedrock containing gold-quartz veins, disseminated gold, or other types of gold-bearing mineral deposits such as porphyry copper, Cu skarn, and polymetallic replacement deposits (Yeend, 1986). Primary gold-bearing deposits typically occur in igneous (Baker, 2002; Seedorff and others, 2005; Hart, 2007; Sinclair, 2007; Taylor, 2007) or metamorphic rocks (Berger and Henley, 1989; Groves and others, 1998; Goldfarb and others, 2005), although sedimentary deposits such as paleoplacers and modified paleoplacers (Pretorius, 1981; Minter, 2006) also occur in some places.

Alluvial placer deposits form in rivers and streams and represent the initial concentration of heavy minerals relative to source rocks within a drainage network. Heavy mineral deposition and concentration occurs where gradients flatten and (or) transport velocities decrease, such as at the inside of meanders, below rapids and falls, beneath boulders, and in vegetation mats (Yeend, 1986). Placer gold deposits are typically found in alluvial gravel and conglomerate. Gold grains and, more rarely, nuggets are most concentrated at the base of gravel deposits where natural traps such as riffles, fractures, bedding planes, or other features are oriented transverse to the water flow. Additional concentration can take place as sediment moves downstream and as older alluvial deposits are reworked by younger systems. The latter takes place in geomorphically stable areas where erosion has proceeded for a long time and multiple generations of sediment and (or) sedimentary rock are recycled into potentially multiple stages of terrace and streambed gravels (Yeend, 1986).

Coastal placer and paleoplacer deposits, or beach placers, form in a range of coastal sedimentary environments that are typically dominated by eolian, wave, and tidal processes (Hamilton, 1995; Van Gosen and others, 2014). Heavy minerals in the coastal environment are derived from sources that could include deeply weathered local bedrock exposures, sediment deposited at river mouths, or offshore sand deposits scoured from the seafloor during storm events. Along wave-dominated coastlines, heavy mineral enrichment occurs in the foreshore and uppermost part of the shoreface environment where sediment is repeatedly reworked by wind, waves, and wave-induced currents. Strong onshore winds winnow shoreface deposits at low tide and ultimately transport sediment inland from the beach environment (Roy, 1999). Longshore transport currents, or littoral drift, move sand along the coast in the direction of prevailing winds, and headlands along drift-aligned coasts trap heavy minerals on the up-drift side of embayments. Most large coastal placer deposits formed along passive tectonic margins with long histories of

erosion and repeated cycles of sea-level change (Force, 1991). Coastal placer deposits formed along convergent and transform tectonic margins are found worldwide but are generally much smaller in size and are dominated by sediment derived from relatively local sources.

The northern part of the CYPA contains approximately 200 km of coastline (fig. 1), but most of the area is inland, and therefore, alluvial placer deposits were the primary focus of this study. The CYPA contains all or part of 18 known placer gold districts; the Hot Springs district, a placer-gold and placer-tin district in the southeastern part of the Tanana quadrangle, is the only one that recovers another commodity in addition to gold (plate 4; Nokleberg and others, 1987). Although placer deposits have the potential to host a variety of economically important minerals and PGE, and although Sn and Ti placer deposits are known around the State (Nokleberg and others, 1987), gold is the only commodity considered herein because it is the primary commodity produced in placer mines throughout Alaska at this time (Athey and others, 2013).

Mineral Resource Potential Estimation Methodology

For placer and paleoplacer Au potential, HUCs were scored on the basis of the following criteria: (1) ARDF records, (2) HMC mineralogy, (3) stream-sediment geochemistry, (4) lithology, and (5) downstream potential. These criteria are described and discussed below and summarized in table 3.

ARDF

An HUC containing one or more ARDF records that scored positive for a placer or paleoplacer occurrence, prospect, or mine (that is, score of nonzero on basis of the word-hit method described above) was given a score of 10 and automatically assigned high potential. The maximum possible score for each HUC on the basis of ARDF records was 10 (table 4).

Heavy Mineral Concentrate (HMC) Mineralogy

An HUC containing one or more HMC samples in which visible gold was present or inferred (that is, value not null) was given a score of 10 and automatically assigned high potential. An HUC containing one or more samples with an HMC report indicating the presence of cassiterite, powellite, scheelite, cinnabar monazite, and (or) thorite (that is, value not null) was given a score of 1 for each of these minerals present. The maximum possible score for each HUC on the basis of HMC mineralogy was 10 or the total number of other non-Au minerals present (table 4).

Stream-Sediment Geochemistry

An HUC containing one or more stream-sediment samples with Au and (or) Ag values in the 75th percentile or higher ($\geq$0.007 ppm for Au, $\geq$0.16 ppm for Ag) was assigned a score of 3 for each element. An HUC containing one or more stream-sediment samples with Ti and (or) W values in the 75th percentile or higher ($\geq$0.57 ppm for Ti, $\geq$2 ppm for W) was given a score of 1 for each element. The maximum possible score for each HUC on the basis of stream-sediment chemistry was 8 (table 4).

Lithology

A generalized lithology layer of mapped igneous-rock units across the State was derived from an anticipated geologic map of Alaska (Wilson, Frederic H., and others, USGS, written commun.) and used to identify areas with permissive lithologies. An HUC was given a score of 3 if it contained plutonic igneous-rock units, a score of 2 if it contained hypabyssal igneous-rock units, or a score of 1 if it contained volcanic or meta-igneous-rock units. For an HUC that contained multiple types of igneous-rock units, the highest single unit score was assigned to the entire HUC. Thus, the maximum possible score for each HUC on the basis of lithology was 3 (table 4). A generalized lithology layer of coarse-grained sedimentary rocks and surficial deposits was also initially used to contribute to the HUC scores. However, a general lack of detailed surficial mapping and challenges in delineating the most prospective coarse-grained sedimentary rocks made it difficult to confidently identify the most suitable surficial and sedimentary units for placer and paleoplacer deposits. Therefore, a weighting for sedimentary rocks and surficial deposits was not assigned, which might limit the ability to identify paleoplacer deposits by this method.

Results and Discussion

Initial total scores ranged from 0 to 32. Table 5 shows how the first four scoring components were used to assign values for potential to each HUC. HUCs with ARDF or mineralogy scores of 10 were automatically assigned high potential, as the presence of a known placer occurrence, prospect, or mine and (or) the presence of visible gold in one or more HMC samples was interpreted to be the most reliable predictors of placer or paleoplacer Au potential among the available datasets. For HUCs that did not meet either of these criteria, a total score of 16 or greater was also assigned high potential (table 5). This cutoff value was chosen because scores of 16 or greater represented maximum possible scores for at least three of the remaining scoring components. HUCs with scores of 6–15 and 0–5 were assigned medium and low potential, respectively. The cutoff value of 6 for medium potential was chosen because scores of 6 or greater generally represented a maximum possible score from at least one of the scoring elements. HUCs with a score of zero that did not have stream-sediment geochemistry data were assigned unknown potential.

Following the preliminary scoring and classification using the four scoring components described above, a fifth scoring component was added to the analysis to account for the possibility of placer occurrences downstream from HUCs with high placer or paleoplacer Au potential (table 4). In ArcGIS, all river and stream segments downstream of each high-potential HUC were selected from NHD and National Atlas datasets. Each HUC containing one or more of these downstream segments was given a score of 6 if it was within 25 km of the upstream high-potential HUC. HUCs that contain one or more downstream segments that are more than 25 km from the upstream high-potential HUC were given a score of 3. HUCs that contain one or more downstream segments, were more than 25 km from the upstream high-potential HUC, and were downstream of an intersection with an equal- or higher-order river segment were given a score of 1. The downstream scoring method excluded HUCs with high potential, and so only total scores for HUCs with medium, low, or unknown potential after the initial scoring process were eligible to change during the subsequent analysis.

The criteria by which the certainty of estimated resource potential was assigned for each HUC are outlined in table 5. Certainty was largely assigned depending on the number of datasets

that contributed to the total score (table 5). The presence of a known placer or paleoplacer occurrence, prospect, or mine, and (or) the presence of visible gold in one or more HMC samples provide a relatively high degree of certainty that placer or paleoplacer Au potential is high in a particular HUC. Therefore, high certainty was assigned to HUCs containing ARDF and (or) mineralogy scores of 10 (table 5). An HUC was also assigned high certainty if four or more datasets contributed to the total score. An HUC with medium certainty had two or three datasets that contributed to the total score. An HUC with unknown potential (that is, a zero score and no stream-sediment geochemistry data of any kind) was automatically assigned a certainty of unknown.

The results of the scoring analysis for placer and paleoplacer Au are shown in plate 3, and accompanying data are presented in appendix E. After adding in the downstream scoring elements, our analysis indicates that 206 HUCs, or 8.2 percent of the 2,460 in the CYPA, have high estimated potential for placer or paleoplacer Au deposits. Of these, all but 3 are also estimated to have high certainty. 511 HUCs (20.8 percent of total) have medium estimated potential, with most (71.4 percent of medium) having medium certainty. Most of the HUCs in the CYPA (1,740, 71 percent of total) have low estimated potential for placer or paleoplacer Au, and all within this category have either high (36.3 percent of low potential) or medium (63.7 percent of low potential) certainty. 480 HUCs have a total score of 0, but only 3 of these (0.1 percent of total) are classified as having unknown potential and certainty because they contain no stream-sediment data.

Throughout the CYPA, areas with high placer Au potential are generally associated with known placer districts (plate 4) as outlined in Nokleberg and others (1987). Regions with the highest concentration of high-scoring HUCs are in the Wiseman and Chandalar quadrangles in the north-central CYPA, along the Yukon and Koyukuk Rivers (fig. 1; plate 4) in the southern CYPA, and in the southern Fairbanks and northern Healy quadrangles in the southeastern CYPA (plate 4). In these and other areas, there are HUCs adjacent to the placer districts that also have high potential, suggesting that ancillary drainages feeding into areas with past and (or) present placer mining activity might also be prospective.

There are a few areas that stand out as having high to medium potential but are not associated with known placer districts. An east-west-trending, discontinuous belt of medium-potential HUCs in the Howard Pass, Killik River, and Chandler Lake quadrangles are on the northern side of the Brooks Range (plate 4). There is a cluster of high- and medium-potential HUCs in the southern Bettles and northern Tanana quadrangles; these HUCs appear to be associated with the outcrop trend of the Ruby batholith, a belt of felsic plutonic rocks that is also prospective for REE and Sn-W-Mo deposits (see plates 2 and 12 for general location and discussions above and below). Two other areas with high and medium potential but not associated with known placer districts are in the central and southern Nulato and eastern Norton Bay quadrangles in the southwestern part of the CYPA. In the Nulato quadrangle, the high-potential HUCs contain known placer prospects in the vicinity of a Cretaceous granitic pluton and multiple Au-Ag-Pb-Zn prospects and occurrences in the Kaiyuh Mountains (plate 4; Cobb, 1972; Patton and Moll-Stalcup, 2000). In the eastern Norton Bay quadrangle, the high-potential HUC contains an ARDF locality describing gold reports but does not list an exact location (ARDF record NR011; Dashevsky, 2002). The drainage is primarily underlain by Cretaceous sedimentary rocks of the western Yukon-Koyukuk Basin (plate 4), and there are no mapped igneous units in the vicinity (Patton and others, 2009). However, there are multiple HUCs in the same region with medium potential for other deposit types (for example, REE deposits; see plate

2) and other HUCs with no data (plate 4). Thus, the western Yukon-Koyukuk Basin in the southwestern part of the CYPA might be a suitable target for more detailed sampling and study.

PGE (-Co-Cr-Ni-Ti-V) Deposits Associated with Mafic-to-Ultramafic Intrusive Rocks

Deposit Group Characteristics

The platinum-group elements (PGE) consist of six metallic elements comprising Ru, Rh, Pd, Os, Ir, and Pt. They share similar physical and chemical properties and therefore tend to occur together in mineral deposits (Harris and Cabri, 1991). The PGE are split into the iridium subgroup (Os, Ir, Ru) and the palladium subgroup (Rh, Pt, Pd), because these two subgroups tend to behave coherently during magmatic processes (Rollinson, 1993). PGE are variably to strongly associated with Co, Cr, Cu, Ni, Ti, and V in deposits associated with mafic-ultramafic (MUM) rocks and with many other elements in non-MUM-related PGE deposits.

PGE are found in many geologic settings and are hosted by igneous and sedimentary rocks; PGE ore deposits form from a variety of physical and chemical processes. For this study, only PGE ore deposit models genetically associated with MUM rocks were considered. Characteristics of MUM-rock-related deposit models are summarized by Naldrett (2004), and the specific deposit types that factored into our assessment are listed in tables 1 and 6. There are other types of ore deposits known in Alaska that have associated PGE enrichments or deposits, and there are also other types of PGE deposit types that are not presently known or are suspected to occur in Alaska (table 6). The scoring criteria outlined below were only optimized for deposits associated with MUM rocks, but some of the more general PGE indicators, such as geochemical data, might reveal potential for a wider variety of deposit types.

Mineral Resource Potential Estimation Methodology

The datasets described below were scored for parameters that identify potential for the occurrence of PGE (Co, Cr, Cu, Ni, Ti, V; see table 6). Datasets were ranked according to their suitability for predicting potential for these elements. For this deposit group, HUCs were scored on the basis of the following criteria: (1) presence of MUM rocks, (2) presence of PGE mineral occurrences, prospects, or mines, (3) PGE- or PGE-indicator-minerals in placers and heavy-mineral-concentrate mineral reports, and (4) geochemical values for Pt, Pd, Os, Ir, Rh, Ru, Co, Cr, Cu, Ni, Ti, and (or) V in (a) heavy mineral concentrate samples, (b) stream-sediment samples, and (c) rock samples. These criteria are described below and summarized in table 6. Although copper is often associated with various PGE models, it also occurs with numerous non-PGE-bearing deposit types. Consequently, copper was excluded from the PGE scoring layers to avoid an overwhelming number of non-PGE-related anomalies.

Lithology

A generalized lithology layer that included all mapped mafic and ultramafic igneous-rock units statewide was used to identify areas of permissive rock types, particularly MUM rocks (Wilson, Frederic H., and others, USGS, written commun.). An HUC received a score of 2 points if it contains mafic or ultramafic igneous rocks as major components of the geologic map units, and a score of 1 point if it contains mafic or ultramafic igneous rocks as minor or incidental components (table 6). For an HUC that contains multiple types or locations of MUM igneous

rocks, the highest score is assigned to the entire HUC. Thus, the maximum possible score for each HUC on the basis of lithology is 2 (table 7).

ARDF

ARDF records for placer occurrences, prospects, and mines were removed from the ARDF layer and incorporated into the Heavy Mineral Concentrate mineralogy section (see below). The remaining lode-related ARDF records were scored for PGE favorability on the basis of the word-hit method described above; keywords included MUM lithologies, associated elements (Pt, Pd, Ir, Os, Rh, Ru, Co, Cr, Ni, Ti, and V), and PGE-bearing minerals (for example, sperrylite, native platinum—for complete list, see appendix C). For lode mineral sites, each highly ranked ARDF record was reviewed after scoring, and occurrences that clearly had no relation to one of the PGE models discussed above were excluded from the list. The remaining list was further classified into ARDF records with (1) PGE reported as major or minor commodities (3 points), (2) chromite and favorable geology (2 points), and (3) permissible geology but no direct evidence for PGE (1 point). The maximum possible score for each HUC on the basis of lode ARDF records was 3 points (table 7).

Heavy Mineral Concentrate (HMC) Mineralogy

For this study, PGE or PGE-indicator minerals in placers in ARDF records were considered equivalent to the same elements in HMC mineralogy records. After applying the word-hit method (described above), the highly ranked ARDF placer list was subdivided into records with: (1) PGE reported as major or minor elements (3 points), (2) chromite or other PGE-related minerals, or questioned PGE identifications (2 points), and (3) mineralogy for MUM rocks in a drainage (for example, jade, serpentine-group minerals) but no direct evidence for PGE (1 point; see table 6). An HUC containing one or more samples with an HMC mineralogy report of chromite, Cu-Co sulfides, Ni-Co sulfides, Ni sulfides, or Cr-Ni silicates received a score of 2 points. A HUC containing one or more samples with an HMC mineralogy report of serpentine or Cr diopside received a score of 1 point. The maximum possible score for each HUC on the basis of ARDF placer records and HMC mineralogy was 3 points (table 7).

Approach for Geochemical Datasets

HMC geochemistry for drainages, stream-sediment geochemistry, and rock geochemistry datasets are also used to assign scores to HUCs. Where possible, the natural breaks method was used to assign scores of 3 points to the ≥91st percentile break for PGE. Similarly, where possible, the natural breaks method was used to assign scores of 2 points to the ≥98th percentile, and 1 point to the ≥91st to <98th percentile breaks for Co, Cr, Ni, Ti, and (or) V.

The spatial distribution of samples assigned to these percentile categories for each element was examined in ArcGIS to check for spatial artifacts. The geochemical datasets contain qualitative emission spectroscopic analyses in addition to analyses run by quantitative analytical methods. The spatial distribution of percentile values determined by natural breaks commonly contains artifacts that result from the "qualitative step levels" for elemental values in emission spectroscopic data. Where artifacts were present, scoring was manually assigned by examining the histogram of values for each element, and visually selecting a reasonable number of anomalous (1 point) and highly anomalous (2 points) values. Additionally, highly anomalous values were initially checked for possible spatial correlation with known PGE occurrences. If the

correlation was high, cutoff values (in ppm) were adjusted downward to allow for a geologically reasonable number of anomalous samples not necessarily associated with known occurrences. Documentation of how points are assigned to each element in the three geochemical datasets is presented in table 7 and discussed by dataset type below.

Heavy Mineral Concentrate (HMC) Geochemistry—An HUC containing one or more HMC geochemical samples with Pt, Pd, Os, and Ir values >0 ppm was given a score of 3 points. No Rh or Ru values were present in the dataset. An HUC containing one or more HMC geochemical samples with TiO_2 values greater than 5 weight percent was given a score of 1 point. For Co, Cr, Ni, and V, scoring was manually assigned by examining their histogram of values and visually selecting a reasonable number of anomalous (1 point) and highly anomalous (2 points) values for each element. The maximum possible score for each HUC on the basis of HMC geochemistry is 3 points (table 7).

Stream-Sediment Geochemistry—An HUC containing one or more stream-sediment geochemical samples with Pt, Pd, Os values in or above the 91st percentile was given a score of 3 points. No Ir, Rh, or Ru values were present in the dataset. For Co, the natural breaks method was used to assign scores of 2 points to the 98th percentile, and 1 point to the 91st percentile values. For Cr, Ni, Ti, and V, scoring was manually assigned by examining their histogram of values and visually selecting a reasonable number of anomalous (1 point) and highly anomalous (2 points) values for each element. The maximum possible score for each HUC on the basis of stream-sediment chemistry was 3 points (table 7).

Rock Geochemistry—For rock geochemistry, elements in the USGS and ADGGS datasets were scored separately. The ADGGS database primarily contains samples collected for evaluating mineral potential. The USGS database contains samples analyzed for background rock-geochemical values, as well as samples collected for evaluating mineral potential. As a result, the natural breaks for each element are significantly different in the two datasets. Past USGS geochemical programs collected hundreds of samples to determine low-level background values for igneous rocks, thus resulting in generally lower mean, median, and natural-break values. For the USGS dataset, an HUC containing one or more rock geochemical samples with Pt >0.004 ppm or Pd>0.005 ppm was given a score of 3 points. For the ADGGS dataset, an HUC containing one or more rock geochemical samples with Pt >0 ppm or Pd >0 ppm was given a score of 3 points. For both the USGS and ADGGS datasets, an HUC containing one or more rock geochemical samples with Ir, Rh, or Ru >0 ppm is given a score of 3 points. No values for Os are present in either dataset. For Co, Cr, Ni, Ti, and V, scoring was manually assigned by examining their histogram of values and visually selecting a reasonable number of anomalous (1 point) and highly anomalous (2 points) values for each element. The maximum possible score for each HUC on the basis of stream-sediment chemistry is 3 points (table 7).

Results and Discussion

Table 8 outlines how PGE (-Co-Cr-Ni-Ti-V) resource potential and certainty were assigned for each HUC. Total scores ranged from 0 to 11. Plate 5 shows the results of the scoring analysis, and accompanying data are presented in appendix E. Of the 2,460 HUCs in the CYPA, there are 127 HUCs (5 percent of total) with high estimated potential for PGE (plate 5, appendix E). Of these, 52 HUCs (40.9 percent of high potential) are also estimated to have high certainty. 1,250 HUCs (51 percent of total) have medium estimated potential, with most (82 percent of medium) having low certainty. 44 percent of the HUCs in the CYPA (1,068 total) have low estimated potential for PGE, although most within this category have either high (62.4 percent of

low) or low (37.6 percent of low) certainty. There are 673 HUCs that have a total score of zero, but only a small number of these (7, 1 percent of total) were assigned unknown potential and certainty.

Future geologic investigations might be best focused on areas that lack information but have relatively high potential scores based on very limited available data. Areas with high potential occur along a discontinuous band in the western part of the northern Brooks Range in the Killik River and Chandler Lake quadrangles and in scattered areas throughout the southern CYPA (plate 6). To more fully understand areas with high and medium PGE potential, future work might include (1) taking the generic MUM-related deposit criteria developed in this study and tailoring it to individual MUM-related, and non-MUM-related PGE models (table 6); (2) using MUM rock geochemistry to determine the spatial distribution, types, and geologic settings of MUM rocks; (3) obtaining quantitative geochemical analyses for historical sediment and rock samples, which originally were only analyzed for a limited number of elements by qualitative emission spectroscopic methods; (4) conducting stream-sediment and rock-geochemical sampling in high- and medium-PGE-potential HUCs to identify lode source(s) of PGE, Co, Cr, Cu, Ni, Ti, and (or) V anomalies within the watersheds; (5) conducting rock sampling to fill gaps in igneous geochemical and geochronology databases; (6) analyzing available geophysical data to identify areas of PGE-hosting lithologies; and (7) conducting geologic mapping in high- and medium-PGE-potential HUCs to delineate MUM rocks or to identify other PGE-hosting lithologies. The PGE scoring criteria described above were only optimized for PGE deposits associated with MUM rocks. Thus, it is possible that scoring parameters relevant to other types of PGE deposits (for example, those not associated with MUM rocks or not presently known to occur in Alaska) might also yield insight into PGE potential.

Carbonate-Hosted Cu (Co-Ag-Ge-Ga) Deposits

Deposit Group Characteristics

Alaskan carbonate-hosted Cu deposits are of two distinct types, the Kennecott and Kipushi types. These deposits commonly contain Ag, and they may also contain three critical elements—Co, Ge, and Ga. Kennecott-type carbonate-hosted Cu deposits are named for the town of Kennecott, Alaska (fig. 1), where deposits were mined out by about 1938 (Price and others, 2014). The district contains northeast-striking, very high-grade (13 percent Cu) veins that fill either normal and reverse faults that cut the Triassic Chitistone Limestone. Silver was recovered (65 g/t), as well as Cu (MacKevett and others, 1997; Price and others, 2014). Deposits show considerable wall-rock replacement by copper sulfides and broad dolomitized alteration envelopes. The deposit bases were along probable bedding-plane faults about 25 m above the contact between the Chitistone Limestone and the underlying Nikolai Greenstone. Over nearly its entire extent in Alaska, the Nikolai Greenstone contains scattered quartz+Cu-sulfide or native Cu±calcite veins or amygdular zones, typically with epidote±calcite±chlorite alteration. Although Cu mineral occurrences are very widespread in the Nikolai Greenstone wherever it occurs, mining has not succeeded for long at any of these occurrences. However, the copper in the Kennecott veins was apparently dissolved from the Nikolai Greenstone during prehnite-pumpellyite facies metamorphism in the Early Cretaceous and then moved upwards and away from zones of higher grade metamorphism (Silberman and others, 1980; MacKevett and others, 1997; Price and others, 2014), suggesting that locations where there is epigenetic Cu mineralization in the Nikolai predict high potential in the overlying Chitistone Limestone or

other carbonate rocks immediately upsection. The Cu occurrences in the basalt are not themselves economically attractive at this time, but the occurrences are surely prospecting guides that might lead to the discovery of Kennecott-type deposits in overlying carbonates.

The Ruby Creek deposit (plate 8 for location) is an Alaskan example of Kipushi-type deposits, which are named for Kipushi, Democratic Republic of Congo (DRC). These are massive base-metal-sulfide replacement bodies or breccia fillings in carbonates, now dolomitized, that are either peneconcordant or cut bedding as high-angle breccia bodies, or both. All deposits classified as Kipushi type by (Cox and Singer, 1986) have Ge-bearing minerals; this appears to be the basis of their classification, as there are other types of Cu-Pb-Zn-sulfide ores in carbonate rocks that lack Ge minerals. The Ruby Creek deposit is hosted by the middle Silurian to Early Devonian Cosmos Hills Sequence (Till and others, 2008). As of April 2014, Ruby Creek had an indicated resource of 14 Mt at 1.08 percent Cu and an additional inferred resource of 165 Mt at 1.57 percent Cu (Davis and others, 2014). Cu-Co-Ge mineralization occurs as sulfide minerals that fill former open space in breccias or replace breccia matrix and wall-rock carbonates within a very large halo of hydrothermal dolomite containing minor sphalerite (Runnells, 1969; Bernstein and Cox, 1986; Hitzman, 1986). Copper sulfide minerals include chalcopyrite, bornite, and chalcocite. Cobalt occurs in carrollite ($CuCo_2S_4$) and cobaltiferous pyrite, and Ge occurs in sulfides are renierite ($Zn_3(AsO_3)_2$) and germanite ($Cu_{13}Fe_2Ge_2S_{16}$). Grades of the trace metals Co, Ge, and Ga in the Ruby Creek deposit have not been published. Elsewhere, Kipushi-type ores may contain approximately 1,000 ppm Ge, but calculations from production figures from Kipushi, DRC, suggest that recovery there ranged from 23 to 600 ppm Ge (Höll and others, 2007).

Mineral Resource Potential Estimation Methodology

For carbonate-hosted Cu deposits, five criteria were used to estimate resource potential—(1) lithology, particularly the presence of carbonate host rocks, (2) sedimentary rock geochemistry, (3) mineralogy of pan concentrates of sediment samples, (4) sediment geochemistry, and (5) presence of known (ARDF) deposits and occurrences with copper in sedimentary rocks, particularly carbonate rocks.

Lithology

Rock-type information is available from map-unit descriptions for an anticipated geologic map of Alaska (Wilson, Frederic H., and others, USGS, written commun.). Using lithologic descriptions, map units with carbonate rocks were divided into two groups—(1) “carbonate, major” and (2) “carbonate, other”—on the basis of whether carbonate rocks form more or less than 50 percent of the map unit, respectively (appendix D). Each HUC that contained any “carbonates, major” units was assigned a score of 3; HUCs that lacked “carbonates, major,” but contained “carbonates, other” were assigned a score of 2. To account for potential down-dip extent of carbonate units, each HUC adjacent to an HUC that scored 2 or 3 was assigned a score of 1 (table 8). Future work could refine this buffering approach by examining bedding attitudes of the carbonate-bearing units and retaining buffer zones only in the downdip direction and removing the buffer zone in the updip direction where carbonate rocks have been eroded.

After the above ranking of HUCs on the basis of lithology, all remaining HUCs that did not score 1–3 were assigned a total potential score of 0, and they were not included in any further scoring procedures. Those HUCs lack the permissive host-rock types for carbonate-hosted Cu deposits.

Rock Geochemistry

Geochemical data for sedimentary and metasedimentary rocks were included from both the AGDB and the ADGGS databases. Three points were assigned to any HUC that contained a sedimentary rock sample with ≥5,000 ppm Cu. Two points were assigned for sedimentary rock samples with <5,000 ppm Cu but ≥1,000 ppm Cu. One point was assigned for a sample containing <1,000 ppm but ≥150 ppm Cu (table 9). To avoid bias where more than one sample occurs in a HUC, only the single sample with the greatest measured Cu concentration was allowed to score in each HUC.

For sedimentary rocks with ≥150 ppm Cu, 1 point was also awarded to any HUC with one or more samples additionally containing ≥45 ppm Co, ≥3 ppm Ge, ≥35 ppm Ga, and (or) ≥1 ppm Ag. (These values follow the recommendation of Huyck [1990], who examined trace elements in black shales, the sedimentary rock type with the highest background values for these four elements.) The metals concentration values are chosen to be consistent with a "metalliferous" black shale as defined there. The trace-element-scoring thresholds are thus designed to award scores only where values anomalous for any sedimentary-rock type are found; concentrations that would seemingly require an epigenetic mineralizing process to reach within carbonate host rocks. Each HUC can score one additional point for each trace element, and therefore, trace element geochemistry of the byproduct metals can contribute as many as 4 points for a single HUC. The maximum possible score for each HUC on the basis of rock geochemistry is then capped at 5 (table 9), so that the rock geochemistry cannot dominate all other scoring factors.

Heavy Mineral Concentrate Mineralogy

An HUC containing one or more samples with an HMC report indicating the presence of chalcopyrite, copper cobalt sulfides, copper silicate, copper sulfides/oxides, azurite, cuprite, enargite, and (or) malachite (that is, value not null) was assigned a score of 1 for each mineral present. The score was additive for each possible mineral present, and therefore the maximum possible score for each HUC on the basis of HMC mineralogy was 8 (table 9).

Stream-Sediment Geochemistry

An HUC containing one or more sediment samples with copper values in the 98th percentile or greater (≥150 ppm) was assigned a score of 3. An HUC containing one or more sediment samples with copper values between the 98th and 91st percentiles (149–76 ppm) was assigned a score of 2, and an HUC containing one or more sediment samples with copper values between the 91st and 75th percentiles (75–50 ppm) was assigned a score of 1.

For Co, Ge, Ga, and Ag, only sediment samples with copper concentrations of ≥50 ppm were considered. For example, this specific scoring procedure worked toward giving no weight to Co that may have been sourced in black shale, no weight for Ge sourced in coal underclay, no weight for Ga sourced in a sedex deposit, and no weight for Ag sourced in an epithermal vein. This approach assigns scoring weight to these trace metals only where they had the proper metal association for a copper in carbonates deposit. A HUC containing one or more stream-sediment samples with ≥50 ppm Cu and Co, Ge, Ga, and (or) Ag concentrations in the 91st percentile or greater (≥36 ppm, ≥5.9 ppm, ≥30 ppm, ≥0.4 ppm, respectively) was given a score of 1 for each trace element. The maximum possible score for each HUC on the basis of sediment chemistry was 7, with 3 possible for Cu and 4 possible for additional trace metals (table 9).

ARDF

The ARDF keyword list and scoring criteria for carbonate-hosted Cu deposits was designed to (1) maximize the probability of identification of occurrences that are consistent with the carbonate-hosted Cu deposits and (2) to minimize the inclusion of unrelated occurrences. Copper is present in a wide variety of mineral deposit types, most of those unrelated to Kipushi- or Kennecott-type deposits. Thus, the ARDF scoring method was designed to account for this potential complexity and overlap. The greatest scoring weight was assigned to ARDF records that were identified as either basaltic Cu or Kipushi deposits (model numbers 23 and 32c, respectively, of Cox and Singer, 1986). Negative scores were assigned if a different deposit type or model number (for example, sediment-hosted massive sulfide deposits, volcanic-hosted massive sulfide deposits, or skarn deposits) was assigned in the ARDF record. Neither positive nor negative scores were assigned for ARDF occurrences that had been classified as polymetallic replacement deposits and polymetallic veins (model numbers 19a and 22c, repectively, of Cox and Singer, 1986) because of possible ambiguities in their classification. There are a number of localities identified where occurrences of polymetallic replacement deposits and (or) polymetallic veins were described near clusters of Cu mineral occurrences in carbonate host rocks. In general, the polymetallic vein and polymetallic replacement classes are not defined in language that is sufficient to determine which deposit type is most appropriate or if they are related to other deposit types. As a result, deposit models 19a and 22c can include features that might be indicative of another type of mineralization but where the specific relations are not completely understood. To account for this possible overlap, the scoring was designed to allow other criteria to score favorably for HUCs with mineral occurrences described that way, rather than to score negatively for such occurrences. A score of 3 was assigned where Cu and (or) Co were listed as a main commodity, whereas scores of –3 were given for each element that is unlikely to be a main commodity in a carbonate-hosted Cu deposit. Negative scores were also given to keywords in the ARDF records that are unlikely to be associated with this type of deposit (appendix C), for example, the word, porphyry, as in a porphyry copper or porphyry molybdenum deposit. The resulting ARDF word-hit results produced maximum scores of 23, and the highest scores typically were for occurrences that were classified either basaltic Cu or Kipushi type. A score of 5 was assigned to each HUC that contained one or more ARDF record with a word-hit model score that was >4 (that is, 4–23), a score of 2 was assigned to each HUC that contained one or more ARDF records with word hit model scores between 3 and 1, and a score of 0 was assigned to any HUC that contained only ARDF records with results of 0 or less.

Results and Discussion

From the above, the greatest total score an HUC could receive was 30 points, though the maximum HUC score in the CYPA and its buffer was 20 for this deposit type. Table 10 outlines the criteria by which resource potential was assigned for each HUC. Those HUCs with scores of ≤3 were classified as having low potential because, although possible host rocks might be present, there was no evidence of any mineralizing process from the remaining 6 types of data. The remaining composite scores of 4 and greater were divided at one natural statistical break (Jenks method), with the two new categories assigned medium and high potential for score ranges of 4–6 and ≥7, respectively. The assigned certainty value for each HUC corresponds to the number of data types that contribute to the potential score as outlined in table 10.

Results of the scoring analysis for carbonate-hosted Cu deposits are shown in plate 7, with accompanying data in appendix E. A total of 141 HUCs (6 percent of 2,460 HUCs in the CYPA) are considered to have high potential. Of those, just over half (79) also have high certainty. There are 425 HUCs (17 percent of the HUCs in the CYPA) with medium potential. The remaining 1,882 HUCs (77 percent of CYPA) have low potential, with almost two-thirds of these (59.1 percent of the low-potential HUCs) also having high certainty. A total of 1,017 HUCs had total scores of 0, but only 12 of these (0.5 percent of CYPA) were classified as having unknown potential and unknown certainty (plate 7, appendix E).

The 100-km buffer zone included Ruby Creek and two similar ARDF occurrences (plate 8). All six HUCs in that area have high potential with five of these at medium certainty (plate 8), and this result helps to validate the scoring method.

The results also identified at least three major belts of high potential for carbonate-hosted Cu deposits close to the boundaries of the CYPA—(1) Sheep Creek belt, (2) the belt of Nikolai Greenstone basaltic Cu occurrences, and (3) the Brooks Range foreland belt. The Sheep Creek belt extends along the south flank of the Brooks Range, with additional occurrences on thrust plates farther north in the interior of the range (plate 8). A group of 10 ARDF occurrences form part of a northeast-southwest belt of high potential in the Wiseman quadrangle, and it may extend discontinuously eastward and northeastward across the Brooks Range into the Philip Smith Mountains and Mount Michelson quadrangles (plate 8).

A belt of high potential southeast of the CYPA boundary (plate 8) is related to basaltic Cu ARDF occurrences, copper geochemical anomalies principally in stream sediments, and some copper minerals in heavy mineral concentrates. This belt is largely identified because of basaltic Cu-type ARDF occurrences along exposures of Nikolai Formation greenstone (plate 8), and it is somewhat analogous with the geology of the Kennecott deposit. However, slightly less than half of those high-potential HUCs also have potential carbonate host rocks upsection from the Nikolai Formation. A parallel belt of high-potential HUCs to the northwest of the Nikolai basaltic Cu occurrences intersects the southeastern part of the CYPA (plate 8) and is more diverse; HUCs along this belt contain basaltic copper occurrences in other greenstones, different carbonate host rocks, fewer ARDF occurrences, and more copper minerals in heavy-mineral concentrates.

The third belt with high potential extends along the Brooks Range foreland (plate 8), but copper concentrations in stream-sediment samples and rocks in this area are typically less than in the areas described above, and there are no ARDF occurrences along this flank of the range that strongly suggest carbonate-hosted Cu deposits. Anomalies along the Brooks Range foreland are mostly associated with the slope facies of the Carboniferous Lisburne Group and with additional chert, shale, and thin carbonate units upsection from the Lisburne through rocks of Jurassic age. Although copper concentrations are generally lower, the copper anomalies of the Brooks Range foreland should be considered because available sampling was sparse and the carbonate rocks, particularly the Lisburne Group, are viable host rocks.

Elsewhere, results suggest high potential for carbonate-hosted Cu deposits where this deposit group is unlikely, and these results mainly occur in places where “carbonate, other” lithologic units contain mineral deposits or prospects with anomalous Cu concentrations or Cu minerals. For example, the Ambler schist belt (plate 8) hosts at least six Cu-rich volcanogenic massive sulfide deposits (Schmidt, 1986). Similarly, the Medfra quadrangle contains a northeast-trending belt of HUCs in the area around Limestone Mountain with high potential, where geochemical anomalies are immediately adjacent to Jurassic intrusions (plate 8). These high potential HUCs likely reflect either skarn or porphyry mineralization, rather than carbonate-

hosted Cu deposits. A group of HUCs with high potential in the northwestern Chandalar quadrangle (plate 8) might reflect Cu anomalies from metamorphosed Devonian-age porphyry Cu deposits and Cu skarns (Newberry and others, 1986), or these HUCs might reflect high potential for carbonate-hosted Cu deposits as part of a discontinuous belt in the Chandalar, Wiseman, Survey Pass, and Ambler River quadrangles.

Sandstone U (-V-Cu) Deposits

Deposit Group Characteristics

Sandstone uranium deposits (ssU) are epigenetic deposits with a worldwide distribution. They form in sandstone host rocks that range in age from Carboniferous to Tertiary. Sandstone uranium deposits are commonly divided into four types—basal, tabular, roll front, and tectonolithologic (table 1; Cuney and Kyser, 2009). Regardless of type, all ssU deposits are thought to form by redox-controlled processes that can be generalized as (1) oxidative mobilization of the uranium from the source rock, commonly granite or tuff, (2) transport of soluble uranyl (U^{6+}) complexes through an oxidized nonmarine-sandstone aquifer, and (3) reduction and precipitation as (U^{4+}) minerals by encounter with reduced host rocks that are laterally continuous or lying below the aquifer in which uranium is transported (Guilbert and Park, 1986; Cuney and Kyser, 2009). Reducing conditions in the host rock are typically a result of entrained carbonized plant matter. In this analysis, all types of ssU deposits were initially targeted, but basal-type deposits are the most likely to occur in Alaska and the CYPA. Other U-enriched deposits that occur within similar host rocks are sediment-hosted V and sediment-hosted Cu deposits (Turner-Peterson and Hodges, 1986).

The best described ssU deposit in Alaska is the Death Valley deposit (ARDF record BN089), located in the Boulder Creek Basin near the eastern end of the Seward Peninsula (see plate 10 for location). It was discovered in 1977 by airborne radiometric survey and has an average grade of 0.27 percent U_3O_8 in beds averaging 3 m thick and has calculated reserves of about 1,000,000 lbs (~453.59 t) U_3O_8 (Dickinson and others, 1987). The host rocks are early-Eocene carbonaceous arkosic sandstones of fluvial or colluvial origin deposited in a graben formed on granitic bedrock (Dickinson and others, 1987). The underlying Late Cretaceous granitic pluton, known as the Darby pluton, forms the western side of the graben. Basalt, coal, and lacustrine laminated sideritic mudstone and turbidites are interbedded with the sandstone. An early-Eocene basalt flow dammed the ancestral river valley, forming the lake in which the lacustrine sediments were deposited (Dickinson and others, 1987).

The deposit history comprises an earlier Eocene(?) primary epigenetic mineralization and later Holocene secondary supergene enrichment. The Darby pluton is considered the likely source for the uranium. Primary mineralization is thought to have developed when uranium was dissolved by oxidizing ground water, carried east from the Darby pluton, and deposited in the reducing environment of the carbonaceous Tertiary sedimentary rocks (Dickinson and others, 1987). The mineralized rocks are fairly widespread in the subsurface, occurring both above and below the Eocene basalt and lacustrine rocks and extending to a depth of about 91 m. Uranium minerals in the primary ore are coffinite ($U(SiO_4)\cdot nH_2O$) in the reduced zones and autunite ($Ca(UO_2)_2(PO_4)_2\cdot 10\text{-}12H_2O$) where the primary ore has been oxidized. The secondary supergene enrichment is related to the present surface exposure and is possibly ongoing, because the involvement of recent surficial mudflows and soil formation processes indicated a recent age (Dickinson and others, 1987). Uranium minerals in the secondary enrichment include meta-

autunite ($Ca(UO_2)_2(PO_4)_2 \cdot 6H_2O$). The uranium-rich rocks of the Death Valley deposit are strongly carbonaceous and have anomalously low manganese (Mn) concentrations. The features of Death Valley are most consistent with those of a basal-type ssU deposit (Dickinson and others, 1987) and the low Mn concentration of the U-bearing rock is inconsistent with roll-front-type deposits (Harshman, 1972).

Mineral Resource Potential Estimation Methodology

The presence of sandstone is a defining characteristic for sandstone uranium deposits. However, because the geologic mapping is generally too coarse and unconsolidated material covers many of the Tertiary sedimentary basins in Alaska, the analysis was not simply limited to HUCs with sandstone lithology. Instead, differing sedimentary-rock lithologic and coal data layers were used to define host rock favorability, and evidence for U-mineralization included (1) uranium distribution (stream sediments, sedimentary rock), (2) bedrock with strong radioactive signature (aerial gamma-ray survey data), (3) U potentially derived from highly differentiated igneous plutons (Fe# displacement), and (or) (4) locations of known or possible ssU occurrences, prospects, and mines (ARDF records). During scoring, host-rock favorability and U-mineralizing process indicators were considered of equal importance. Data density was also considered as discussed below. Scoring components and criteria are listed in table 11.

Lithology

A generalized sedimentary rock layer was derived from an anticipated geologic map of Alaska (Wilson, Frederic H., and others, USGS, written commun.) using search terms that were based on the map unit descriptions (see appendix D). The generalized sedimentary rock layer includes all the mapped units where sedimentary rocks were listed as either a “major” or an “other” component of the unit description. Because unconsolidated materials cover many of the sedimentary basins, a generalized lithology layer of unconsolidated sediment was also developed.

Sandstone U deposits in North America, including the Death Valley deposit in Alaska (plate 10), are commonly hosted in Tertiary sandstone, specifically Tertiary arkosic sandstone (Guilbert and Park, 1986; Cuney and Kyser, 2009). To capture the high favorability of these rocks, map units described as Tertiary arkosic sandstone and Tertiary/Cretaceous sandstone were extracted from the generalized sedimentary rock layer, regardless of whether these characteristics were a “major” or an “other” component in the unit descriptions. HUCs containing Tertiary arkosic sandstone and Tertiary/Cretaceous sandstones were assigned scores 4 and 3, respectively (table 11). HUCs containing part of the generalized sedimentary rock layer were given a score of 2. If an HUC contained unconsolidated sediment that was within a 3-km buffered area surrounding favorable sedimentary lithologies, the HUC was assigned a score of 1. For HUCs that met more than one of these lithological criteria, only the highest score was used. Thus, the maximum possible score for lithology was 4 (table 11).

Coal

Coal-bearing sedimentary sections typically also contain rocks from fluvial, lacustrine, and (or) coastal sedimentary environments. The first two environments match the targeted host rocks for sandstone uranium deposits. Thus, to capture the favorability of sedimentary rocks that contain solid organic matter, Tertiary to Tertiary/Cretaceous coal-bearing rock units were

identified from the published map of Alaska's coal resources (Merritt and Hawley, 1986). A HUC containing one or more coal-bearing units was given a score of 1 (table 11). This score was applied to an HUC independent of any other lithology score.

Stream-Sediment and Sedimentary-Rock Geochemistry

The uranium distribution in both sediments and sedimentary rocks was used to define areas with anomalously high uranium content. Analyses of sedimentary rock are the most direct determination of the uranium content; however, the spatial distribution of available sedimentary-rock data is more limited than that of the stream-sediment data. In addition, rock samples might have been collected for a specialized purpose, such as background determination, and such information might not be available as metadata together with the analytic result. For these reasons, the maximum score for U content in sedimentary rock was 2 and was assigned to HUCs containing one or more sedimentary rock samples greater than or equal to the 98th-percentile value for uranium (≥40 ppm). A score of 1 was assigned to HUCs with a sedimentary rock sample greater than or equal to the 91st-percentile and less than the 98th-percentile values for uranium (≥11 and <40 ppm).

The uranium content in stream sediment is a less direct measure in comparison with sedimentary rock, because stream-sediment samples can integrate the contributions from multiple sources upstream of the collection point. However, because of the dataset's greater areal extent and uniformity of purpose compared to the sedimentary rock data, the maximum possible score for stream-sediment uranium data was set at 3. HUCs with a stream-sediment sample greater than or equal to the 98th-percentile value for uranium (≥20 ppm) scored 3; those with a stream-sediment sample greater than or equal to the 91st-percentile and less than the 98th-percentile values (≥5.8 ppm and <20 ppm) for uranium scored two, and those with a stream-sediment sample greater than or equal to the 75th-percentile and less than the 91st-percentile values for uranium (≥3.5 ppm and <5.8 ppm) scored 1 (table 11).

Both the sedimentary rock and stream-sediment geochemistry datasets were scored independently and, in both instances, a single HUC could contain multiple samples. For HUCs containing multiple samples, scoring was limited to the highest scoring single sample within the HUC. Because the two geochemistry datasets were scored independently, an HUC could receive a score of 2 for uranium content greater than or equal to the 98th percentile in a sedimentary-rock sample and 3 for a uranium content greater than or equal to the 98th percentile in a stream-sediment sample, if both were present in the HUC.

Igneous-Rock Geochemistry

Igneous rocks are the likely sources of U in some ssU deposits. Because of the behavior of U in magmas, the most likely source plutons for U are highly differentiated igneous rocks. There are few U analyses in the igneous-rock dataset and, therefore, an indicator approach was used. Uranium is highly incompatible and, as a result, is commonly in higher concentrations in late-stage differentiates and more highly evolved, silica-rich compositions. To identify highly differentiated and potentially U-rich igneous bodies, we used the $Fe\#_{displacement}$ metric described above (Frost and Frost, 2008). An HUC containing one or more igneous rock samples with SiO_2>70 percent and $Fe\#_{displacement}$>0 was assigned a score of 1 (table 11).

Aerial Gamma-Ray Survey Data

Data from the aerial gamma-ray surveys include measurement of the naturally occurring radioactive element ^{238}U across Alaska (Duval, 2001). Uranium data are reported in equivalent ppm (eq. U ppm). HUCs containing data with U equivalents ≥5 (eq. U ppm) received a score of 2, and HUCs between eq. U ppm ≥2 and <5 scored 1 (table 11). The maximum score for each HUC was assigned on the basis of the maximum eq. U ppm value anywhere within the HUC.

ARDF

Alaska Resource Data File records were searched for prospective ssU occurrences using the keywords and associated scores for ssU deposits in appendix C. The results from the word-hit search were further limited to only those records with U as a "main" or "other" commodity. These records were reviewed individually and retained if (1) the deposit-type model type was ssU or roll-front, (2) if no deposit type was given and lode, granite, vein, dike, phosphates, or skarn were not present in any of the descriptive fields, or (3) if the deposit type was a placer with U present as either a major or minor commodity. The retained ARDF records contributed a score of 1 for the HUC they occur in (table 11).

Results and Discussion

A score of 14 was the maximum total attainable using the scoring procedure for ssU deposits described above (table 11). Table 12 outlines the criteria by which estimated mineral resource potential and certainty were assigned. Because the best described ssU deposit in Alaska (the Death Valley deposit) is outside of the CYPA (plate 10), our classification of estimated mineral resource potential and certainty was informed by initial analysis of HUCs across the entire State. In the statewide analysis, HUC scores ranged from 0 to 10, and the HUC containing the Upper Tubutulik River and the Death Valley deposit scored seven. Thus, a score of seven and higher was assigned high potential. HUCs with scores of 4–6 and 0–3 were assigned medium and low potential, respectively. Although it was possible for a HUC to receive a total score of 4 based on lithology alone or a combination of the lithology and coal score, no HUC was allowed to receive a medium potential rating based solely on host rock favorability lacking any indication of a U-mineralizing process. HUCs with total scores of 4 derived only host-rock favorability were assigned low potential (table 12).

The classification of certainty was based on the number of datasets that contributed out of a possible seven (table 12). High certainty was assigned when 5–7 datasets contributed to the total score, and medium and low certainty were assigned when 3–4 and 0–2 datasets contributed, respectively. Two exceptions to this are that (1) an HUC with a score from a reviewed and retained ARDF record was always assigned high certainty and (2) an HUC with a total score of zero was assigned high certainty. A value of unknown was only assigned to an HUC if it (1) lacked stream-sediment data and had a total score of zero or (2) lacked stream-sediment data and the total score was completely based on the lithology, lithology + coal, or the aeroradiometric data score.

Results for ssU are shown in plate 9, and accompanying data are presented in appendix E. Of the 2,460 HUCs in the CYPA, 51 (2 percent of total) have high potential for ssU. Of these, 46 (90.2 percent of high-potential HUCs) also have high certainty and 5 (9.8 percent of high potential) had medium certainty. 543 HUCs (22 percent of total) have medium potential, with either high (51 percent of medium potential) or medium (49 percent of medium potential)

certainty. 75 percent of the HUCs in the CYPA (1,847 total) have low potential for ssU, and most in this category have either high (36 percent of low potential) or medium (64 percent of low potential) certainty. There are 251 HUCs with a total score of zero, but only a small number of these (4) were assigned unknown potential and unknown certainty.

The results identified three general areas of high potential for ssU deposits at or within the boundaries of the CYPA. high potential HUCs occur within the trend of the Ruby Batholith, the northeastern portion of the Hogatza igneous belt (Shungak and Hughes quadrangles), and an area bordering the Fairbanks and Healy quadrangles (plate 10). The high potential HUCs typically contain favorable lithologies such as sedimentary rock and Tertiary/Cretaceous sediments or arkose sandstone. Coal is present in 33 percent of the high potential HUCs. These high potential HUCs also commonly contain one or more of the following: (1) favorable ARDF records, (2) sediment data above the 98th percentile value for U content (≥ 20 ppm), (3) radiometric uranium equivalents >2 eq. U ppm, and (or) (4) a highly differentiated and potentially U-rich igneous body.

Within the CYPA, medium-potential HUCs cluster around the high-potential HUCs, except for a cluster of 16 medium-potential HUCs that cross the Hughes/Melozitna quadrangle boundary and another cluster of 42 HUCs that cross the Kateel River, Nulato, and Norton Bay quadrangle boundaries in the southwestern portion of the CYPA (plate 10). The host-rock setting for the cluster of 16 medium-potential HUCs is the generalized sedimentary lithologic unit and coal is not present. Within this grouping, all of the 16 HUCs have stream-sediment samples at or above the 75th percentile, and 7 have U content between the 91st and 98th percentile value. All 16 HUCs also have radiometric uranium equivalents >2 and ≤5 eq. U ppm.

The host rock setting for the cluster of 42 medium-potential HUCs is the generalized sedimentary class and 41 of 42 have coal present. Thirty-seven of these HUCs have a stream-sediment sample above the 75th percentile value for U content, with six between the 91st and 98th percentile value for U content. Half of the 42 HUCs in the belt have radiometric uranium equivalents >2 and ≤5 eq. U ppm.

To better characterize the areas of high and medium potential for the ssU deposit model, future work might include rock and stream-sediment geochemical and mineralogical sampling in these areas to better determine the U source(s) and geologic mapping might be refined to better delineate extent and characteristics of the sedimentary deposits.

Sn-W-Mo (-Ta-In-fluorspar) Deposits Associated with Specialized Granites

The mineral commodities Sn, W, Mo, Ta, In, and fluorspar (industry term for fluorite, cubic CaF_2) do not always occur as a group, but they are commonly found in various combinations closely associated with highly evolved felsic intrusive rocks that are grouped herein as specialized granites (for example, Reed, 1986). Specialized granites include granite porphyries, peraluminous granites, and high-silica (>73 percent SiO_2; Rogers and Greenberg, 1990; Blatt and others, 2006) granites. Such granites tend to be found in tectonic environments that relate to thickening, contraction, or extension of continental crust. With some exceptions, the common petrogenetic characteristics of specialized granites and their associated dikes and sills are that they (1) are late-stage magmatic phases containing elevated concentrations of incompatible elements as a result of fractional crystallization and (2) have sources that include continental crust. Mineral deposits associated with specialized granites mainly occur in dikes, veins, stockworks, and greisens or hydrothermally altered zones near the top of granite intrusions or in skarns in carbonate wall rock adjacent to the other features just named near the top of the

granite. In systems associated with specialized granites, Sn ore minerals are mainly cassiterite and less commonly stannite, W is mainly found in scheelite and wolframite, and Mo is mainly found in molybdenite. Tantalum occurs mainly in columbotantalite and less often in wodginite or microlite. Indium typically occurs as a substitution in sphalerite, cassiterite, and (or) stannite, and is found rarely as roquesite.

Specialized granites in this model include a range of compositions because many factors can influence production and crystallization of silicic magma. The formation of specialized granites can include late phases associated with large magma systems or localized anatectic melts, and a common characteristic of these diverse granites is their relatively small volume. For example, granite porphyries that contain Sn, W, and Mo mineralization form at lower temperatures and lower sulfidation states and also tend to be smaller in size than Cu and Cu-Au porphyries (Seedorff and others, 2005). Most economic concentrations of Sn, W, Mo, Ta, and In, with or without fluorspar, are associated with peraluminous granites. Peraluminous granites have high ASI values, are corundum normative, and commonly contain aluminous minerals such as cordierite, garnet, muscovite, andalusite, sillimanite, topaz, tourmaline, and biotite. Pegmatites, veins, and dikes that contain elevated concentrations of Sn, Ta, W, Mo, Cs, and Li are classified as lithium-cesium-tantalum (LCT) pegmatites (Černý and others, 2005), which commonly occur within and peripheral to the cupolas of peraluminous and highly evolved granites (Černý, 1991; Černý and others, 2005; Johan and others, 2012). Indium is a common impurity in Zn-, Sn-, and Cu-sulfides, and in Sn-oxides (cassiterite) in Sn-W veins, pegmatites, and skarns associated with evolved granitic rocks (Černý and others, 2005; Ishihara and others, 2006; Sinclair and others, 2006). Fluorine and H_2O are important agents for transport of Sn, In, Ta, and W in fluids exsolved from peraluminous granite melts (Dobson, 1982; Swanson and others, 1990; Černý and others, 2005; Johan and others, 2012). Highly fractionated, LCT granites and pegmatites are also thought to be enriched in F by anatectic crustal melts (Černý, 1991). This possibility is consistent with the high initial $^{87}Sr/^{86}Sr$ ratios for peraluminous Sn-granites in Australia (Clemens and Wall, 1984; Blevin and Chappell, 1992) and in Alaska (see table 1 for localities; Hudson and Arth, 1983; Arth and others, 1989).

Specialized granites associated with Sn deposits generally have elevated Sn concentrations relative to average granite (Černý and others, 2005). However, W, Mo, Ta, and In do not always vary directly with Sn concentration in granite. In some systems, Ta varies inversely with Sn and increases upward in the mineral columbotantalite (Puchner, 1986). Porphyry-Sn granites are not common and are only well documented in Bolivia (Grant and others, 1980).

Mineable deposits of tin are mainly found in skarns, greisens, simple Sn-veins and Sn-polymetallic veins (table 1). Greisens associated with evolved granites consist of quartz, white mica, and cassiterite, with or without scheelite, molybdenite, pyrite, and (or) fluorite, that form in the upper roof zones of hydrothermally altered granite (endogreisen), or as alteration of wall rocks of the intrusions (exogreisen). Additional minerals found less commonly in greisen include tourmaline, topaz, garnet, axinite, arsenopyrite, sphalerite, and chalcopyrite. A characteristic mineral that occurs in greisens in Sn-granites is lithium (Li) rich annite (formerly “zinnwaldite”), where annite is the iron-rich end member of the biotite-phlogopite micas. Alaska has a well-known province of Sn granites and associated Sn occurrences on the northwestern Seward Peninsula (Hudson and Arth, 1983), as well as widely scattered Sn occurrences in interior Alaska between the central Alaska Range and the central Brooks Range and to the west of the Alaska Range (fig. 1; Hudson and Reed, 1997). Key deposits and occurrences in Alaska are summarized in table 1. Tin has also been mined from alluvial placers, mainly as cassiterite.

Concentrations of tungsten are recognized in both oxidized (magnetite-series) and reduced (ilmenite-series) granites; porphyry-W deposits are rare (table 1; Seedorff and others, 2005). Granite porphyries that contain W are described in the Fairbanks area in Alaska (fig. 1; Newberry and others, 1990). Tungsten is typically concentrated in veins and greisens around the margins of highly evolved granites (Werner and others, 1998), and is mined mainly from skarns in carbonate wall rocks adjacent to the granites and from veins (table 1). Although high W contents result from extended melt fractionation, W contents of granites associated with scheelite skarns are not commonly elevated relative to other igneous rocks (Newberry and Swanson, 1986; Černý and others, 2005). It is common for W-skarns to contain Sn, for Sn-skarns to contain W, and for W-skarns to contain some Mo. Fluorspar is typically found as either a principal product with Sn and W in vein, greisen, and skarn deposits associated with highly evolved granites or as an unrecovered accessory mineral in rocks mined for W or Sn (Richards and others, 2003). Late stage Sn-, Zn-, and Cu-sulfide veins and breccias that post-date W-Mo mineralization can contain significant concentrations of indium (Sinclair and others, 2006). In southeastern Japan, ilmenite granites contain late-stage cassiterite-wolframite (Sn-W) quartz veins that contain as much as 0.8 percent Indium, in association with scheelite-molybdenite skarn deposits (Ishihara and others, 2006). Scheelite-skarns and -veins associated with ilmenite-series granites within the CYPA near Fairbanks (fig. 1; Newberry and Swanson, 1986) might have similar potential for In concentrations.

Magmatic-associated Mo deposits include a broad range of compositions for shallowly emplaced to hypabyssal intrusive rocks, but molybdenum is mined principally from two types of deposits—(1) Climax-type porphyry Mo systems, where it is the principal product (White and others, 1981; Seedorff and Einaudi, 2004), and (2) porphyry Cu (-Mo) deposits, where it is a byproduct of mining large-tonnage, low-grade copper deposits (Seedorff and others, 2005). In the range of compositions between those two granite porphyry types is a group of deposits classified as low-fluorine porphyry Mo deposits (Theodore, 1986; Ludington and Plumlee, 2009). In the Climax-type deposits, molybdenum is associated with high-K, aluminous granite and rhyolite porphyry with more than 73 weight percent SiO_2 (White and others, 1981). The specialized granite-scoring model herein is intended to identify Climax-type and low-F porphyry Mo-type deposits. It does not target the more prevalent porphyry Cu (-Mo) deposits (Cox, 1986), although it might identify areas prospective for porphyry Cu deposits because of associated Mo enrichments.

Late intrusive or hydrothermal activity associated with specialized granites can remobilize Sn, W, Mo, Ta, and In. However, high-volatile (especially F) contents in near-solidus melts make it difficult to distinguish magmatic versus aqueous fluid effects (Černý and others, 2005, and references therein).

There are few known Sn-W-Mo deposits in Alaska at present (table 1), and there are no known deposits in the CYPA at this time. Most known Sn-W-Mo prospects and occurrences in the CYPA are either placer deposits containing cassiterite or other Sn- or Ta- bearing minerals or relatively localized features such as veins, skarns, or greisens associated with larger igneous bodies (table 1).

Mineral Resource Potential Estimation Methodology

To estimate mineral resource potential for Sn, W, Mo , Ta, In, and fluorspar deposits in specialized granites in the CYPA, the following five criteria were scored: (1) specialized granite compositions indicated by element ratios, (2) igneous rock geochemistry, (3) presence or absence

of known economic mineral occurrences, deposits, or mines, (4) stream-sediment geochemistry, and (5) aerial gamma-ray survey data. The significance and application of these criteria are briefly described below and summarized in table 13.

Igneous-Rock Geochemistry

Igneous-rock geochemical data were used to identify permissive rock types for Sn-W-Mo deposits, particularly rocks meeting the classification of specialized granite as described above. These distinctive igneous rock compositions are relatively easy to identify using geochemical data from individual rock samples or suites of rock samples, and the distribution of igneous rock samples across the CYPA provides more detail than geological maps typically portray, especially considering the compositional complexity of many igneous systems and a general lack of detailed geologic mapping. The method of discriminating the presence of specialized granites described herein offers three advantages—(1) geochemistry provides an objective test of key compositional criteria for identification of permissive rock compositions; (2) geochemical data are also spatially referenced to dikes and small satellite bodies that can be associated with Sn-W-Mo mineralization but are not typically captured in mapped units; and (3) rock-sample data correspond to discrete locations within an HUC, which provides greater geospatial precision for rock compositions than is provided by granite map units that commonly span several HUCs. For these reasons, igneous-rock geochemistry was favored over using geological map units alone to better identify the specific compositions of interest across the area.

Two scoring components based on igneous rock geochemical criteria were used to identify specialized granite compositions that have potential to host Sn-W-Ta-Mo-In and fluorspar mineral deposits (table 13). The first scoring component is defined based on the values derived from two ratios—(1) the aluminum saturation index, or ASI (modal Al/[(Ca-1.67×P)+Na+K]; Shand, 1947), and modal Al/[Na+K] (ANK), which allows differentiation between peraluminous (ASI>1), metaluminous (ANK>1), and peralkaline (ANK>1) rock types (Maniar and Piccoli, 1989), and (2) the Ga/Al ratio, which at 10,000×Ga/Al>2.6 can distinguish alkaline and subalkaline igneous rock types (Whalen and others, 1987), and which also serves as a proxy monitor of fluorine contents because of the higher solubility of GaF_6 relative to AlF_6. This ratio also has utility for identifying Sn and In concentrations because these elements are positively correlated with F in granite. The Ga/Al ratio has only been calibrated for granitic (intermediate and felsic) rock compositions (Whalen and others, 1987), and, because highly fractionated igneous rocks were the target of this deposit model, scoring of both the ASI and Ga/Al parameters was limited to igneous rocks with >65 weight percent SiO_2.

The second scoring component was composed of 6 factors based on contents of key elements in the granites, including SiO_2 and concentrations of the 5 target metals. Scores were assigned for contents of SiO_2>73 weight percent in order to identify specialized granites high in silica that might, in particular, correspond to siliceous porphyries that contain Mo deposits. The cutoff at 73 wteight percent silica was chosen based on the normalized average silica composition of four different suites of granite (Rogers and Greenberg, 1990) and based on published silica values for granite porphyries that contain Mo at Climax (White and others, 1981) and at Quartz Hill (Ashleman and others, 1997). Points were assigned for igneous rocks in the geochemical database that have In, Mo, Sn, Ta, and W abundances at or above the 91st percentile, which significantly exceed average upper continental crustal abundances for these elements (table 14; Taylor and McLennan, 1995).

As with other models, nonsystematic rock sampling and incomplete igneous-rock exposure across the CYPA area led to variable coverage of igneous-rock geochemical data, so for each chemical scoring component (peraluminous, Ga/Al, and single element concentrations), a single point was assigned if a sample within an HUC exceeded cutoff values in table 13, for a maximum igneous rock score of 8 points (table 13).

ARDF

Mineral occurrence records compiled in the ARDF database were scored on the basis of keywords in the various descriptive fields as described in the introduction of this report. Keywords of interest included individual elements and commodities (for example, Sn, W, Ta, In, and Mo) and host minerals (for example, fluorite, cassiterite, scheelite, and wolframite) in the records (see appendix D). Fluorite described in ARDF records provides the only direct indication for its actual presence across the CYPA, because fluorine was not routinely or reliably measured for rock or stream-sediment samples in the geochemical databases. The cumulative keyword hits contributed to a net ARDF keyword score, with net scores higher than 4 representing favorable occurrences based on statistical analysis and verification by inspection of individual records. The results of the ARDF scoring output were reviewed for each record to ensure that known occurrences received appropriate scores and that occurrences unlikely to contain potential for Sn, W, Ta, Mo, In, and (or) F mineralization were not ranked inappropriately. Many ARDF localities that received high keyword scores were placer deposits, which were considered useful to include in the ranking process because, for example, placer cassiterite or scheelite suggest the presence of a nearby igneous source for those minerals. An ARDF keyword score higher than 19 corresponded to mineral occurrences with keyword hits for multiple categories in an ARDF record, suggesting high resource potential. By this reasoning, on the basis of statistical breaks in the ARDF score distribution, localities with scores of 4 to 19 were assigned 1 point, and localities with scores of 20 or higher were assigned 2 points (table 13). Although some HUCs contain more than one ARDF locality, the maximum score for any ARDF locality in the HUC provides the maximum score for the HUC, so a single HUC can have a maximum ARDF score of 2 points.

Stream-Sediment Geochemistry

Stream-sediment concentrations for five representative elements (In, Mo, Sn, Ta, W) were scored at two levels for this deposit model (table 13). A score of 1 point was assigned for stream-sediment concentrations of the target elements from the 91st to the 98th percentile and a score of 2 points for values in the 98th percentile or greater. Each HUC was scored based on the maximum possible value of any single stream-sediment sample it contained, such that the maximum possible score for a stream-sediment sample that had high values in all the target elements is 10.

Aerial Gamma-Ray Survey Data

Equivalent thorium concentrations (eq. ppm Th) in aerial gamma-ray surveys were measured by proxy from gamma-rays emitted from radioactive ^{208}Tl, the daughter product of ^{232}Th decay. These data help to identify igneous rocks associated with potential for incompatible elements, such as Sn, W, and Ta, that are commonly accompanied by Th. As stated above, aerial radiometric Th values correlate with Th concentrations in stream sediments, suggesting that the

radiometric surveys indicate areas that might be fed by material from Th- and incompatible-element-bearing rocks. HUCs with Th values ≥75th percentile (~6 eq. ppm Th; Duval, 2001) were assigned a score of 1 point, a smaller percentage of the total score than other parameters because elevated Th values may, but do not necessarily, correspond to possible enrichments of Sn, W and (or) Ta. As with the other datasets, each HUC was limited to a score based on its maximum radioactivity, with a maximum value of 1 point (table 13).

Results and Discussion

The results of attribute analyses showed that the variety of rock types that hosted enriched concentrations of Sn, W, Ta, Mo, In, and F could not be applied to a discrete map unit, and in many cases could be overstated if assigned to a plutonic complex mapped as a single unit. This is consistent with descriptions of known occurrences at which concentrations of these commodities are almost entirely associated with veins and greisens associated with late phases of a variety of granitic rocks. These types of localized features are not commonly mapped as discrete units in the regional-scale maps available for Alaska. Thus, although "specialized granite" defines the best approximation of a host-rock type for a deposit model for theses commodities, the location of specialized granites is more precisely designated by analytical-data-point locations than by map units, and discrete sample locations within HUCs can (1) constrain the location of specialized granite phases within a larger generalized intrusive body and (2) identify the location of intrusive phases too small to appear at a regional map scale and isolated as dikes or veins in the host rocks of an intrusive body.

In the scoring method created for the Sn-W-Mo (-fluorspar-Ta-In) deposit model, stream-sediment geochemistry contributed as much as 50 percent of the total HUC score, which is considered valid for this dataset because it has the most comprehensive and systematic coverage for the CYPA and is quantitative evidence for the presence of the target elements. Igneous rock geochemistry, the best predictor of appropriate host rock types for undiscovered Sn, W, Mo, Ta, In, and (or) fluorspar resources in igneous rocks at a regional scale, accounted for as much as 35 percent of the total HUC score. ARDF localities, although important for showing locations of known Sn, W, Mo, Ta, In, and (or) fluorspar concentrations and indirectly suggesting the possibility of additional deposits in the vicinity, require prior knowledge or entry into the existing database, do not represent systematic evaluation of the project area, and more importantly, do not necessarily predict undiscovered resources in areas that do not contain known occurrences; therefore, ARDF localities contributed only as much as 10 percent of the total HUC score. Gamma-ray survey data contributed as much as 5 percent of total HUC score, because these data do not constitute as strong a predictor of the targeted deposits as do the other factors.

The total possible score an HUC could receive for Sn-W-Mo (-Ta-In-fluorspar) deposits was 21 points, and the maximum score for any HUC in the CYPA and buffer was 15 (appendix E). Composite scores were subdivided at natural statistical breaks by the Jenks method into three categories corresponding to low, medium, and high potential, with score ranges of 0–1, 2–5, and 6-21 points, respectively (table 15). Certainty values were assigned based on the number of datasets that contributed to the total score for each HUC, such that low, medium, and high values correspond to contributions of 0–1, 2–3, and 4–5 datasets, respectively (table 15).

Results of the scoring analysis for Sn-W-Mo (-Ta-In-fluorspar) deposits are shown in plate 11, and accompanying data are in appendix E. A total of 97 HUCs (4 percent of HUCs in the CYPA) are considered to have high potential to contain a mineral occurrence of this type. Of

those, 70 also have high certainty. There are 624 HUCs (25 percent of HUCs in the CYPA) that have medium potential. The remaining 1,724 HUCs (70 percent of the CYPA) have low potential on the basis of our scoring method. A total of 1,215 HUCs have total scores of 0; only 17 of these (<1 percent of CYPA) were classified as having unknown potential and certainty (plate 11, appendix E) because of a lack of data.

The areas that stand out as having the highest potential for Sn-W-Mo (-Ta-In-fluorspar) mineralization in the CYPA and its buffer zone include (1) areas underlain by Devonian felsic intrusive rocks in the southern Brooks Range, (2) areas near middle to Late Cretaceous intrusive rocks in the Hogatza igneous belt, (3) parts of the middle Cretaceous Ruby batholith, (4) areas near Late Cretaceous to early Tertiary intrusive rocks in the Tofty belt and discrete locations in the Sischu-Prindle igneous belt, and (5) the southeastern Yukon-Tanana upland (plate 12). Areas with moderate potential include (1) the Brooks Range, although generally with low certainty, (2) the Hogatza igneous belt, (3) most of the Ruby batholith and its inferred southwestern extension in the Kaiyuh Mountains area, (4) isolated HUCs, some of which are known to contain igneous rocks in the Yukon-Koyukuk Basin, (5) discrete locations in the Sischu-Prindle igneous belt, (6) a broad area of poor rock exposure to the southwest of known intrusive rocks east of Fairbanks, and (7) areas near known Cretaceous-Tertiary intrusive suites in the Yukon Tanana uplands and the northern foothills of the Alaska Range in the southeastern part of the CYPA (plate 12).

Three areas of interest that contain groups of HUCs that have medium to high potential but low certainty (based on limited available data) are (1) the area west of Fairbanks, (2) the area in the southeastern CYPA in the northern foothills of the Alaska Range near the Ptarmigan Creek deposits, and (3) the area in the southwestern CYPA in the vicinity of the Kaiyuh Mountains near the Illinois Creek and Round Top deposits. It is uncertain whether areas with low potential might be more favorable if additional data were available, but combinations of available datasets in some cases suggest the presence of appropriate rocks in regions of poor exposure. For example, in some areas where igneous rocks are not mapped, stream sediments have high values for Sn, W, Mo, Ta, and (or) In, raising the possibility of potentially permissive rocks in areas where they were not previously documented. Specific areas that have high stream-sediment values for the target elements but lack information with respect to bedrock compositions, and lack known occurrences of the target commodities, include the Yukon Tanana uplands near Fairbanks and the southeastern corner of the CYPA (plate 12). These results suggest that areas with significant potential but low certainty warrant further investigation.

Summary

The method described herein provides means by which to assemble and analyze disparate datasets in a geospatial environment to map mineral resource prospectivity across broad areas such as the CYPA in Alaska. It is worth noting that the data distribution for the datasets used herein is generally not always consistent across the State. In particular, the number and spatial distribution of geochemistry sample localities differs significantly among 1:250,000-scale quadrangles throughout the State (Granitto and others, 2013). In some areas, ARDF records cluster around known occurrences, prospects, or mines and (or) they cluster in areas with easier means of access such as along roads or rivers. Attempts were made to equalize scores potentially skewed through uneven sampling by limiting the number of scores per database that could be applied to each HUC. The ability and opportunity to analyze and query the results has also been preserved by providing complete data regarding the individual scoring components and score results for each deposit group (appendix E). For those datasets such as the AGDB2, ADGGS

geochemical data, and ARDF that are publicly available, it is possible for an individual user to compile the same data and evaluate sampling trends and compare them to our scoring results across the CYPA.

The results described above highlight numerous areas, some of them large, rated with high potential for one or more of the selected deposit groups within the CYPA. The CYPA has recognizable potential for REE deposits associated with the Hogatza plutonic belt and parts of the Ruby batholith. Another area of high potential surrounds a known carbonatite occurrence near Tofty, Alaska, in the Hot Springs placer district. Placer-gold potential is relatively high along drainages scattered across the CYPA. Prospecting for and production from relatively small placer-gold deposits were widespread in the past and have continued to the present. Areas with high potential for PGE deposits associated with mafic and ultramafic rocks are in the northwestern Brooks Range to the west of the CYPA and in the Killik River quadrangle within the CYPA. Another area of high PGE potential flanks the Ruby batholith to the northwest, generally within and near the Kanuti River drainage. High potential for carbonate-hosted copper deposits exists outside the CYPA within the Gates of the Arctic National Park and Preserve along the south flank of and into the core of the Brooks Range. That discontinuous belt of high potential extends far to the northeast and includes areas within the CYPA in the Wiseman, Chandalar, and Philip Smith Mountains quadrangles. Other areas with high potential for copper deposits in carbonate rocks are in the southeastern CYPA and in the Brooks Range foreland. Sandstone uranium potential within the CYPA appears most closely associated with areas proximal to felsic intrusive igneous rocks such as the Hogatza plutonic belt and the Ruby batholith; the potential appears highest for a basal-type sandstone uranium deposit analogous with the Death Valley (Boulder Creek) deposit adjacent to the Darby pluton on the eastern Seward Peninsula. The highest potential for Sn-W-Mo-fluorspar deposits is associated with the Hogatza belt and Ruby batholith plutons, but high potential also occurs along the Tofty-Livengood belt of intrusive igneous rocks and in scattered areas within the Yukon-Tanana uplands.

Future geologic investigations might focus on areas that lack information but have relatively high potential scores based on limited available data. Land use planning decisions will benefit most from additional data in areas with low degrees of certainty because, in these areas, a lack of relevant data precludes sufficient evaluation of mineral potential. Mineral exploration targets will be most confidently pursued in areas of known potential.

Data Resources

Alaska Resource Data File (ARDF)—http://ardf.wr.usgs.gov/
Alaska Geochemical Database Version 2.0 (AGDB2)—http://pubs.usgs.gov/ds/759/
National Uranium Resource Evaluation (NURE) Hydrogeochemical and Stream Sediment Reconnaissance data—http://pubs.usgs.gov/of/1997/ofr-97-0492/
Alaska Division of Geological and Geophysical Surveys (ADGGS) WebGeochem geochemical sample analysis search—http://www.dggs.alaska.gov/webgeochem/
Alaska aerial gamma-ray surveys—http://pubs.usgs.gov/of/2001/of01-128/
Map of Alaska's coal resources (Merritt and Hawley, 1986)—http://www.dggs.dnr.state.ak.us/pubs/pubs?reqtype=citation&ID=2636

References Cited

Ames, D.E., Davidson, A., and Wodicka, N., 2008, Geology of the giant Sudbury polymetallic mining camp, Ontario, Canada: Economic Geology, v. 103, no. 5, p. 1057–1077.

Angiboust, S., Fayek, M., Power, I. M., Camacho, A., Calas, G., and Southam, G., 2012, Structural and biological control of the Cenozoic epithermal uranium concentrations from the Sierra Peña Blanca, Mexico: Mineralium Deposita, v. 47, no. 8, p. 859–874.

Arbogast, B.F., ed., 1990, Quality assurance manual for the Branch of Geochemistry, U.S. Geological Survey, U.S. Geological Survey Open-File Report 90–668, 184 p.

Arbogast, B.F., ed., 1996, Analytical methods manual for the Mineral Resource Surveys Program, U.S. Geological Survey, U.S. Geological Survey Open-File Report 96–525, 248 p.:

Armbrustmacher, T.J., 1989, Minor element content, including radioactive elements and rare-earth elements, in rocks from the syenite complex at Roy Creek: Mount Prindle area, Alaska: U.S. Geological Survey Open-File Report 89–0146, 11 p.

Arth, J.G., Criss, R.E., Zmuda, C.C., Foley, N.K., Patton, W.W., and Miller, T.P., 1989, Remarkable isotopic and trace element trends in potassic through sodic Cretaceous plutons of the Yukon-Koyukuk Basin, Alaska, and the nature of the lithosphere beneath the Koyukuk terrane: Journal of Geophysical Research, Solid Earth, v. 94, no. B11, p. 15,957–915,968.

Ashleman, J., Taylor, C., and Smith, P., 1997, Porphyry molybdenum deposits of Alaska, with emphasis on geology of Quartz Hill deposit, southeastern Alaska: Economic Geology Monograph, v. 9, p. 334–354.

Athey, J.E., Harbo, L.A., Lasley, P.S., and Freeman, L. K., 2013, Alaska's mineral industry, 2012: Alaska Division of Geological and Geophysical Surveys Special Report 68, p. 61.

Baker, T., 2002, Emplacement depth and carbon dioxide-rich fluid inclusions in intrusion-related gold deposits: Economic Geology, v. 97, no. 5, p. 1111–1117.

Barker, J.C., 1985, Sampling and analytical results of a mineral reconnaissance in the Selawik Hills area, northwestern Alaska: U.S. Bureau of Mines Open-File Report 43–85, 67 p.

Barker, J.C., 1991, Investigation of rare-earth elements and zirconium in the Windy Fork peralkaline pluton, west-central Alaska: U.S. Bureau of Mines Field Report, 36 p.

Barker, J.C., and Foley, J.Y., 1986, Tin reconnaissance of the Kanuti and Hodzana Rivers uplands, central Alaska: U.S. Bureau of Mines Information Circular 9104, 27 p.

Barker, J.C., and Swainbank, R.C., 1986, A tungsten-rich porphyry molybdenum occurrence at Bear Mountain, northeast Alaska: Economic Geology, v. 81, no. 7, p. 1753–1759.

Barker, S.L.L., Hickey, K.A., Cline, J.S., Dipple, G.M., Kilburn, M.R., Vaughan, J.R., and Longo, A.A., 2009, Uncloaking invisible gold; Use of nanoSIMS to evaluate gold, trace elements, and sulfur isotopes in pyrite from Carlin-type gold deposits: Economic Geology, v. 104, no. 7, p. 897–904.

Barnes, S.-J., and Lightfoot, P.C., 2005, The formation of magmatic nickel-copper-PGE sulfide deposits, *in* Hedenquist, J.W., Thompson, J.F.H., Goldfarb, R.J., and Richards, J.P., eds., Economic Geology one hundredth anniversary volume 1905–2005: Littleton, Colorado, Society of Economic Geologists, p. 179–213.

Barnes, S.J., Godel, B., Gürer, D., Brenan, J.M., Robertson, J., and Paterson, D., 2013, Sulfide-olivine Fe-Ni exchange and the origin of anomalously Ni rich magmatic sulfides: Economic Geology, v. 108, no. 8, p. 1971–1982.

Bea, F., 1996, Residence of REE, Y, Th and U in granites and crustal protoliths; Implications for the chemistry of crustal melts: Journal of Petrology, v. 37, no. 3, p. 521–552.

Beaty, D.W., Landis, G.P., and Thompson, T.B., 1990, Carbonate-hosted sulfide deposits of the Central Colorado mineral belt: Economic Geology Monograph 7, 424 p.
Bentzen, E.H., Ghaffari, H., Eng, P., Galbraith, L., Hammen, R.F., Robinson, R.J., Hafez, S.A., and Annavarapu, S., 2013, Preliminary economic assessment; Bokan Mountain rare earth element project, near Ketchikan, Alaska: Vancouver, British Columbia, Canada, Ucore Metals, Inc. [prepared by Tetra Tech, Inc.], document no. 1196000100-REP-R0001-02, 219 p.
Berger, B.R., and Henley, R.W., 1989, Advances in the understanding of epithermal gold-silver deposits, with special reference to the western United States, *in* Kcays, R.R., Ramsay, W.R.H., and Groves, D.I., eds., The geology of gold deposits; The perspective in 1988: Economic Geology Monograph 6, p. 405–423.
Berger, V.I., Singer, D.A., and Orris, G.J., 2009, Carbonatites of the World, Explored Deposits of Nb and REE--database and Grade and Tonnage Models, U.S. Geological Survey Open-File Report 2009–1139, 17 p. and database.
Bernstein, L.R., and Cox, D.P., 1986, Geology and sulfide mineralogy of the Number One Orebody, Ruby Creek copper deposit, Alaska: Economic Geology, v. 81, no. 7, p. 1675–1689.
Bittenbender, P.E., Bean, K.W., Kurtak, J.M., and Deininger, J., Jr., 2007, Mineral assessment of the Delta River mining district area, east-central Alaska, U.S. Bureau of Land Management, Alaska Technical Report 57, 676 p.
Blatt, H., Tracy, R.J., and Owens, B., 2006, Petrology: igneous, sedimentary, and metamorphic, 3d ed.: New York, W.H. Freeman and Company, 533 p.
Blevin, P.L., and Chappell, B.W., 1992, The role of magma sources, oxidation states and fractionation in determining the granite metallogeny of eastern Australia: Transactions of the Royal Society of Edinburgh; Earth Sciences, v. 83, no. 1-2, p. 305–316.
Bliss, J., ed., 1992, Developments in Mineral deposit modeling: U.S. Geological Survey Bulletin 2004, p. 168 p.
Bluemel, B., Leijd, M., Dunn, C., Hart, C.J., Saxon, M., and Sadeghi, M., 2013, Biogeochemical expression of rare earth element and zirconium mineralization at Norra Kärr, Southern Sweden: Journal of Geochemical Exploration, v. 133, p. 15–24.
Blundy, J., and Wood, B., 2003, Mineral-melt partitioning of uranium, thorium and their daughters: Reviews in Mineralogy and Geochemistry, v. 52, no. 1, p. 59–123.
Borg, G., Frotzscher, M., and Ehling, B., 2005, Metal content and spatial distribution of Au and PGE in the Kupferschiefer of the Mansfeld/Sangerhausen mining district, Germany: Mineral Deposit Research; Meeting the Global Challenge, proceedings of the eighth biennial SGA meeting, p. 885–888.
Boyle, D.R., 1982, The formation of basal-type uranium deposits in south central British Columbia: Economic Geology, v. 77, no. 5, p. 1176–1209.
Burleigh, R.E., 1992, Tin mineralization at the Won Prospect, west-central Alaska: U.S. Bureau of Mines Open-File Report 85–92, p. 21 p.
Burton, P.J., 1981, Radioactive mineral occurrences, Mount Prindle area, Yukon-Tanana uplands, Alaska: Fairbanks, University of Alaska, M.S. thesis, 72 p.
Castor, S.B., 2008, The Mountain Pass rare-earth carbonatite and associated ultrapotassic rocks, California: The Canadian Mineralogist, v. 46, no. 4, p. 779–806.
Černý, P., 1991, Rare-element granitic pegmatites, Part I; Anatomy and internal evolution of pegmatitic deposits: Geoscience Canada, v. 18, p. 49–67.
Černý, P., Blevin, P.L., Cuney, M., and London, D., 2005, Granite-related ore deposits, *in* Hedenquist, J.W., Thompson, J.F.H., Goldfarb, R.J., and Richards, J.P., eds., Economic

Geology one hundredth anniversary volume 1905–2005: Littleton, Colorado, Society of Economic Geologists, p. 337–370.
Chao, E.C., Back, J., Minkin, J., Tatsumoto, M., Wang, J., Conrad, J., McKee, E., Hou, Z., Meng, Q., and Huang, S., 1997, The sedimentary carbonate-hosted giant Bayan Obo REE-Fe-Nb ore deposit of Inner Mongolia, China; A cornerstone example for giant polymetallic ore deposits of hydrothermal origin, U.S. Geological Survey Bulletin 2143, n.p.
Cheilletz, A., Clark, A.H., Farrar, E., Pauca, G.A., Pichavant, M., and Sandeman, H.A., 1992, Volcano-stratigraphy and $^{40}Ar/^{39}Ar$ geochronology of the Macusani ignimbrite field; monitor of the Miocene geodynamic evolution of the Andes of southeast Peru: Tectonophysics, v. 205, no. 1, p. 307-327.
Clemens, J.D., and Wall, V.J., 1984, Origin and evolution of a peraluminous silicic ignimbrite suite; the Violet Town Volcanics: Contributions to Mineralogy and Petrology, v. 88, no. 4, p. 354–371.
Cobb, E.H., compiler, 1972, Metallic mineral resources map of the Nulato quadrangle, Alaska: U.S. Geological Survey Miscellaneous Field Studies Map MF-423, 1 sheet, scale 1:250,000.
Cox, D.P., 1986, Descriptive model of porphyry Cu *in* Cox, D.P., and Singer, D.A., eds., Mineral deposit models: U.S. Geological Survey Bulletin, 1693, p. 76.
Cox, D.P., and Singer, D.A., eds.,1986, Mineral deposit models: U.S. Geological Survey Bulletin 1693, 379 p.
Cuney, M., and Kyser, T.K., 2009, Recent and not-so-recent developments in uranium deposits and implications for exploration: Mineralogical Association of Canada, Short Course 39, 257 p.
Czamanske, G.K., Haffty, J., and Nabbs, S.W., 1981, Pt, Pd, and Rh analyses and beneficiation of mineralized mafic rocks from the La Perouse Layered Gabbro, Alaska: Economic Geology, v. 76, no. 7, p. 2001–2011.
Dashevsky, S.S., 2002, Alaska Resource Data File, Norton Bay Quadrangle, Alaska: U.S. Geological Survey Open-File Report 02–75, 27 p.
Davis, B., Sim, R., and Austin, J., 2014, Technical Report on the Bornite Project, Northwest Alaska, USA: Vancouver, British Columbia, Canada, NovaCopper Inc. [Report prepared by BD Resource Consulting, Inc., SIM Geological Inc., and International Metallurgical & Environmental Inc.], NI 43-101, 142 p.
Dickinson, K.A., Cunningham, K.D., and Ager, T.A., 1987, Geology and origin of the Death Valley uranium deposit, Seward Peninsula, Alaska: Economic Geology, v. 82, no. 6, p. 1558–1574.
Dobson, D.C., 1982, Geology and alteration of the Lost River tin-tungsten-fluorine deposit, Alaska: Economic Geology, v. 77, no. 4, p. 1033–1052.
Dostal, J., Karl, S. M., Keppie, J.D., Kontak, D.J., Shellnutt, J.G., and Murphy, B., 2013, Bokan Mountain peralkaline granitic complex, Alexander terrane (southeastern Alaska): evidence for Early Jurassic rifting prior to accretion with North America: Canadian Journal of Earth Sciences, v. 50, no. 6, p. 678–691.
Dostal, J., Kontak, D.J., and Karl, S.M., 2014, The early Jurassic Bokan Mountain peralkaline granitic complex (southeastern Alaska); Geochemistry, petrogenesis and rare-metal mineralization: Lithos, v. 202, p. 395–412.
Duval, J.S., 2001, Aerial gamma-ray surveys in Alaska: U.S. Geological Survey Open-File Report 01–128.
Eby, G.N., 1990, The A-type granitoids; A review of their occurrence and chemical characteristics and speculations on their petrogenesis: Lithos, v. 26, p. 115–134.

Eckstrand, O.R., ed., 1985, Canadian mineral deposit types; a geological synopsis: Geological Survey of Canada, Economic Geology Report 36, 68 p.
Eckstrand, O.R., and Hulbert, L. J., 2007, Magmatic nickel-copper-platinum group element deposits *in* Goodfellow, W.D., ed., Mineral deposits of Canada; A synthesis of major deposit-types, district metallogeny, the evolution of geological provinces, and exploration methods: Geological Association of Canada, Mineral Deposits Division, Special Publication no. 5, p. 205–222.
Flanigan, B., 1998, Genesis and mineralization of ore deposits in the Illinois Creek region, west central Alaska: Anchorage, University of Alaska, M.S. thesis, 125 p.
Foley, J., and Barker, J., 1986, Uranium occurrences in the northern Darby Mountains, Seward Peninsula, AK: U.S. Bureau of Mines Information Circular 9103, 27 p.
Foley, J.Y., and Barker, J.C., 1984, Chromite deposits along the Border Ranges fault, southern Alaska (in two parts); 1. Field investigations and descriptions of chromite deposits, Avondale, Maryland: U.S. Bureau of Mines Information Circular 8990, 58 p.
Foley, J., Light, T., Nelson, S., and Harris, R., 1997, Mineral occurrences associated with mafic-ultramafic and related alkaline complexes in Alaska: Economic Geology, v. 9, p. 396–449.
Force, E.R., 1991, Geology of titanium-mineral deposits: Geological Society of America Special Papers, v. 259, p. 1–112.
Frimmel, H., Groves, D., Kirk, J., Ruiz, J., Chesley, J., and Minter, W., 2005, The formation and preservation of the Witwatersrand goldfields, the world's largest gold province *in* Hedenquist, J.W., Thompson, J.F.H., Goldfarb, R.J., and Richards, J.P., eds., Economic Geology one 1905–2005 anniversary volume: Littleton, Colorado, Society of Economic Geologists, p. 769–797.
Frost, B.R., and Frost, C.D., 2008, A geochemical classification for feldspathic igneous rocks: Journal of Petrology, v. 49, no. 11, p. 1955–1969.
Frost, C.D., and Frost, B.R., 2011, On ferroan (A-type) granitoids; their compositional variability and modes of origin: Journal of Petrology, v. 52, no. 1, p. 39–53.
Frost, B.R., Barnes, C.G., Collins, W.J., Arculus, R.J., Ellis, D.J., and Frost, C.D., 2001, A geochemical classification for granitic rocks: Journal of Petrology, v. 42, no. 11, p. 2033–2048.
Garnett, R.H.T., and Bassett, N. C., 2005, Placer deposits, *in* Hedenquist, J.W., Thompson, J.F.H., Goldfarb, R.J., and Richards, J.P., eds., Economic Geology one hundredth anniversary volume 1905–2005: Littleton, Colorado, Society of Economic Geologists, p. 813–843.
Ghaffari, H., Morrison, D.R.S., Ruijter, M.A. d., Živković, A., Hantelmann, T., Ramsey, D., and Cowie, S., 2011, Preliminary assessment of the Pebble project Southwest Alaska: Vancouver, British Columbia, Canada, Northern Dynasty Minerals, Ltd. [produced by Terra Tech, Inc.], document no. 1056140100-REP-R0001-00, 529 p.
Goldfarb, R.J., Baker, T., Dubé, B., Groves, D.I., Hart, C.J.R., and Gosselin, P., 2005, Distribution, character, and genesis of gold deposits in metamorphic terranes, *in* Hedenquist, J.W., Thompson, J.F.H., Goldfarb, R.J., and Richards, J.P., eds., Economic Geology one hundredth anniversary volume 1905–2005: Littleton, Colorado, Society of Economic Geologists, p. 407–450.
Granitto, M., Bailey, E.A., Schmidt, J.M., Shew, N.B., Gamble, B.M., and Labay, K.A., 2011, Alaska Geochemical Database (AGDB)—Geochemical Data for Rock, Sediment, Soil, Mineral and Concentrate Sample Media: U.S. Geological Survey Data Series 637, 31 p. and database, 1 DVD.
Granitto, M., Schmidt, J.M., Shew, N.B., Gamble, B.M., and Labay, K.A., 2013, Alaska Geochemical Database, Version 2.0 (AGDB2)—including "best value" data compilations for

rock, sediment, soil, mineral, and concentrate sample media: U.S. Geological Survey Data Series 759, 20 p. and database, 1 DVD.
Grant, J.N., Halls, C., Sheppard, S.M., and Avila, W., 1980, Evolution of the porphyry tin deposits of Bolivia, *in* Ishihara, S., and Takenouchi, S., eds., Granitic magmatism and related mineralization: The Society of Mining Geologists of Japan, Mining Geology Special Issue, no. 8, p. 151–173.
Groves, D., Goldfarb, R., Gebre-Mariam, M., Hagemann, S., and Robert, F., 1998, Orogenic gold deposits; A proposed classification in the context of their crustal distribution and relationship to other gold deposit types: Ore Geology Reviews, v. 13, p. 7–27.
Guilbert, J.M., and Park, C.F., 1986, The geology of ore deposits: Long Grove, Illinois, Waveland Press, Inc., 985 p.
Hamilton, N.T.M., 1995, Controls on the global distribution of coastal titanium-zirconium placers: International Geology Review, v. 37, no. 9, p. 755–779.
Harris, D.C., and Cabri, L.J., 1991, Nomenclature of platinum-group-element alloys; review and revision: The Canadian Mineralogist, v. 29, no. 2, p. 231–237.
Harshman, E.N., 1972, Geology and uranium deposits, Shirley Basin area, Wyoming: U.S. Geological Survey Professional Paper 745, 82 p.
Hart, C.J.R., 2007, Reduced intrusion-related gold systems, *in* Goodfellow, W.D., ed., Mineral deposits of Canada; A synthesis of major deposit-types, district metallogeny, the evolution of geological provinces, and exploration methods: Geological Association of Canada, Mineral Deposits Division, Special Publication no. 5, p. 95–112.
Helsel, D.R., 2012, Statistics for censored environmental data using Minitab and R: New York, John Wiley and Sons, 344 p.
Himmelberg, G.R., and Loney, R.A., 1995, Characteristics and petrogenesis of Alaskan-type ultramafic-mafic intrusions, southeastern Alaska: U.S. Geological Survey Professional Paper 1564, 47 p.
Hitzman, M.W., 1986, Geology of the Ruby Creek copper deposit, southwestern Brooks Range, Alaska: Economic Geology, v. 81, no. 7, p. 1644–1674.
Höll, R., Kling, M., and Schroll, E., 2007, Metallogenesis of germanium—A review: Ore Geology Reviews, v. 30, no. 3–4, p. 145–180.
Hudson, T., and Arth, J.G., 1983, Tin granites of Seward Peninsula, Alaska: Geological Society of America Bulletin, v. 94, no. 6, p. 768–790.
Hudson, T., and Reed, B., 1997, Tin deposits in Alaska *in* Goldfarb, R.J., and Miller, L.D., eds., Mineral deposits of Alaska: Economic Geology Monograph, no. 9, p. 450–465.
Hulbert, L.J., 1997, Geology and metallogeny of the Kluane mafic-ultramafic Belt, Yukon Territory, Canada; eastern Wrangellia; a new Ni-Cu-PGE metallogenic terrane: Geological Survey of Canada Bulletin 506, 265 p.
Hulbert, L.J., Carne, R.C., Gregoire, D.C., and Paktunc, D., 1992, Sedimentary nickel, zinc, and platinum-group-element mineralization in Devonian black shales at the Nick Property, Yukon, Canada; a new deposit type: Exploration and Mining Geology, v. 1, no. 1, p. 39–62.
Huyck, H.L, 1990, When is a metalliferous black shale not a black shale, *in* Grauch, R.I., and Huyck, H.L.O., compilers, Metalliferous black shales and related ore deposits—Proceedings, 1989 United States Working Group Meeting, International Geological Correlation Program Project 254: U.S. Geological Survey Circular 1058, p. 42–56.
Irvine, T.N., and Baragar, W.R.A., 1971, A guide to the chemical classification of the common volcanic rocks: Canadian Journal of Earth Sciences, v. 8, no. 5, p. 523–548.

Ishihara, S., Hoshino, K., Murakami, H., and Endo, Y., 2006, Resource evaluation and some genetic aspects of indium in the Japanese ore deposits: Resource Geology, v. 56, no. 3, p. 347–364.
Johan, Z., Strnad, L., and Johan, V., 2012, Evolution of the Cínovec (zinnwald) granite cupola, Czech Republic; Composition of feldspars and micas, a clue to the origin of W, Sn mineralization: The Canadian Mineralogist, v. 50, no. 4, p. 1131–1148.
Kamona, A., and Günzel, A., 2007, Stratigraphy and base metal mineralization in the Otavi Mountain Land, Northern Namibia—a review and regional interpretation: Gondwana Research, v. 11, no. 3, p. 396–413.
Kampunzu, A., Cailteux, J., Kamona, A., Intiomale, M., and Melcher, F., 2009, Sediment-hosted Zn–Pb–Cu deposits in the Central African Copperbelt: Ore Geology Reviews, v. 35, no. 3, p. 263–297.
Keith, T.E.C., Page, N.J., Oscarson, R.L., and Foster, H.L., 1987, Platinum-group element concentrations in a biotite-rich clinopyroxenite suite, Eagle C-3 quadrangle, Alaska, *in* Hamilton, T.D., and Galloway, J.P., eds., Geologic studies in Alaska by the U.S. Geological Survey during 1986: U.S. Geological Survey Circular 998, p. 62–68.
Kelley, K.D., Lang, J.R., and Eppinger, R.G., 2013, The giant Pebble Cu-Au-Mo deposit and surrounding region, southwest Alaska; Introduction: Economic Geology, v. 108, no. 3, p. 397–404.
Kimball, A.L., Still, J.C., and Rataj, J.L., 1978, Mineral resources, *in* Brew, D.A., Johnson, B.R., Grybeck, D., Griscom, A., Barnes, ed., Mineral resources of the Glacier Bay National Monument Wilderness Study Area: U.S. Geological Survey Open-File Report 78–494, p. 1C–375C.
Kogarko, L., Lahaye, Y., and Brey, G., 2010, Plume-related mantle source of super-large rare metal deposits from the Lovozero and Khibina massifs on the Kola Peninsula, Eastern part of Baltic Shield; Sr, Nd and Hf isotope systematics: Mineralogy and Petrology, v. 98, no. 1–4, p. 197–208.
Kooiman, G., McLeod, M., and Sinclair, W., 1986, Porphyry tungsten-molybdenum orebodies, polymetallic veins and replacement bodies, and tin-bearing greisen zones in the Fire Tower Zone, Mount Pleasant, New Brunswick: Economic Geology, v. 81, no. 6, p. 1356–1373.
Kwak, T., and Askins, P., 1981, Geology and genesis of the F-Sn-W (-Be-Zn) skarn (wrigglite) at Moina, Tasmania: Economic Geology, v. 76, no. 2, p. 439–467.
Kwak, T.A.P., 1987, W-Sn skarn deposits and related metamorphic skarns and granitoids: Amsterdam, Netherlands, Elsevier, 468 p.
Le Bas, M., Kellere, J., Kejie, T., Wall, F., William, C., and Peishan, Z., 1992, Carbonatite dykes at Bayan Obo, Inner Mongolia, China: Mineralogy and Petrology, v. 46, no. 3, p. 195–228.
Le Bas, M.J., Le Maitre, R.W., Streckeisen, A., and Zanettin, B., 1986, A chemical classification of volcanic rocks based on the total alkali silica diagram: Journal of Petrology, v. 27, no. 3, p. 745–750.
Le Maitre, R.W., ed., 2002, Igneous Rocks; A Classification and Glossary of Terms: A Classification and Glossary of Terms; Recommendations of the International Union of Geological Sciences Subcommission on the Systematics of Igneous Rocks, 2d ed.: Cambridge, United Kingdom, Cambridge University Press, 236 p.
Li, C., Ripley, E.M., and Naldrett, A.J., 2009, A new genetic model for the giant Ni-Cu-PGE sulfide deposits associated with the Siberian flood basalts: Economic Geology, v. 104, no. 2, p. 291–301.

Linnen, R.L., Samson, I.M., Williams-Jones, A.E., and Chakhmouradian, A.R., 2014, Geochemistry of the Rare-Earth Element, Nb, Ta, Hf, and Zr Deposits, chap. 21 *in* Holland, H.D., and Turekian, K.K., eds., Geochemistry of mineral deposits: Treatise on Geochemistry (2d ed.), vol. 13, p. 543–568.

Loney, R.A., and Himmelberg, G.R., 1989, The Kanuti ophiolite, Alaska: Journal of Geophysical Research, Solid Earth, v. 94, no. B11, p. 15,869–815,900.

Long, K.R., Van Gosen, B.S., Foley, N.K., and Cordier, D., 2010, The principal rare earth elements deposits of the United States—A summary of domestic deposits and a global perspective: U.S. Geological Survey Scientific Investigations Report 2010–5220, p. 96.

Ludington, S., and Plumlee, G.S., 2009, Climax-type porphyry molybdenum deposits: U.S. Geological Survey Open-File Report 2009–1215, 16 p.

Ludington, S.D., Hammarstrom, J., and Piatak, N., 2009, Low-fluorine stockwork molybdenite deposits: U.S. Geological Survey Open-File Report 2009–1211, 9 p.

MacKevett, E.M., Jr., Cox, D.P., Potter, R.W., II, and Silberman, M.L., 1997, Kennecott-type deposits in the Wrangell Mountains, Alaska; High-grade copper ores near a basalt-limestone contact, *in* Goldfarb, R.J., and Miller, L.D., eds., Mineral deposits of Alaska: Economic Geology Monograph 9, p. 66–89.

Maniar, P.D., and Piccoli, P.M., 1989, Tectonic discrimination of granitoids: Geological Society of America Bulletin, v. 101, no. 5, p. 635–643.

Mernagh, T.P., Wyborn, L.I.A., and Jagodzinski, E.A., 1998, 'Unconformity-related' U ± Au ± platinum-group-element deposits: Australian Geological Survey Organization, Journal of Australian Geology & Geophysics, v. 17, no. 4, p. 197–205.

Merritt, R.D., and Hawley, C.C., 1986, Map of Alaska's coal resources: Alaska Dept. of Natural Resources, Division of Mining and Geological and Geophysical Surveys Special Report 37, 1 sheet, scale 1:2,500,000.

Middlemost, E., 1990, Mineralogy and petrology of the rauhaugites of the Mt Weld carbonatite complex of Western Australia: Mineralogy and Petrology, v. 41, no. 2–4, p. 145–161.

Miesch, A.T., 1976, Sampling designs for geochemical surveys—Syllabus for a short course, U.S. Geological Survey Open-File Report 76–772, 127 p.:

Miller, J.D., Jr., Green, J.C., Severson, M.J., Chandler, V.W., Hauck, S.A., Peterson, D.M., and Wahl, T.E., 2002, Geology and mineral potential of the Duluth complex and related rocks of northeastern Minnesota: Minnesota Geological Survey Report of Investigations 58, 207 p.

Miller, T.P., and Ferrians, O., Jr., 1968, Suggested areas for prospecting in the central Koyukuk River region, Alaska: U.S. Geological Survey Circular 570, 12 p.

Miller, T.P., Moll, E., and Patton W.W., Jr., 1980, Uranium- and thorium-rich volcanic rocks of the Sischu Creek area, Medfra quadrangle, Alaska: U.S. Geological Survey Open-File Report 80–803, 9 p.

Minter, W.E.L., 2006, The sedimentary setting of Witwatersrand placer mineral deposits in an Archean atmosphere, *in* Kesler, S.E., and Ohmoto, H., eds., Evolution of early Earth's atmosphere, hydrosphere, and biosphere—Constraints from ore deposits: Geological Society of America Memoir 198, p. 105–119.

Moroni, M., Girardi, V., and Ferrario, A., 2001, The Serra Pelada Au-PGE deposit, Serra dos Carajás (Pará State, Brazil); geological and geochemical indications for a composite mineralising process: Mineralium Deposita, v. 36, no. 8, p. 768–785.

Naldrett, A., 2004, Magmatic sulfide deposits; Geology, geochemistry and exploration: Berlin, Springer, 727 p.

Naldrett, A.J., Asif, M., Krstic, S., and Li, C., 2000, The composition of mineralization at the Voisey's Bay Ni-Cu sulfide deposit, with special reference to platinum-group elements: Economic Geology, v. 95, no. 4, p. 845–865.
National Research Council, 2008, Minerals, Critical Minerals, and the U.S. Economy: Washington, D.C., The National Academies Press, 264 p.
Newberry, R.J., and Brew, D.A., 1989, Epigenetic hydrothermal origin of the Groundhog Basin-Glacier Basin silver-tin-lead-zinc deposits, southeastern Alaska, in Dover, J.H., ed., Geologica studies in Alaska by the U.S. Geological Survey, 1988: U.S. Geological Survey Bulletin 1903, p. 113–121.
Newberry, R., and Solie, D.N., 1995, Data for plutonic rocks and associated gold deposits in Interior Alaska, Division of Geological & Geophysical Surveys Public Data File 95–25, 62 p.
Newberry, R.J., and Swanson, S.E., 1986, Scheelite skarn granitoids; An evaluation of the roles of magmatic source and process: Ore Geology Reviews, v. 1, p. 57–81.
Newberry, R., Burns, L., Swanson, S., and Smith, T., 1990, Comparative petrologic evolution of the Sn and W granites of the Fairbanks-Circle area, interior Alaska: Geological Society of America Special Papers, v. 246, p. 121–142.
Newberry, R.J., Dillon, J.T., and Adams, D.D., 1986, Regionally metamorphosed, calc-silicate-hosted deposits of the Brooks Range, northern Alaska: Economic Geology, v. 81, no. 7, p. 1728–1752.
Nokleberg, W.J., Bundtzen, T.K., Berg, H., Brew, D., Grybeck, D., Robinson, M., Smith, T., and Yeend, W., 1987, Significant metalliferous lode deposits and placer districts of Alaska, U.S. Geological Survey Bulletin 1786, 104 p.
Northrop, H.R., Goldhaber, M.B., Landis, G.P., Unruh, J.W., Reynolds, R.L., Campbell, J.A., Wanty, R.B., Grauch, R.I., Whitney, G., and Rye, R.O., 1990, Genesis of the tabular-type vanadium-uranium deposits of the Henry Basin, Utah: Economic Geology, v. 85, no. 2, p. 215–269.
Notholt, A., Highley, D., and Deans, T., 1990, Economic minerals in carbonatites and associated alkaline igneous rocks: Transactions of the Institution of Mining and Metallurgy. Section B., Applied Earth Science, v. 99, p. 59–B124.
Nyman, M.W., Sheets, R.W., and Bodnar, R.J., 1990, Fluid-inclusions evidence for the physical and chemical conditions associated with intermediate-temperature PGE mineralization at the New Rambler Deposit, southeastern Wyoming: The Canadian Mineralogist, v. 28, no. 3, p. 629–638.
Patton, W.W., Jr., compiler, 1992, Ophiolitic terrane of the western Brooks Range, Alaska: U.S. Geological Survey Open-File Report 92-20D, 7 p.
Patton, W.W., Jr., and Moll-Stalcup, E.J., 2000, Geologic map of the Nulato Quadrangle, west-central Alaska: U.S. Geological Survey Geologic Investigations Series I–2677, 41 p., 1 sheet, scale 1:250,000.
Patton, W.W., Jr., Wilson, F.H., Labay, K.A., and Shew, N., 2009, Geologic Map of the Yukon-Koyukuk Basin: U.S. Geological Survey Scientific Investigations Map 2909, 30 p., 3 sheets, scale 1:500,000.
Pearce, J.A., 1996, A user's guide to basalt discrimination diagrams, *in* Wyman, D.A., and Bailes, A.H., eds., Trace element geochemistry of volcanic rocks; applications for massive sulphide exploration: Geological Association of Canada, Short Course Notes 12, p. 79–113.
Pearce, J.A., Harris, N.B.W., and Tindle, A.G., 1984, Trace element discrimination diagrams for the tectonic interpretation of granitic rocks: Journal of Petrology, v. 25, no. 4, p. 956–983.

Philpotts, J., Taylor, C., Evans, J., and Emsbo, P., 1993, Newly discovered molybdenite occurrences at Dora Bay, Prince of Wales Island, southeast Alaska, and preliminary scanning electron microscope studies *in* Dusel-Bacon, C., and Till, A.B., eds., Geologic studies in Alaska by the U.S. Geological Survey: U.S. Geological Survey Bulletin 2068, p. 187–196.
Philpotts, J.A., Taylor, C., Tatsumoto, M., and Belkin, H., 1998, Petrogenesis of late-stage granites and Y-REE-Zr-Nb-enriched vein dikes of the Bokan Mountain stock, Prince of Wales Island, Southeastern Alaska: U.S. Geological Survey Open-File Report 98–459, 71 p.
Pollard, P.J., 1995, A special issue devoted to the geology of rare metal deposits; geology of rare metal deposits; an introduction and overview: Economic Geology, v. 90, no. 3, p. 489–494.
Portnov, A., 1987, Specialization of rocks toward potassium and thorium in relation to mineralization: International Geology Review, v. 29, no. 3, p. 326–344.
Preto, V., 1978, Setting and genesis of uranium mineralization at Rexspar: Canadian Institute of Mining and Metallurgical Bulletin, v. 71, no. 800, p. 82–88.
Pretorius, D.A., 1981, Gold and uranium in quartz-pebble conglomerate, *in* Skinner, B.J., ed., Economic Geology, seventy-fifth anniversary volume, 1905–1980, El Paso, Texas, Society of Economic Geologists, p. 117–138.
Price, J.B., Hitzman, M.W., Nelson, E.P., Humphrey, J.D., and Johnson, C.A., 2014, Wall-rock alteration, structural control, and stable isotope systematics of the high-grade copper orebodies of the Kennecott district, Alaska: Economic Geology, v. 109, no. 3, p. 581–620.
Puchner, C.C., 1986, Geology, alteration, and mineralization of the Kougarok Sn deposit, Seward Peninsula, Alaska: Economic Geology, v. 81, no. 7, p. 1775–1794.
Raimbault, L., Cuney, M., Azencott, C., Duthou, J.-L., and Joron, J.L., 1995, Geochemical evidence for a multistage magmatic genesis of Ta-Sn-Li mineralization in the granite at Beauvoir, French Massif Central: Economic Geology, v. 90, no. 3, p. 548–576.
Rankin, A., 2005, Carbonatite-associated rare metal deposits; composition and evolution of ore-forming fluids—the fluid inclusion evidence, *in* Samson, I. and Linnen., R., eds., Rare-element geochemistry and ore deposits: Geological Association of Canada-Mineralogical Association of Canada Short Course Series, v. 17, p. 299–314.
Reed, B.L., 1986, Descriptive model of Sn greisen deposits *in* Cox, D.P., and Singer, D.A., eds., Mineral deposit models: U.S. Geological Survey Bulletin 1693, p. 70.
Reifenstuhl, R., Dover, J., Newberry, R., Clautice, K., Liss, S., Blodgett, R., and Weber, F., 1998, Interpretive geologic bedrock map of the Tanana A-1 and A-2 quadrangles, central Alaska: Alaska Division of Geological & Geophysical Surveys Public Data File 98–37B, v. 1.1, 17 p., 1 sheet, scale 1:63,360.
Richards, J., Dang, T., Dudka, S., and Wong, M., 2003, The Nui Phao tungsten-fluorite-copper-gold-bismuth deposit, northern Vietnam; An opportunity for sustainable development: Exploration and Mining Geology, v. 12, no. 1–4, p. 61–70.
Richardson, D., and Birkett, T., 1996, Peralkaline rock-associated rare metals: Geology of Canadian Mineral Deposit Types, p. 523–540.
Richter, D. H., 1967, Geology of the Upper Slana-Mentasta Pass Area, Southcentral Alaska, Alaska Division of Mines and Minerals Geologic Report 30, 30 p., 2 sheets, scale 1:63,360
Rogers, J.J., and Greenberg, J.K., 1990, Late-orogenic, post-orogenic, and anorogenic granites; distinction by major-element and trace-element chemistry and possible origins: The Journal of Geology, v. 98, no. 3, p. 291–309.
Rollinson, H.R., 1993, Using geochemical data; Evaluation, presentation, interpretation: New York, Routledge, Longman Scientific and Technical series, 352 p.

Roy, P.S., 1999, Heavy mineral beach placers in southeastern Australia; their nature and genesis: Economic Geology, v. 94, no. 4, p. 567–588.
Runnells, D.D., 1969, The mineralogy and sulfur isotopes of the Ruby Creek copper prospect, Bornite, Alaska: Economic Geology, v. 64, no. 1, p. 75–90.
Saltus, R.W., Riggle, F.E., Clark, B.T., and Hill, P. L., 1999, Merged aeroradiometric data for Alaska; a web site for distribution of gridded data and plot files: U.S. Geological Survey Open-File Report 99–0016, 13 p.
Schmidt, J.M., 1986, Stratigraphic setting and mineralogy of the Arctic volcanogenic massive sulfide prospect, Ambler District, Alaska: Economic Geology, v. 81, no. 7, p. 1619–1643.
Schulz, K.J., Chandler, V.W., Nicholson, S.W., Piatak, N., Seal, R.R., II, Woodruff, L.G., and Zientek, M.L., 2010, Magmatic sulfide-rich nickel-copper deposits related to picrite and (or) tholeiitic basalt dike-sill complexes—A preliminary deposit model: U.S. Geological Survey Open-File Report 2010–1179, 25 p.
Seedorff, E., Dilles, J.H., Proffett Jr., J.M., Einaudi, M.T., Zurcher, L., Stavast, W.J.A., Johnson, D.A., and Barton, M.D., 2005, Porphyry deposits; Characteristics and origin of hypogene features, *in* Hedenquist, J.W., Thompson, J.F.H., Goldfarb, R.J., and Richards, J.P., eds., Economic Geology one hundredth anniversary volume 1905–2005: Littleton, Colorado, Society of Economic Geologists, p. 251–298.
Seedorff, E., and Einaudi, M.T., 2004, Henderson porphyry molybdenum system, Colorado; I. Sequence and abundance of hydrothermal mineral assemblages, flow paths of evolving fluids, and evolutionary style: Economic Geology, v. 99, no. 1, p. 3–37.
Shand, S.J., 1947, Eruptive rocks, their genesis, composition, and classification, with a chapter on meteorites: New York, J. Wiley & Sons, 444 p.
Sheard, E.R., Williams-Jones, A.E., Heiligmann, M., Pederson, C., and Trueman, D.L., 2012, Controls on the concentration of zirconium, niobium, and the rare earth elements in the Thor Lake Rare Metal Deposit, Northwest Territories, Canada: Economic Geology, v. 107, no. 1, p. 81–104.
Silberman, M.L., MacKevett, E.M., Connor, C.L., and Matthews, A., 1980, Metallogenic and tectonic significance of oxygen isotope data and whole-rock potassium-argon ages of the Nikolai Greenstone, McCarthy Quadrangle, Alaska: U.S. Geological Survey Open-File Report 80–2019, 31 p.
Sinclair, W., Kooiman, G., Martin, D., and Kjarsgaard, I., 2006, Geology, geochemistry and mineralogy of indium resources at Mount Pleasant, New Brunswick, Canada: Ore Geology Reviews, v. 28, no. 1, p. 123–145.
Sinclair, W.D., 2007, Porphyry deposits, *in* Goodfellow, W.D., ed., Mineral deposits of Canada; A synthesis of major deposit-types, district metallogeny, the evolution of geological provinces, and exploration methods: Geological Association of Canada, Mineral Deposits Division, Special Publication no. 5, p. 223–243.
Singer, D.A., 1993, Basic concepts in three-part quantitative assessments of undiscovered mineral resources: Nonrenewable Resources, v. 2, no. 2, p. 69–81.
Singer, D.A., and Menzie, W.D., 2010, Quantitative mineral resource assessments: An integrated approach: Oxford, United Kingdom, Oxford University Press, 232 p.
Slingerland, R., and Smith, N.D., 1986, Occurrence and formation of water-laid placers: Annual Review of Earth and Planetary Sciences, v. 14, no. 1, p. 113–147.
Solie, D., Bundtzen, T., Bowman, N., and Cruse, G., 1993, Land selection unit 18 (Melozitna, Ruby, Nulato, and Kateel River quadrangles); References, DGGS sample locations,

geochemical and major oxide data: Alaska Division of Geological & Geophysical Surveys Public Data File 93–18, 20 p., 1 sheet, scale 1: 250,000.
Staatz, M., Sharp, B., and Hetland, D., 1979, Geology and mineral resources of the Lemhi Pass thorium district, Idaho and Montana: U.S. Geological Survey Professional Paper 1049-A, 90 p., 2 pls.
Staatz, M.H., 1983, Geology and description of thorium and rare-earth deposits in the southern Bear Lodge Mountains, northeastern Wyoming, U.S. Geological Survey Professional Paper 1049-D, 52 p., 2 pls.
Still, J.C., 1984, Copper, gold, platinum, and palladium sample results from the Klukwan mafic/ultramafic complex, southeast Alaska: U.S. Bureau of Mines Open-File Report 84–21, p. 53 p.
Still, J.C., Hoekzema, R.B., Bundtzen, T.K., Gilbert, W.G., Wier, K.R., Burns, L.E., and Fechner, S.A., 1991, Economic geology of Haines-Klukwan-Porcupine area, southeastern Alaska: Alaska Division of Geological & Geophysical Surveys Report of Investigation 91–4, 156 p.
Swanson, S.E., Newberry, R.J., Coulter, G.A., and Dyehouse, T.M., 1990, Mineralogical variation as a guide to the petrogenesis of the tin granites and related skarns, Seward Peninsula, Alaska, *in* Stein, H.J., and Hannah, J.L., eds., Ore-bearing granite systems; petrogenesis and mineralizing processes: Boulder, Colorado, Geological Society of America Special Paper 246, p. 143–160.
Sweetapple, M.T., and Collins, P.L., 2002, Genetic framework for the classification and distribution of Archean rare metal pegmatites in the North Pilbara Craton, Western Australia: Economic Geology, v. 97, no. 4, p. 873–895.
Taggart, J.E., ed., 2002, Analytical methods for chemical analysis of geologic and other materials, U.S. Geological Survey Open-File Report 2002–223 [variously paged].
Taylor, B.E., 2007, Epithermal gold deposits, *in* Goodfellow, W.D., ed., Mineral deposits of Canada; A synthesis of major deposit-types, district metallogeny, the evolution of geological provinces, and exploration methods: Geological Association of Canada, Mineral Deposits Division, Special Publication no. 5, p. 113–139.
Taylor, S.R., and McLennan, S.M., 1995, The geochemical evolution of the continental crust: Reviews of Geophysics, v. 33, no. 2, p. 241–265.
Theodore, T., 1986, Descriptive model of porphyry Mo, low-F, *in* Cox, D.P., and Singer, D.A., Mineral deposit models: U.S. Geological Survey Bulletin, 1693, p. 120.
Thompson, T.B., 1988, Geology and uranium-thorium mineral deposits of the Bokan Mountain granite complex, southeastern Alaska: Ore Geology Reviews, v. 3, no. 1, p. 193–210.
Thorne, R.L., and Wells, R.R., 1956, Studies of the Snettisham magnetite deposit, southeastern Alaska: U.S. Bureau of Mines Report of Investigations 5195, 41 p.
Till, A.B., Dumoulin, J.A., Harris, A.G., Moore, T.E., Bleick, H.A., and Siwiec, B.R., 2008, Bedrock geologic map of the southern Brooks Range, Alaska, and accompanying conodont data, U.S. Geological Survey Open-File Report 2008–1149, 88 p., 2 sheets, scales 1:500,000 and 1:600,000.
Tolstykh, N.D., Foley, J.Y., Sidorov, E.G., and Laajoki, K.V.O., 2002, Composition of the platinum-group minerals in the Salmon River placer deposit, Goodnews Bay, Alaska: The Canadian Mineralogist, v. 40, no. 2, p. 463–471.
Turner-Peterson, C., and Hodges, C., 1986, Descriptive model of sandstone U, in Cox, D.P., and Singer, D.A., Mineral deposit models: U.S. Geological Survey Bulletin1693, p. 209–210.

Upton, B., Emeleus, C., Heaman, L., Goodenough, K., and Finch, A., 2003, Magmatism of the mid-Proterozoic Gardar Province, South Greenland; chronology, petrogenesis and geological setting: Lithos, v. 68, no. 1, p. 43–65.
Van Gosen, B.S., Fey, D.L., Shah, A.K., Verplanck, P.L., and Hoefen, T.M., 2014, Deposit model for heavy-mineral sands in coastal environments: U.S. Geological Survey Scientific Investigations Report 2010–5070-L, 51 p.
Vasyukova, O., and Williams-Jones, A.E., 2014, Fluoride–silicate melt immiscibility and its role in REE ore formation; Evidence from the Strange Lake rare metal deposit, Québec-Labrador, Canada: Geochimica et Cosmochimica Acta, v. 139, p. 110–130.
Verplanck, P.L., Van Gosen, B.S., Seal, R.R., and McCafferty, A.E., 2014, A deposit model for carbonatite and peralkaline intrusion-related rare earth element deposits: U.S. Geological Survey Scientific Investigations Report 2010-5070-J: 58 p.
Wall, F., 2013, Rare earth elements, in Gunn, G., ed., Critical Metals Handbook: Oxford, United Kingdom, J. Wiley & Sons, p. 312–339.
Warner, J.D., Mardock, C.L., and Dahlin, D.C., 1986, A columbium-bearing regolith on Upper Idaho Gulch, near Tofty, AK: U.S. Bureau of Mines Information Circular 9105, 29 p.
Wenrich, K.J., 1985, Mineralization of breccia pipes in northern Arizona: Economic Geology, v. 80, no. 6, p. 1722–1735.
Werner, A.B.T., Sinclair, W.D., and Amey, E.B., 1998, International strategic minerals summary report—tungsten: U.S. Geological Survey Circular 930-O, 74 p.
Whalen, J., Currie, K., and Chappell, B., 1987, A-type granites; geochemical characteristics, discrimination and petrogenesis: Contributions to Mineralogy and Petrology, v. 95, no. 4, p. 407–419.
Whalen, J.B., Anderson, R.G., Struik, L.C., and Villeneuve, M.E., 2001, Geochemistry and Nd isotopes of the François Lake plutonic suite, Endako batholith; host and progenitor to the Endako molybdenum camp, central British Columbia: Canadian Journal of Earth Sciences, v. 38, no. 4, p. 603–618.
White, W., Bookstrom, A., Kamilli, R., Ganster, M., Smith, R., Ranta, D., and Steininger, R., 1981, Character and origin of Climax-type molybdenum deposits, *in* Skinner, B.J., Economic Geology Seventy-Fifth Anniversary Volume (1905–1980): Lancaster, Pennsylvania, The Economic Geology Publishing Company, p. 270–316.
Winchester, J.A., and Floyd, P.A., 1977, Geochemical discrimination of different magma series and their differentiation products using immobile elements: Chemical Geology, v. 20, p. 325–343.
Yang, K.-F., Fan, H.-R., Santosh, M., Hu, F.-F., and Wang, K.-Y., 2011, Mesoproterozoic carbonatitic magmatism in the Bayan Obo deposit, Inner Mongolia, North China; Constraints for the mechanism of super accumulation of rare earth elements: Ore Geology Reviews, v. 40, no. 1, p. 122–131.
Yeend, W.E., 1986, Descriptive model of placer Au-PGE, *in* Cox, D.P., and Singer, D.A., eds., Mineral deposit models: U.S. Geological Survey Bulletin 1693, p. 261–263.
Yefimov, A., Borodayev, Y.S., Mozgova, N., and Nenasheva, S., 1990, Bismuth mineralization of the Akchatau molybdenum-tungsten deposit, central Kazakhstan: International Geology Review, v. 32, no. 10, p. 1017–1027.
Zientek, M.L., 2012, Magmatic ore deposits in layered intrusions—Descriptive model for reef-type PGE and contact-type Cu-Ni-PGE deposits: U.S. Geological Survey Open-File Report 2012–1010, p. 44 p.

Zientek, M.L., Causey, J.D., Parks, H.L., and Miller, R.J., 2014, Platinum-group elements in southern Africa—Mineral inventory and an assessment of undiscovered mineral resources, *in* Zientek, M.L., Hammarstrom, J.M., and Johnson, K.M., eds., Global mineral resource assessment: U.S. Geological Survey Scientific Investigations Report 2010–5090-Q, 126 p.
Zientek, M.L., Cooper, R.W., Corson, S.R., and Geraghty, E.P., 2002, Platinum-group element mineralization in the Stillwater Complex, Montana, *in* Cabri, L.J., ed., The geology, geochemistry, mineralogy and mineral beneficiation of platinum-group elements: Canadian Institute of Mining, Metallurgy and Petroleum Special Volume 54, p. 459–481.

Tables

Table 1. Mineral deposit groups and types considered in this study, and their commodities, characteristics, and representative localities.

Mineral deposit group	Commodities (critical elements in **bold**)	Deposit types	World examples	Alaska deposits* and occurrences	Ore deposit model references	Deposit and occurrence references#
REE-Th-Y-Nb(-U-Zr) deposits associated with peralkaline to carbonatitic igneous rocks	**REE, Th,** Y, **Nb**, U, Zr	Carbonatite	Bayan Obo, China; Mount Weld, Australia; Mountain Pass, California	Tofty	Verplanck and others (2014); model 10 in Cox and Singer (1986); model 16 in Eckstrand (1985); Berger and others (2009)	Yang and others (2011); Middlemost (1990); Castor (2008); Reifenstuhl and others (1998)
		Alkaline intrusive	Thor Lake, Canada; Lovozero, Russia	Windy Fork, Ruby batholith, Darby Mountains	Long and others (2010); Verplanck and others (2014)	Sheard and others (2012); Kogarko and others (2010); Barker (1991); Arth and others (1989); Foley and Barker (1986)
		Syenite or peralkaline granite REE-Zr-U-Nb	Strange Lake, Canada; Ilimaussaq, Greenland; Norra Kärr, Sweden	Bokan Mountain*, Dora Bay, Roy Creek	Linnen and others (2014); Verplanck and others (2014)	Vasyukova and Williams-Jones (2014); Upton and others (2003); Bluemel and others (2013); Dostal and others (2014); Philpotts and others (1993); Armbrustmacher (1989)
		Thorium-REE Veins	Lemhi Pass, Idaho-Montana; Bear Lodge, Wyoming	Bokan Mountain*	Staatz and others (1979); Bliss (1992)	Staatz and others (1979); Staatz (1983); Dostal and others (2014)
		Plutonic-volcanic U-REE	Nopal, Mexico; Rexspar, Canada	Selawik Hills; Sischu Mountain	Cox and Singer (1986)	Angiboust and others (2012); Preto (1978); Barker (1985); Miller and others (1980)
Placer and paleoplacer Au	Au, **PGE**, Ag, **Sn, W**, Cr, **Ti**	Alluvial placer	Thousands	Hundreds	Model 39a in Cox and Singer (1986)	Nokleberg and others (1987)
		Alluvial paleoplacer		Tofty district	Frimmel and others (2005)	Garnett and Bassett (2005)
		Coastal placer	Richards Bay, South Africa		Model 39c in Cox and Singer (1986)	Van Gosen and others (2014)
PGE (-Co-Cr-Ni-Ti-V) deposits associated with mafic and ultramafic igneous rocks	**PGE**, Cu, Ni, Ti, **V**	Alaska-Ural type PGE		Goodnews Bay; Union Bay	Model 9 in Cox and Singer (1986)	Naldrett (2004)
		Duluth-Noril'sk Cu-Ni-PGE	Noril'sk, Russia; Wellgreen, Yukon, Canada	Spirit Mountain (ARDF VA 080) *	Models 5a & 5b in Cox and Singer (1986); Zientek (2012)	Hulbert (1997); Li and others (2009)
		Synorogenic -synvolcanic Ni-Cu-PGE	Selebi-Phikwe, Botswana	Brady Glacier	Models 5a & 5b in Cox and Singer (1986); Schulz and others (2010)	Barnes and Lightfoot (2005)
		Fe-Ti-V-rich mafic-ultramafic rocks with PGE; (see, also, table 6)		Klukwan; Snettisham		Still (1984); Thorne and Wells (1956)
Carbonate-hosted Cu(-Co-Ag-Ge-Ga) deposits	Cu, Ag	Kennecott type; related to basaltic copper	Keweenawan native copper district, Michigan	Kennecott veins*	Model 23 in Cox and Singer (1986); model 10 in Eckstrand (1985)	MacKevett and others (1997): Price and others (2014)
	Cu, **Co, Ge, Ga**	Kipushi type	Kipushi, Democratic Republic of Congo; Tsumeb, Namibia	Ruby Creek*	Model 32c in Cox and Singer (1986)	Kampunzu and others (2009); Kamona and Günzel (2007)
Sandstone U (-V-Cu) deposits	U, **V,** Cu	Roll-front	Shirley Basin district, Wyoming		Model 30c in Cox and Singer (1986)	Harshman (1972)
		Tabular	Grants Belt, New Mexico.; Uravan district, Colorado			Northrop and others (1990)
		Basal	Okanagan highlands, B.C., Canada	Death Valley (Boulder Creek)*	Model 6.4 in Eckstrand (1985)	Boyle (1982)
		Tectono-lithologic	Orphan mine, Arizona		Model 32e in Bliss (1992)	Wenrich (1985)

Sn-W-Mo (Ta-In-fluorspar) deposits associated with specialized granites	**Sn, W, Mo, F, In, Ta**	Sn porphyry, greisen, skarn, peraluminous granite	Podlesi and Cinovec, Czech Republic; Beauvoir, France; Chlorolque, Bolivia; Mancusani, Peru; Moina, Australia; Cinovec, Czech Republic; Akchatau and Kara Oba, Kazakhstan	Ruby batholith, Rocky Mountain, Mount Prindle, Groundhog Basin; Lost River*, Kougarok*, Sleitat*, Sithylemenkat	Linnen and others (2014); Models 14b, 15c in Cox and Singer (1986); Kwak (1987)	Cérny and others (2005); Raimbault and others (1995); Cheilletz and others (1992); Hudson and Arth (1983); Newberry and others (1990); Newberry and Brew (1989); Kwak and Askins (1981); Cérny and others (2005); Yefimov and others (1990); Dobson, 1982; Hudson and Arth (1983); Puchner (1986); Hudson and Reed (1997); Barker and Foley (1986)
		Sn veins, Sn-polymetallic veins, pegmatites	Wodgina, Australia; Tanco, Canada	Waterpump Creek*,Won, McIntyre, Groundhog Basin*	Models 15b and 20b in Cox and Singer (1986); Linnen and others (2014)	Sweetapple and Collins (2002); Cérny and others (2005); Flanigan (1998); Burleigh (1992); Reifenstuhl and others (1998); Newberry and Brew (1989)
		W porphyry, greisen, skarn	Pine Creek, California; Mactung, Canada; Mount Pleasant, Canada	Stepovich*; Spruce Hen*; Tanana*; Gillmore Dome	Models 14a and 15a in Cox and Singer (1986); Kwak (1987)	Kooiman and others (1986); Newberry and others (1990); White and others (1981); Barker and Swainbank (1986); Barker (1985)
		Climax-type Mo	Climax, Henderson	Bear Mountain, Zane Hills	Model 16 in Cox and Singer (1986); Seedorff and others (2005); Ludington and Plumlee (2009)	White and others (1981); Barker and Swainbank (1986); Barker (1985)
		Porphyry Mo, low-F	Endako, Canada	Quartz Hill*, Nunatak	Model 21b in Cox and Singer (1986); Ludington and others (2009)	Whalen and others (2001); Ashleman and others (1997); Kimball and others (1978)

* Deposits (indicated by asterisk) are localities with reported inventory or past production.

References in this column contain maps or coordinates for specific deposits, occurrences, and (or) prospects worldwide and in Alaska. References are in the same order as localities are listed in columns four and five.

Table 2. Scoring template for analysis of REE-Th-Y-Nb (-U-Zr) potential within each hydrologic unit code in the Central Yukon Planning Area.

[ARDF, Alaska resource data file; REE, rare earth elements; AGDB2, Alaska geochemical database version 2.0; ADGGS, Alaska Division of Geological and Geophysical Surveys; NURE, National uranium resource evaluation database; MALI displacement, MALI deviation from a published geochemical threshold; Fe# displacement, Fe# deviation from a published geochemical threshold; ppm, concentration in parts per million; HUC, hydrologic unit code]

Category	Dataset/layer	Component	Selection and score
ARDF records	ARDF	REE model keywords[1]	2 points if REE keyword score ≥5 1 point if REE keyword score >2 *and* <5
Igneous-rock geochemistry[2]	AGDB2 + ADGGS + literature	MALI displacement[3]	1 point if MALI value >0
		10,000×Ga/Al[4]	1 point if 10,000×Ga/Al >2.6
		Fe# displacement[5]	1 point if Fe# displacement >0.05
		Nb/Y ratio	1 point if Nb/Y≥1
Sediment geochemistry[6]	AGDB2 + ADGGS + NURE	Nb ppm 91st and 98th percentile	2 points if Nb ppm ≥23 1 point if Nb ppm ≥17 *and* <23
		Ce ppm 91st and 98th percentile	2 points if Ce ppm ≥166 1 point if Ce ppm ≥103 *and* <166
		Yb ppm 91st and 98th percentile	2 points if Yb ppm ≥8.4 1 point if Yb ppm ≥5.6 *and* <8.4
		Th ppm 91st and 98th percentile	2 points if Th ppm ≥28.1 1 point if Th ppm ≥13.4 *and* <28.1
Aeroradiometric data[7]	Aerial gamma-ray survey data	Th/K ratio	2 points if Th/K value >12 1 point if Th/K value >5 *and* ≤12

[1]See appendix C for list of REE keywords and scoring template for ARDF; maximum single score for an HUC contributes to the total score, although any ARDF score >1 results in an assignment of high potential.

[2]Igneous-rock geochemistry scores are additive for a total possible score of 4 for each HUC.

[3]MALI, modified alkali-lime index (Na_2O+K_2O-CaO). Score applied only to igneous rocks with SiO_2>56 weight percent.

[4]10,000×Ga/Al scores applied only to igneous rocks with SiO_2>60 weight percent.

[5]Fe# (FeO/[FeO + MgO]) displacement calculated using the Fe# versus SiO_2 array proposed by Frost and Frost (2008).

[6]Maximum single score for each element in HUC is used. Element scores are additive for possible total of 8.

[7]Mean score for an HUC contributes to the total score. Data from Duval (2001).

Table 3. Matrix of mineral resource potential versus certainty classification for REE-Th-Y-Nb (-U-Zr) deposits associated with peralkaline-to-carbonatitic intrusive rocks.

[REE, rare earth elements; ARDF, Alaska resource data file; HUC, hydrologic unit code]

REE-Th-Nb-Y-(Zr-U)	Estimated certainty[1]				
	Low	Medium	High		
Unknown Total score = 0 *and* no sediment data points in HUC *or* aerial gamma-ray survey is only data set represented *and* no sediment data points in HUC	ARDF score >1 *or* total score ≥6 (p) 1 dataset not null(c)	ARDF score >1 *or* total score ≥6 (p) 2–3 datasets not null (c)	ARDF score >1 *or* total score ≥6 (p) 4 datasets not null (c)	High	Estimated potential[1]
	Total score 3–5 (p) 1 dataset not null (c)	Total score 3–5 (p) 2–3 datasets not null (c)	Total score 3–5 (p) 4 datasets not null (c)	Medium	
	Total score 1–2 (p) 1 dataset not null (c)	Total score 1–2 (p) 2–3 datasets not null (c)	Total score 1-2 *or* Total score = 0 *and* sediment data points in HUC (p, c)	Low	

[1]Abbreviations (p) and (c) in cells denote which components contribute to assignment of potential and certainty, respectively.

Table 4. Scoring template for analysis of placer and paleoplacer Au potential in hydrologic unit codes within the Central Yukon Planning Area.

[ARDF, Alaska resource data file; AGDB2, Alaska geochemical database version 2.0; ADGGS, Alaska Division of Geological and Geophysical Surveys; NURE, National uranium resource evaluation database; ppm, concentration in parts per million; HUC, hydrologic unit code; NHD, National Hydrologic Dataset]

Category	Dataset/layer	Component	Selection and score
ARDF records	ARDF	Placer model keywords[1]	10 points if total >0
Pan Concentrate Mineralogy[2]	AGDB2	Gold	10 points if Au is present
		Cassiterite	1 point if cassiterite is present
		Powellite	1 point if powellite is present
		Scheelite	1 point if scheelite is present
		Cinnabar	1 point if cinnabar is present
		Monazite	1 point if monazite is present
		Thorite	1 point if thorite is present
Sediment geochemistry[3]	AGDB2 + ADGGS + NURE	Au ppm 75th percentile	3 points if Au ppm ≥0.007
		Ag ppm 75th percentile	3 point if Ag ppm ≥0.16
		Ti ppm 75th percentile	1 point if Ti ppm ≥0.57
		W ppm 75th percentile	1 point if W ppm ≥2.0
Lithology[4]	Digital geologic map of Alaska	Plutonic major component of map unit	3 points if present
		Plutonic minor component of map unit	2 points if present
		Hypabyssal igneous map unit	2 points if present
		Volcanic igneous map unit	1 point if present
		Metaigneous map unit	1 point if present
Downstream of high potential[5]	NHD	River/stream <25 km downstream of HUC with high potential	6 points if present
		River/stream >25 km downstream of HUC with high potential	3 points if present
		River/stream downstream of HUC with high potential past intersection with equal or higher order segment	1 point if present

[1]See appendix C for list of placer model keywords and scoring template for ARDF.

[2]Pan Concentrate Mineralogy—If Au is not null, only use the highest value of 10; otherwise, score is additive for other possible minerals.

[3]Stream-sediment geochemistry—Scores are additive for possible total of 8.

[4]Lithology—if more than one lithologic type is present, only use the type with the highest value.

[5]Downstream analysis excludes HUCs with high potential; if more than one type of segment is present only use the type with the highest value

Table 5. Matrix of mineral resource potential versus certainty classification for placer and paleoplacer Au deposits.

[ARDF, Alaska resource data file; HUC, hydrologic unit code]

Placer Au	Estimated certainty[1]				
	Low	Medium	High		
Unknown Total score = 0 *and* no sediment data points in HUC	n/a	Total score ≥16 (p) 2–3 datasets not null (c)	ARDF score = 10 *or* pan concentrate score = 10 *or* total score ≥16 (p) ARDF score = 10 *or* pan concentrate score = 10 *or* 4–5 datasets not null (c)	High	Estimated potential[1]
	Total score 6–15 (p) 1 dataset not null (c)	Total score 6–15 (p) 2–3 datasets not null (c)	Total score 6–15 (p) 4–5 datasets not null (c)	Medium	
	Total score 1–5 (p) 1dataset not null (c)	Total score 1–5 (p) 2–3 datasets not null (c)	Total score 1–5 (p) *and* 4–5 datasets not null (c) *or* Total score = 0 *and* sediment data points in HUC (p,c)	Low	

[1]Abbreviations (p) and (c) in cells denote which components contribute to assignment of potential and certainty, respectively.

Table 6. Platinum group element (PGE) ore deposit types.

PGE deposit models	Example / locations	References
PGE ore deposit models considered in mineral potential evaluation		
Alaska-Ural type	Goodnews Bay, southwest Alaska Union Bay, southeast Alaska	Foley and others (1997) Himmelberg and Loney (1995)
Ophiolites	Angayucham-Tozitna terranes, northern Alaska	Loney and Himmelberg (1989); Patton (1992)
Layered magmatic PGE	Stillwater, Montana	Zientek and others (2002)
Magmatic-sulfide PGE	Wellgreen, Yukon and Fish Lake Complex, Alaska, both in the Wrangellia terrane	Hulbert (1997)
Synorogenic Ni-Cu-PGE	Brady Glacier, Mount Fairweather trend, southeast Alaska	Czamanske and others (1981)
Large-igneous-province/flood-basalt and feeder-zone Ni-Cu-PGE	Norilsk, Russia[3]; Duluth Complex, Minnesota[4]	[3]Li and others (2009) [4]Miller and others (2002)
Troctolite-anorthosite-granite-hosted Ni-Cu-Co±PGE	Voisey's Bay, Newfoundland and Labrador, Canada	Naldrett and others (2000)
PGE found with chromite in island-arc crustal sections	Red Mountain, Kenai Peninsula, Alaska	Foley and Barker (1984)
Fe-Ti±V-rich mafic/ultramafic (MUM) rocks with PGE	Klukwan, Snettisham, southeast Alaska;	Still and others (1991)
PGE ore deposit models known in Alaska but not factored into mineral potential assessment		
PGE-enriched porphyry Cu-Mo-Au deposits	Pebble, Alaska	Kelley and others (2013) Ghaffari and others (2011)
PGE-enriched composite plutons	Butte Creek, Alaska	Keith and others (1987)
Differentiated igneous complexes	Mentasta Pass, Alaska Range, Alaska	Richter (1967)
PGE-enriched skarns adjacent to PGE-bearing mafic-ultramafic intrusions	Unnamed skarn occurrence, West Fork Rainy Creek, Mount Hayes quadrangle, Alaska	Bittenbender and others (2007)
PGE-bearing placer deposits in unconsolidated sediments	Goodnews Bay, Alaska	Tolstykh and others (2002)
PGE ore deposit models not presently known in Alaska and not optimized for in this assessment		
Hydrothermal PGE deposits	New Rambler, Wyoming Kupferschiefer, Germany	Nyman and others (1990) Borg and others (2005)
Black shale-hosted PGE	Nick Property, Yukon	Hulbert and others (1992)
Unconformity related U±Au±PGE	Rum Jungle, Australia	Mernagh and others (1998)
Supergene PGE	Serra Pelada, Brazil	Moroni and others (2001)
Meteorite impacts	Sudbury, Ontario	Ames and others (2008)
Komatiites	Kambalda, Australia	Barnes and others (2013)

Table 7. Scoring template for analysis of PGE (-Co-Cr-Ni-Ti-V) potential in hydrologic unit codes within the Central Yukon Planning Area.

[PGE, platinum group elements; MUM, mafic-ultramafic; ARDF, Alaska resource data file; AGDB2, Alaska geochemical database version 2.0; ADGGS, Alaska Division of Geological and Geophysical Surveys; HMC, heavy metal concentrate; ppm, concentration in parts per million; HUC, hydrologic unit code]

Category	Dataset/layer	Component	Selection and score
Lithology[1]	Digital geologic map of Alaska	MUM rocks, major component	2 points if present
		MUM rocks, minor or incidental component	1 point if present
ARDF records[3]	ARDF	PGE model keywords[2]	3 points if PGE reported as major or minor commodities 2 points if chromite and favorable geology 1 point if permissible geology but no direct evidence for PGE
Pan concentrate Mineralogy[3]	AGDB2 + ARDF	ARDF placers	3 points if PGE reported as major or minor elements 2 points if chromite or other PGE-related minerals, or questioned PGE identifications 1 point if mineralogy for MUM rocks in a drainage, but no direct evidence for PGE
		Ore-related mineral comment	2 points if chromite ('CHR') is present
			2 points if copper cobalt sulfide ('Cu_Co sulfs') is present
			2 points if nickel cobalt sulfide ('Ni_Co sulfs') is present
			2 points if nickel sulfide ('Ni sulfs') is present
		Rock-forming mineral comment	2 points if chromium nickel silicate ('Cr-Ni silicates') is present
			1 point if serpentinite ('SRP') is present
			1 point if chrome diopside ('Cr-D') is present
		Chalcopyrite	1 point if not null
Pan concentrate geochemistry[3]	AGDB2	HMC geochemistry	3 points if Ir_ppm >0
			3 points if Os_ppm >0
			3 points if Pd_ppm >0
			3 points if Pt_ppm >0
			3 points if Rh_ppm >0
			3 points if Ru_ppm >0
			2 points if Co_ppm >500 1 point if Co_ppm >150 *and* ≤500
			2 points if Cr_ppm >7000 1 point if Cr_ppm >2000 and ≤ 7000
			2 points if Ni_ppm >700 1 point if Ni_ppm >200 *and* ≤700
			1 point if Ti_pct >5.0
			2 points if V_ppm >1500 1 point if V_pp >700 *and* ≤1500

Sediment geochemistry[3]	AGDB2	Sediment geochemistry	2 points if Co_ppm ≥70 (98th percentile) 1 point if Co_ppm ≥36 *and* ≤70 (91st percentile)
			2 points if Cr_ppm ≥500 1 point if Cr_ppm ≥200 *and* <500
			2 points if Ni_ppm ≥150 1 point if Ni_ppm ≥84 *and* <150
			2 points if Ti_pct ≥1.11 1 point if Ti_pct ≥0.79 *and* <1.11
			2 points if V_ppm ≥500 1 point if V_ppm ≥299 *and* <500
			3 points if Os_ppm ≥0.016 (91st percentile)
			3 points if Pd_ppm ≥0.005 (91st percentile)
			3 points if Pt_ppm ≥0.015 (91st percentile)
Rock geochemistry[3]	AGDB2	Rock geochemistry	2 points if Co_ppm >200 1 point if Co_ppm >100 *and* ≤200
			2 points if Cr_ppm >2000 1 point if Cr_ppm >700 *and* ≤2000
			2 points if Ni_ppm >1500 1 point if Ni_ppm >500 *and* ≤1500
			2 points if TiO2_pct >3.0 1 point if TiO2_pct >2.0 *and* ≤3.0
			2 points if V_ppm >1000 1 point if V_ppm >500 *and* ≤1000
			3 points if Ir_ppm >0
			3 points if Pd_ppm >0.005
			3 points if Pt_ppm >0.004
			3 points if Rh_ppm >0
			3 points if Ru_ppm >0
	DGGS	Rocks geochemistry	2 points if Co_ppm >70 1 point if Co_ppm >30 *and* ≤70
			2 points if Cr_ppm >2000 1 point if Cr_ppm >700 *and* ≤2000
			2 points if Ni_ppm >500 1 point if Ni_ppm >50 *and* ≤500
			2 points if TiO2_pct >3.0 1 point if TiO2_pct >2.0 *and* ≤3.0
			2 points if V_ppm >100 1 point if V_ppm >50 *and* ≤100
			3 points if Ir_ppm >0
			3 points if Pd_ppm >0
			3 points if Pt_ppm >0
			3 points if Rh_ppm >0
			3 points if Ru_ppm >0

[1]Digital geologic map of Alaska (Wilson, Frederic H., and others, USGS, written commun.) is source of lithology layers. Maximum HUC score is 2 points.

[2]See appendix C for list of PGE model keywords and scoring template for ARDF; maximum HUC score is 3 points.

[3]Maximum HUC score is 3 points.

Table 8. Matrix of mineral resource potential versus certainty classification for PGE (-Co-Cr-Ni-Ti-V) deposits.

[ARDF, Alaska resource data file; HUC, hydrologic unit code]

PGE (Co, Cr, Ni, Ti, V)	Estimated certainty[1]				
	Low	Medium	High		
Unknown Total score = 0 *and* no sediment data points in HUC *or* no sediment data points in HUC *and* Lithology is only dataset >0	Total score >5 1– datasets not null (c)	Total score >5 (p) 4–5 datasets not null (c)	ARDF score ≥ 3 *or* total score >5 (p) ARDF score ≥ 3 *or* 6 datasets not null (c)	High	Estimated potential[1]
	Total score 2–5 (p) 1–3 datasets not null (c)	Total score 2–5 (p) 4–5 datasets not null (c)	Total score 2–5 (p) 6 datasets not null (c)	Medium	
	Total score = 1 (p) 1–3 datasets not null (c)	Total score = 1 (p) 4–5 datasets not null (c)	Total score = 1 *or* total score = 0 *and* sediment data points in HUC (p,c)	Low	

[1]Abbreviations (p) and (c) in cells denote which components contribute to assignment of potential and certainty, respectively.

Table 9. Scoring template for analysis of carbonate-hosted Cu (-Co-Ag-Ge-Ga) potential in the hydrologic unit codes within the Central Yukon Planning Area.

[ARDF, Alaska resource data file; AGDB2, Alaska geochemical database version 2.0; ADGGS, Alaska Division of Geological and Geophysical Surveys; HMC, heavy metal concentrate; ppm, concentration in parts per million; HUC, hydrologic unit code]

Category	Dataset/Layer	Component	Selection and score
Lithology[1]	Digital geologic map of Alaska	Carbonate rocks, major component	3 points if present
		Carbonate rocks, minor or incidental component	2 point if present
ARDF records[2]	ARDF	Cu carbonate model keywords[2]	5 points if keyword score ≥4 2 points if keyword score >0 *and* <4
Pan concentrate Mineralogy[3]	AGDB2	Ore-related mineral comment	1 point if copper cobalt sulfide minerals ('Cu-Co sulfs') are present
			1 point if copper silicate minerals ('Cu SiO4 mnrls') are present
			1 point if copper sulfide and (or) copper oxide minerals ('CuS/O') are present
			1 point if azurite ('AZR') is present
			1 point if cuprite ('CUP') is present
			1 point if enargite ('ENG') is present
			1 point if malachite ('MAL') is present
		Chalcopyrite	1 point if present
Sediment geochemistry[3]	AGDB2	Sediment geochemistry	3 points if Cu_ppm ≥ 150 (98th percentile) 2 points if Cu_ppm ≥76 *and* <150 (91st percentile) 1 point if Cu_ppm ≥ 50 *and* <76 (75th percentile)
Sediment trace geochemistry[5]	AGDB2	Sediment trace geochemistry	1 point if Cu_ppm ≥50 *and* Co ppm ≥36
			1 point if Cu_ppm ≥50 *and* Ge_ppm ≥5.9
			1 point if Cu_ppm ≥50 *and* Ga_ppm ≥30
			1 point if Cu_ppm ≥50 *and* Ag_ppm ≥0.4
Rock geochemistry[4]	AGDB2	Cu ppm	3 points if Cu_ppm ≥5000 2 points if Cu_ppm ≥1000 *and* <5000 1 point if Cu_ppm ≥150 *and* <1000
	DGGS	Cu ppm	3 points if Cu_ppm ≥5000 2 points if Cu_ppm ≥1000 *and* <5000 1 point if Cu_ppm ≥150 *and* <1000
Rock trace geochemistry[5]	AGDB2	Co ppm, Ge ppm, Ga ppm, Ag ppm, with Cu ppm	1 point if Cu_ppm ≥150 *and* Co ppm ≥45
			1 point if Cu_ppm ≥150 *and* Ge_ppm ≥3
			1 point if Cu_ppm ≥150 *and* Ag_ppm ≥1
			1 point if Cu_ppm ≥150 *and* Ga_ppm ≥35
	DGGS	Co ppm, Ge ppm, Ga ppm, Ag ppm, with Cu ppm	1 point if Cu_ppm ≥150 *and* Co_ppm ≥45
			1 point if Cu_ppm ≥150 *and* Ge_ppm ≥3
			1 point if Cu_ppm ≥150 *and* Ag_ppm ≥ 1
			1 point if Cu_ppm ≥150 *and* Ga_ppm ≥35

[1]Digital geologic map of Alaska (Wilson, Frederic H., and others, USGS, written commun.) is source of lithology layers. Maximum HUC score is 3 points. Only HUCs that contain carbonates or are in a one HUC ring around these HUCs will be scored for the other layers. All unscored HUCs will have a total score of null, low potential, and high certainty.

[2]See appendix C for list of Cu carbonate model keywords and scoring template for ARDF; maximum HUC score is 5 points.

[3]Maximum HUC score is 8 points.

[4]Maximum HUC score is 3 points.

[5]Maximum HUC score is 4 points.

Table 10. Matrix of mineral resource potential versus certainty classification for carbonate-hosted Cu (-Co-Ag-Ge-Ga) deposits.

[ARDF, Alaska resource data file; HUC, hydrologic unit code]

Cu (Co-Ag-Ge-Ga)	Estimated certainty[1]				
	Low	Medium	High		
Unknown Total score = 0 *and* no sediment data points in HUC *or* no sediment data points in HUC *and* Lithology is only dataset >0	Total score ≥7 (p) 1-2 datasets not null (c)	Total score ≥7 (p) 3-4 datasets not null (c)	Total score ≥7 (p) 5-7 datasets not null (c)	High	Estimated potential[1]
	Total score 4–6 (p) 1-2 datasets not null (c)	Total score 4–6 (p) 3-4 datasets not null (c)	Total score 4–6 (p) 5-7 dataset not null (c)	Medium	
	Total score 1-3 (p) 1-2 datasets not null (c)	Total score 1-3 (p) 3-4 datasets not null (c)	Total score = 0 *and* sediment data points in HUC *or* Total score is null (p,c)	Low	

[1]Abbreviations (p) and (c) in cells denote which components contribute to assignment of potential and certainty, respectively.

Table 11. Scoring template for analysis of sandstone U (-V-Cu) potential in the hydrologic unit codes within the Central Yukon Planning Area.

[ARDF, Alaska resource data file; AGDB2, Alaska geochemical database version 2.0; ADGGS, Alaska Division of Geological and Geophysical Surveys; NURE, National uranium resource evaluation database; ppm, concentration in parts per million; HUC, hydrologic unit code]

Category	Dataset/layer	Component	Selection and score
ARDF records	ARDF	Reviewed records from ssU model keywords[1]	1 point if present
Lithology[2]	Digital geologic map of Alaska	Arkose sandstone	4 points if present
		Tertiary/ Cretaceous sedimentary rocks	3 points if present
		Sedimentary rocks	2 points if present
		Unconsolidated geologic units within 3km buffer around sedimentary rocks	1 point if present
Coal	Map of Alaska's coal resources (Merritt, and Hawley, 1986)	Upper Cretaceous to Tertiary coal	1 point if present
Igneous-rock geochemistry	AGDB2 + ADGGS + literature	Fe# displacement [3]	1 point if Fe# displacement >0
Sedimentary-rock geochemistry[4]	AGDB2 + ADGGS + NURE	U_ppm 98th percentile	2 points if U_ppm ≥40
		U_ppm 91st percentile	1 point if U_ppm ≥11 *and* <40
Sediment geochemistry[4]	AGDB2 + ADGGS + NURE	U_ppm 98th percentile	3 points if U_ppm ≥20 ppm
		U_ppm 91st percentile	2 points if U_ppm ≥5.8 *and* <20
		U_ppm 75th percentile	1 point if U_ppm ≥3.5 *and* <5.8
Aeroradiometric data[5]	Aerial gamma-ray survey data	U equivalent ppm	2 points if mean _ppm value >5 1 point if mean U_ppm value >2 *and* ≤5

[1] See appendix C for list of ssU keywords and scoring template for ARDF; see text for reviewing criteria.

[2] Lithology scores are the highest ranking sedimentary lithology present anywhere in the HUC.

[3] Fe# (FeO/[FeO + MgO]) displacement calculated using the Fe# versus SiO_2 array proposed by Frost and Frost (2008); applied only if SiO_2 >70 percent.

[4] Maximum single score for each element in HUC is used.

[5] HUC score based on mean eU value. Data from Duval (2001).

Table 12. Matrix of mineral resource potential versus certainty classification for sandstone U (-V-Cu) deposits.

[ARDF, Alaska resource data file; HUC, hydrologic unit code]

ssU	Estimated certainty[1]				
	Low	Medium	High		
Unknown No sediment data points in HUC *and* total score = 0; *or* no sediment data points in HUC *and* the total score entirely derived from the lithology, coal, or aerorad scores	Total score ≥7 (p) 1-2 datasets not null (c)	Total score ≥7 (p) 3–4 datasets not null (c)	Total score ≥7 (p) 5–7 datasets not null *or* an ARDF record meeting the reviewed criteria for ssU is present[2] (c)	High	Estimated potential[1]
	Total score 4-6 (p) 1-2 datasets not null (c)	Total score 4–6 (p) 3–4 datasets not null (c)	Total score 4 - 6 (p) 5-7 datasets not null *or* an ARDF record meeting the reviewed criteria for ssU is present[2] (c)	Medium	
	Total score 0-3 (p) 1-2 datasets not null (c)	Total score 0–3 (p) 3–4 datasets not null (c)	Total score 0–3 (p) 5-7 datasets not null *or* an ARDF record meeting the reviewed criteria for ssU is present[2] (c)	Low	

[1]Abbreviations (p) and (c) in cells denote which components contribute to assignment of potential and certainty, respectively.

[2]ssU ARDF recorded review criteria. Records with U as a "main" or "other" commodity were retained if (1) the deposit-type model type was sandstone uranium or roll-front, (2) if no deposit type was given and the "lode," granite, vein, dike, phosphates, or skarn were not present in any of the descriptive fields, (3) if the deposit type was a placer with U present as either a major or minor commodity.

[3]For a HUC to receive a medium potential the total score could not arise solely from the lithology or the lithology + coal; such HUCs were assigned low potential.

Table 13. Scoring template for analysis of Sn-W-Mo (-Ta-In-fluorspar) potential in the hydrologic unit codes of the Central Yukon Planning Area.

[ARDF, Alaska resource data file; AGDB2, Alaska geochemical database version 2.0; ADGGS, Alaska Division of Geological and Geophysical Surveys; NURE, National uranium resource evaluation database; ppm, concentration in parts per million; HUC, hydrologic unit code]

Category	Dataset/Layer	Component	Selection and score
ARDF records	ARDF	Sn-W-Mo-F keywords[1]	2 points if Sn-W-Mo-F keyword score ≥20 1 point if Sn-W-Mo-F keyword score >4 *and* <20
Igneous-rock geochemistry ratios[2]	AGDB2 + ADGGS + literature	Peraluminous[3]	1 point if classified as peraluminous
		10,000×Ga/Al[4]	1 point if 10,000×Ga/Al ≥2.6
Igneous rock geochemistry[2]	AGDB2 + ADGGS + literature	In ppm 91st percentile	1 point if In_ppm ≥0.4387
		Mo ppm 91st percentile	1 point if Mo_ppm ≥50
		Sn ppm 91st percentile	1 point if Sn_ppm ≥70
		Ta ppm 91st percentile	1 point if Ta_ppm ≥2.5206
		W ppm 91st percentile	1 point if W_ppm ≥50
		High silica	1 point if SiO2_pct ≥73
Sediment geochemistry[5]	AGDB2 + ADGGS + NURE	In_ppm 91st and 98th percentiles	2 points if In_ppm ≥0.17 1 point if In_ppm >0.08 *and* <0.17
		Mo_ppm 91st and 98th percentiles	2 points if Mo_ppm ≥10 1 point if Mo_ppm ≥5 *and* <10
		Sn_ppm 91st and 98th percentiles	2 points if Sn_ppm ≥39 1 point if Sn_ppm >4 *and* <39
		Ta_ppm 91st and 98th percentiles	2 points if Ta_ppm ≥2.2 1 point if Ta_ppm ≥1 *and* <2.2
		W_ppm 91st and 98th percentiles	2 points if W_ppm ≥21 1 point if W_ppm ≥5.2 *and* <21
Aeroradiometric data[6]	Aerial gamma-ray survey data	Th[7] 75th percentile	1 point if Th value ≥6

[1]See appendix C for list of Sn-W-Mo-F keywords and scoring template for ARDF; maximum single score for a HUC is used as the total score.

[2]Igneous rock geochemistry scores are additive.

[3]See text for description of peraluminous classification criteria. Score applied only to igneous rocks with SiO_2 >65 weight percent.

[4]10,000×Ga/Al scores applied only to igneous rocks with SiO_2 >65 weight percent.

[5]Maximum single score for each element in HUC is used. Element scores are additive for possible total of 10.

[6]Data from Duval (2001).

[7]Apparent Th as ^{208}Thallium (parts per million equivalent thorium).

Table 14. Average element concentrations in the upper continental crust.

Element	Average concentration in the upper continental crust, in parts per million*
In	0.05
Mo	1.5
Sn	5.5
Ta	2.2
W	2.0

*From Taylor and McLennan (1995)

Table 15. Matrix of mineral resource potential versus certainty classification Sn-W-Mo (-Ta-In-fluorspar) deposits in specialized granites.

[ARDF, Alaska resource data file; HUC, hydrologic unit code]

Sn-W-Mo (Ta-In-fluorspar)	Estimated certainty[1]				
	Low	Medium	High		
Unknown Total score = 0 *and* no sediment data points in HUC	ARDF score >1 *or* total score ≥6 (p) 1 data set not null (c)	ARDF score >1 *or* total score ≥6 (p) 2–3 data sets not null (c)	ARDF score >1 *or* total score >6 (p) 4–5 datasets not null (c)	High	Estimated potential[1]
	Total score 3–4 (p) 1 data set not null (c)	Total score 3–4 (p) 2–3 data sets not null (c)	Total score 3–4 (p) 4–5 datasets not null (c)	Medium	
	Total score 1 (p) 1 data set not null (c)	Total score 1 (p) 2–3 data sets not null (c)	Total score = 0 *and* sediment data points in HUC (p,c) *or* Total score 1 (p) and 4-5 data sets not null (c)	Low	

[1]Abbreviations (p) and (c) in cells denote which components contribute to assignment of potential and certainty, respectively.